Friedrich Schiller Universität Jena
Biologisch-Pharmazeutische Fakultät

Max Planck Institut für Chemische Ökologie
Abteilung für Biochemie

Characterization of UDP-glycosyltransferases responsible for benzoxazinoid detoxification in *Spodoptera frugiperda*

Masterarbeit
zur Erlangung des Grades eines
Master of Science

vorgelegt von

Elena Seibel
aus Gera

Jena, May 24, 2017

Betreuer:
Prof. Dr. Jonathan Gershenzon
Prof. Dr. Christian Hertweck

List of Abbreviations

ACN	Acetonitrile
BOA	2-Benzoxazolinone
BLAST	Basic Local Alignment Search Tool
BXD	Benzoxazinoid
cDNA	complementary DNA
cps	counts per second
ddH_2O	Double distilled water
DNA	Desoxyribonucleic acid
DMK	Deutsches Mais Komitee
ddNTP	Didesoxyribonucleotide triposphate
L-DOPA	*L*-3,4-dihydroxyphenylalanine
DIMBOA	2,4-dihydroxy-7-methoxy-2*H*-1,4-benzoxazin-3(4*H*)-one
DMSO	Dimethyl sulfoxide
DTT	Dithiothreitol
EDTA	Ethylenediaminetetraacetic acid
EIC	Extracted ion chromatogram
FA	Formic acid
GT	Glycosyltransferase
HPLC	High pressure liquid chromatography
6-OH-BOA	6-Hydroxy-2-benzoxazolinone
HMBOA	2-Hydroxy-7-methoxy-2*H*-1,4-benzoxazin-3(4*H*)-one
LB	Lysogeny broth
LC-MS	Liquid chromatography–mass spectrometry
LC-MS/MS	Liquid chromatography-tandem mass spectrometry
MBOA	6-Methoxy-2-benzoxazolinone
MRM	Multiple Reaction Monitoring
NTC	Non-transfected control
NMR	Nuclear magnetic resonance
PCR	Polymerase chain reaction
PVDF	Polyvinylidene flouride
rpm	Revolutions per minute
RT-qPCR	Real-time quantitative PCR
RNA	Ribonucleic acid
SDS	Sodium docecyl sulfate
SfUGT	UDP-glucosyltransferase from *Spodoptera frugiperda*
UDP	Uridine-5'-diphosphate
UGT	UDP-Glycosyltransferase
U	Units
USDA	U. S. Department of Agriculture

List of Figures

List of Tables

Contents

1 Zusammenfassung

Der Herbst-Heerwurm *Spodoptera frugiperda* ist ein polyphager Schädling ökonomisch bedeutender Nutzpflanzen, einschließlich Mais. Die wichtigste Gruppe chemischer Abwehrstoffe im Mais sind Benzoxazinoide (BXDs). Diese Sekundärmetaboliten werden als stabile Glukoside in der Pflanzenzelle gelagert und, nach Pflanzenbefraß, durch spezifische Glukosidasen aktiviert, wobei toxische Aglukone freigesetzt werden. Obwohl diese strukturell diverse Gruppe eine effiziente Verteidigung gegenüber vielen Schädlingen darstellt, ist *S. frugiperda* in der Lage auf Mais zu fressen, ohne Vergiftungssymptome zu zeigen. Obwohl die Konjugation dieser Verbindungen mit Glukose, katalysiert von UDP-Glykosyltransferasen (UGTs), lange als potentieller BXD-Entgiftungsmechanismus vermutet wurde, waren die verantwortlichen Enzyme für diese Reaktion bisher unbekannt. Erst kürzlich hat die Analyse des Transkriptoms von *S. frugiperda* die Identifikation von fünf UGT-Kandidaten mit Aktivität gegenüber dem Benzoxazinon DIMBOA oder dessen Abbauprodukt, dem Benzoxazolinon MBOA ermöglicht. Interessanterweise formte nur SfUGT5 (2*S*)-DIMBOA-Glc, das Hauptentgiftungsprodukt von DIMBOA. Dieses wurde in hohen Mengen in den Exkrementen von *S. frugiperda* nach Maisbefraß detektiert und ist ein Epimer der vom Mais produzierten Originalverbindung, (2*R*)-DIMBOA-Glc.
Im Rahmen dieser Arbeit erfolgte die weitere Charakterisierung dieser fünf Kandidaten im Bezug auf ihre Substratspezifität und relative Expression der entsprechenden Gene in verschiedenen Geweben. Die heterolog exprimierten Enzyme zeigten eine breite Substratspezifität gegenüber Xenobiotika und Pflanzenabwehrstoffen, wie Flavonoide, Terpenoide, Coumarine und simple Phenole. Im Vergleich zu den anderen UGTs, war SfUGT5 spezifischer für BXDs, was eine wichtige Rolle in der Resistenzbildung von *S. frugiperda* gegenüber dem stark verbreiteten und toxischen BXD vermuten lässt. Alle UGTs waren entweder in den Fettkörperchen, Darmgewebe oder den Malpighischen Gefäßen exprimiert, was für ihre Rolle als Entgiftungsenzyme spricht; zwei Kandidaten zeigten Expression in den Hoden. Die Funktion von UGTs in reproduktiven Organen is bisher jedoch unklar. Außerdem erfolgte die Expression und funktionelle Charakterisierung von fünf neuen UGT-Kandidaten, welche potentiell an der BXD-Detoxifizierung in *S. frugiperda* beteiligt sind; darunter vier Enzyme, die eine relativ geringe Aktivität gegenüber MBOA und HMBOA zeigten. Interessanterweise zeigte ein Enzym eine ähnlich hohe Aktivität und (Stereo)-Spezifität gegenüber DIMBOA und HMBOA, wie zuvor für SfUGT5 berichtet wurde. Die Ergebnisse dieser Arbeit erweitern das Wissen über den BXD-Metabolismus und der daran beteiligten Enzyme in *S. frugiperda*. Daher könnte diese Arbeit eine Basis für die weitere Erforschung der Rolle von UGTs in der Detoxifizierung von BXDs und anderen Xenobiotika in dieser und anderen Insektenspezies bilden.

2 Abstract

The fall armyworm *Spodoptera frugiperda* is a generalist herbivore and serious pest species on a number of economically important crop plants including maize. As many other members of the grass family, maize produces benzoxazinoids (BXDs) as major chemical defensive compounds against herbivores. These nitrogen-containing cyclic secondary metabolites are stored as stable glucosides in the plant cell and are activated by specific glucosidases upon herbivory, releasing toxic aglucones. Even though maize (*Zea mays*) is well defended by these metabolites, *S. frugiperda* larvae are able to feed and develop on maize of all growth stages, without showing symptoms of toxicity. Although glucose conjugation by UDP-glucosyltransferases (UGTs) has been suggested to be involved in the detoxification of benzoxazinoids by *S. frugiperda*, the responsible enzymes for this reaction were previously unknown. Only recently, the investigation of the transcriptome of *S. frugiperda*, after feeding on maize, revealed 39 putative UGT candidates out of which five candidates showed activity towards the benzoxazinone aglucone DIMBOA or its benzoxazolinone degradation product MBOA *in vitro*. Among them, only SfUGT5 formed (2*S*)-DIMBOA-Glc, the major detoxification product detected in the frass of *S. frugiperda* after feeding on maize, and epimer of the plant-derived compound (2*R*)-DIMBOA-Glc.

In this work, we further characterize these five candidates regarding their substrate specificity and relative expression levels of the corresponding genes in different larval tissues, and examine further enzyme candidates for activity towards BXDs. The UGT candidates were expressed in insect cells and a range of structurally diverse compounds was assessed as potential substrates. The expressed enzymes generally had a wide substrate specificity towards xenobiotics and plant allelochemicals, such as flavonoids, terpenoids, coumarins and simple phenols. However, SfUGT5 that was previously implicated to be involved in DIMBOA detoxification, was more specific towards BXDs, supporting a major role in the resistance of *S. frugiperda* against this highly abundant and toxic BXD. All UGTs were expressed in either fat bodies, gut or Malpighian tubules, consistent with their potential function in detoxification, and two candidates were expressed in the testes. The role of UGTs in reproductive organs is unclear and is worth to be investigated in future studies. Furthermore we heterologously expressed and characterized five new UGT candidates with potential contribution in BXD metabolism in *S. frugiperda*; out of these enzymes four showed relatively low activity towards MBOA and HMBOA, and one enzyme showed similar stereospecific activity and selectivity towards DIMBOA and HMBOA, as those previously observed for SfUGT5. The findings from this study expand the knowledge of BXD metabolism and the involved enzymes in this maize pest and will form the basis for future investigations on the role of UGTs in the detoxification of BXDs and other xenobiotics in this and other species.

3 Introduction

3.1 Maize (*Zea mays*)

Maize (*Zea mays*) belongs to the family of Gramineae (Poaceae), one of the largest plant families, including around 12,000 species. Modern maize was domesticated in Southern Mexico circa 9,000 years ago from its progenitor Balsas teosinte (*Z. mays* spp. *parviglumis*). Although genetically close related, maize and Balsas teosinte differ remarkably in their phenotypic appearance, most striking is the difference in their female inflorescence or ears. Teosinte ear possesses only about 5 to 12 kernels, each sealed tightly in a hard casing to ensure its protection. In comparison, modern maize ears possess about 500 or more kernels which are firmly attached to the central axis without adequate protection from predators [1]. The loss of the protective casing during domestication allows for easy harvest, increasing the yield of maize production. On the other hand, the exposure of the kernels makes them highly vulnerable to pathogens and herbivores [2].

Nowadays, maize is one of the most important staple crops with a worldwide production of around 1,000 million metric tons per year on an area of around 180 million hectares (Projection USDA, April 2017). Especially in developing countries maize is indispensable; together with rice and wheat, it provides around 30% of the food calories to more than 4.5 billion people in 94 developing countries. However, in a global perspective the major use of maize is as livestock feed, 63% of the maize demand is accounted by this area [3]. In Germany, around 60% of the total maize production area is reserved only for cattle farming. In addition, around 10% of the area corresponds to demand for bio-fuel production (DMK, 2009).

Both, biotic and abiotic stress factors can severely reduce maize yield: abiotic factors include the physical, chemical and moisture characteristics of the soil and climatic conditions; biotic factors include plant genotype, soil fauna, pests, and diseases [4]. Advances in maize hybrid breeding led to the cultivation of hundreds of landraces worldwide [5], adapted to specific local needs, environments and abiotic stresses, facilitating the cultivation of maize in practically every part of the world. Due to the aritificial selection, along improvements in fertilizers and pesticides, maize production has doubled in the past 40 years [3]. However, domestication and artificial selection has also been shown to negatively influence resistance to pathogens and insects [6]. Between 2001 - 2003, the loss of global maize production due to animal pests, including insect herbivores, was estimated to 6 - 19% worldwide [7].

More than 90 insect species are known to feed on cultivated maize, with feeding behaviors that cover all parts of the plant, from roots to the aerial parts [8]. To cope with the variety of damages caused by different herbivores, maize utilizes diverse defense strategies, mainly chemical adaptations (figure 1). Maize defense metabolites include compounds which increase leaf toughness, small organic metabolites and also macromolecules, as dietary fibers and proteins. For instance, high silica contents in maize leaves and stem were shown to interfere with feeding and boring of Asiatic Rice Borer [9]. The dietary fiber lignin and other cell wall components were shown to increase leaf toughness and act as nutritional or physical barriers to insect feeding [10]. Several classes of small organic molecules have been connected to maize defense: terpenoids,

alkaloids, steroids, phenolics, including flavonoids, polypeptides, as protease inhibitors and various glycosides [11]. Phenolic compounds, as the flavonol glycoside maysin and the carboxylic acid ester chlorogenic acid were shown to provide resistance towards herbivores in maize silk and foliar tissue, respectively [8]. However, benzoxazinoids (BXDs), a group of nitrogen-containing secondary metabolites, suggested as key defense compounds of many cereals [12], are among the best-studied maize chemical defenses.

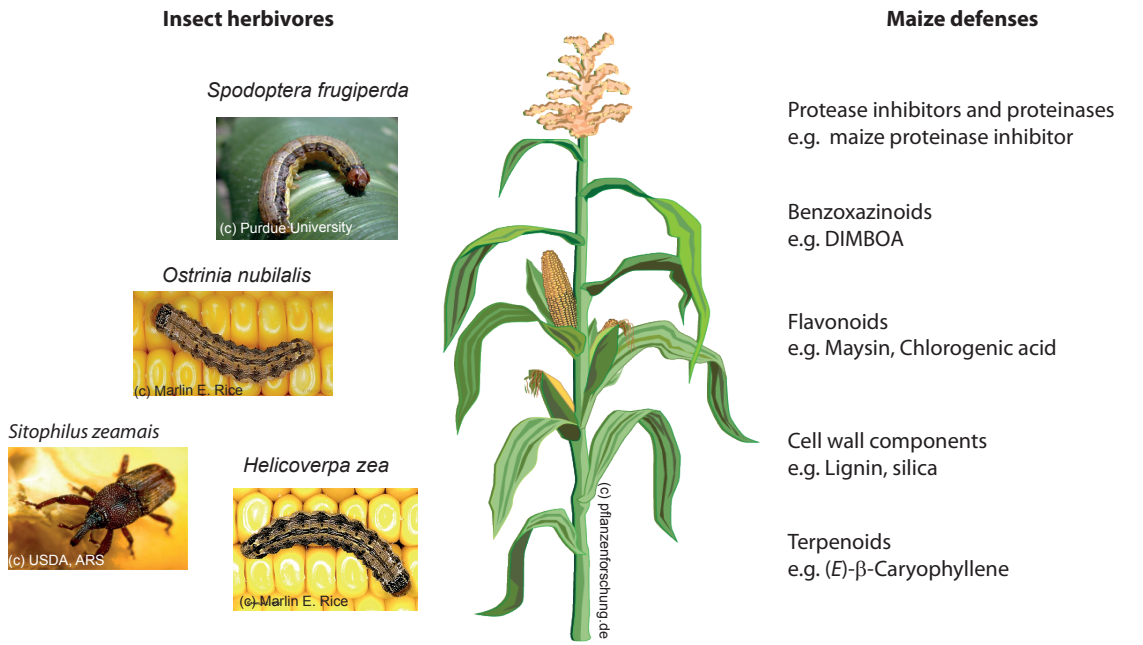

Figure 1: Summary of common maize-fedding insect herbivores and counter defenses produced by maize.

3.2 Benzoxazinoids (BXDs)

Benzoxazinoids are specialized secondary metabolites which occur in many grasses (Gramineae or Poaceae), including crop plants as maize, wheat, rye and are also found in dicotyledon plant families: Acanthaceae, Ranunculaceae, Lamiaceae, among others [12]. They contain a 2-hydroxy-2*H*-1,4-benzoxazin-3(4*H*)-one skeleton (figure 2) and can be chemically divided according to the substituent group R^1 into lactams (R^1 = H), hydroxamic acids (R^1 = OH) and *N*–*O*-methylated derivatives (R^1 = OMe). Benzoxazinoids are known for their broad biological activities as antifeedant, insecticidal, antimicrobial and allelopathic agents [12]. Indole serves as substrate for BXD biosynthesis and results from the conversion of indole-3-glycerol phosphate by indole-3-glycerol phosphate lyase Bx1, representing the branching point from primary metabolism [13]. To protect themselves from autotoxicity, benzoxazinoids are mainly stored in large amounts (concentrations up to several mmol/kg tissue) as stable, inactive, non-toxic glucosides in the plant vacuole, spatially separated from the activating β-glucosidases which in monocots are generally localized in the chloroplast. Hence, like other prominent examples of plant defense compounds, such as glucosinolates or cyanogenic glycosides, benzoxazinoids be-

long to the group of two-component defense systems [14]. It is important to note that the plant exclusively forms benzoxazinone-(2*R*)-2-β-D-glucosides [15].

Upon tissue damage by, for instance, a chewing herbivore, the loss of cell integrity leads to the hydrolysis of the inactive glucosides and benzoxazinone aglucones are released. These unstable intermediates spontaneously degrade to form benzoxazolinones, and both compound classes are biologically active towards the herbivore. This degradation process is facilitated by the alkaline environment [16] in the gut lumen of many herbivores of the lepidopteran species [17]. As this mechanism generates a diversity of structures, benzoxazinone glucosides and their aglucones as well as the benzoxazolinone degradation products are commonly summarized as benzoxazinoids (BXDs). The BXD nomenclature is based on acronyms derived from the systematic names of the compounds, as, for instance, DIMBOA for 2,4-**di**hydroxy-7-**m**ethoxy-2*H*-1,4-**b**enz**o**x**a**zin-3(4*H*)-one. The mechanism of hydrolysis and degradation and the structural diversity of BXDs are illustrated in figure 2.

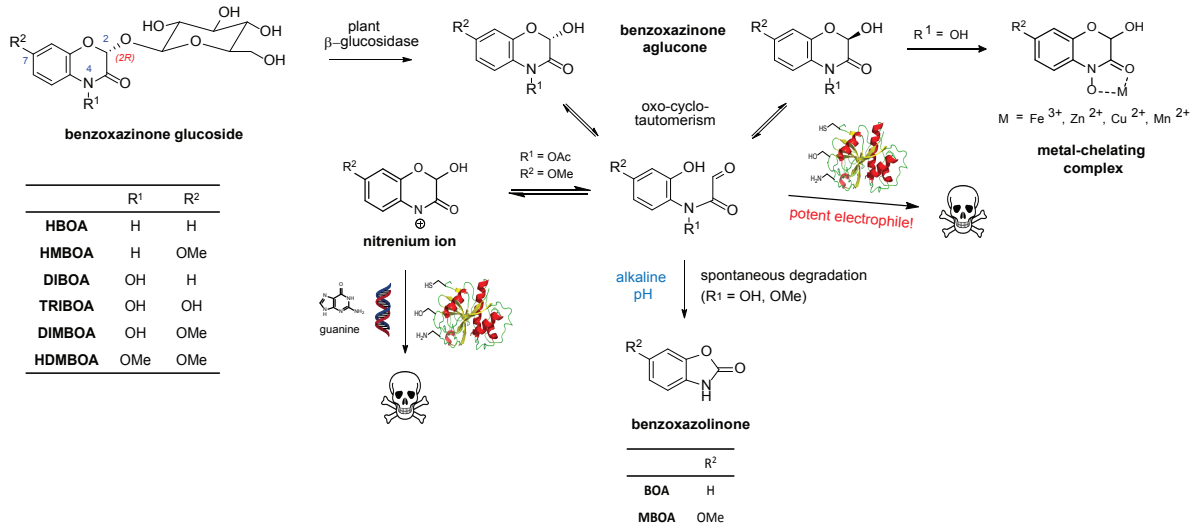

Figure 2: Structural diversity and suggested modes of action of naturally occurring benzoxazinone glucosides, the aglucones formed after hydrolysis and their spontaneous degradation products benzoxazolinones, commonly summarized as benzoxazinoids (adapted from Wouters et. al. [18]).

3.2.1 Plant distribution and mode of action of benzoxazinoids

BXDs are widely distributed in the plant but the abundance of BXDs differs among plant species, tissues, development stages and after induction by biotic factors [18]. In cultivated maize, a maximum concentration of 8 mmol/kg fresh weight was reported, in wheat and rye the concentrations were even higher [12]. The main BXD in rye is DIBOA-Glc, whereas DIMBOA-Glc is most abundant in the aerial parts of maize and wheat. HDMBOA-Glc is the dominant BXD in roots. Distribution of BXDs in leaves is also dependent of their age: while DIMBOA-Glc is predominant in young leaves from growth stages L2 to L4, HMBOA- and DIBOA-glucosides are more abundant in older leaves from growth stage L5 to L7 [19]. While most BXDs are constitutively expressed in the plant, HDMBOA-Glc was shown to be induced upon herbivory [20] with higher induction in young leaves than in old leaves [19].

The reactivity of the unstable benzoxazinone aglucones strongly depends on the substituent R^1, leading to various structural features and thus, diverse modes of action (figure 2). Whereas benzoxazinone glucosides are specifically produced as (2*R*)-form during BXD biosynthesis, the aglucones are cyclic hemiacetals that undergo oxo-cyclo ring-chain tautomerism via a reversible ring opening reaction in aqueous medium and therefore occur as racemic mixture of (2*R*) and (2*S*) aglucone. The open form transition state is an α-oxo-aldehyde and was shown to be relevant for biological activities, described for BXDs. It is a potent electrophile and is suggested to unspecifically react with nucleophilic residues in proteins such as thiols, amines and hydroxy-groups and therefore cause enzyme inhibition. However, the reaction of hydroxamic acids (e.g. DIMBOA) with nucleophiles was shown to be faster than for lactams (e.g. HMBOA), most likely due to the electron-withdrawing effect from the hydroxamic acid hydroxy group [15].
For hydroxamic acids the formation of a highly electrophilic nitrenium ion that results from metabolic *O*-acetylation and subsequent 7-MeO group-supported heterolytic cleavage of the N–O-bond was suggested [21]. This species was also shown to react with the DNA base guanine, and therefore act as mutagenic agent [22]. Both studies on this reactivity were performed with a synthetic derivative of DIMBOA, 4-acetoxy-7-methoxy-2-*H*-1,4-benzoxazin-3(4*H*)-one (4-*N*-OAc-D-DIMBOA) which lacks the 2-hydroxy group an thus is locked in the closed form. However, introduction of a 2-hydroxy group enhanced the reactivity of 4-acetoxy derivatives towards nucleophiles [23]. Other studies on BXD reactivity have reported that hydroxamic acids are able to act as metal chelators, suggesting potential for the inhibition of metallo enzymes containing bivalent metal ions [24]. In accordance with the reactivity of BXDs as electrophile, DIMBOA was shown to inhibit serine proteases by reacting with serine in the catalytic center of enzymes such as papain, α-chymotrypsin and trypsin [25, 26]. Inhibition studies with partially purified preoteinases from the European corn borer (*Ostrinia nubilalis*) suggested that DIMBOA toxicity primarly results from its role as digestive toxin [26]. In contrast to lactams, hydroxamic acids and *N*-*O*-methyl derivatives degrade spontaneously to benzoxazolinones by different proposed degradation mechanisms [23]. This degradation is especially facilitated by the alkaline gut environment which is common for most lepidopteran species [17], hence leading to specific biological activities towards this insect order.

3.2.2 Biological activity of BXDs towards lepidopteran insects

Accordingly to the broad modes of action, BXDs were shown to influence the feeding behavior of insects. Especially chewing herbivores, such as lepidopteran larvae, are exposed to high amounts of BXD aglucones due to the disruption of the plant cell during feeding [18]. In studies on the European corn borer (*Ostrinia nubilalis*) DIMBOA and its degradation product MBOA were shown to increase mortality and development times to pupation and adult emergence when supplemented to artificial diet. However, 10 to 20 times higher concentrations of MBOA were needed to cause similar toxicity as caused by DIMBOA [27–29]. Interestingly, lactams as HMBOA and HBOA, which do not degrade to benzoxazolinones, did not inhibit larval growth whereas other

hydroxamic acids, as for instance DIBOA, showed increased toxicity [29]. Thus, degradation of hydroxamic acids to benzoxazolinones correlates with increased toxicity although benzoxazolinones themselves are less toxic. In general, DIMBOA concentrations as low as 100 μg/g in maize whorl tissues was shown to be sufficient to reduce leaf consumption by the European corn borer.

In contrast, comparative studies on genus *Spodoptera* have shown contrary effects of BXDs. In these studies, toxicity of BXDs towards the broad generalist *S. littoralis* and *S. frugiperda* which is more specialized for grasses, were examined. When feeding on artificial diet containing 40 μg/g DIMBOA (level found in intact maize plants), no negative effect is observed on *S. littoralis* and *S. frugiperda*. However, DIMBOA concentrations of 200 μg/g diet (level found in herbivory-induced maize plants) had a negative effect on larval growth of *S. littoralis* but did not show any effect on *S. frugiperda*, confirming its better adaptation to grasses [30]. In comparison, a concentration of 330 μg/g MBOA did not have a negative effect on the growth of both, *S. frugiperda* and *S. littoralis*, suggesting that the genus *Spodoptera* in general is more resistance towards BXDs compared to genus *Ostrinia* discussed above [31]. When comparing the feeding preferences on different maize growth stages, *S. littoralis* preferred to feed on older leaves, possibly to avoid high concentrations of induced BXDs. In comparison, *S. frugiperda* predominantly fed on younger leaves despite of high BXD content [13]. Since *S. frugiperda* performs better on maize compared to the generalist *S. littoralis*, it seems to be more efficient in detoxifying BXDs.

3.3 Fall armyworm (*Spodoptera frugiperda*) and detoxification of BXDs

The fall army worm, *Spodoptera frugiperda* (J. E. Smith), is an agricultural pest of tropical-subtropical origin with wide distribution throughout the American continent [32,33]. It is known to feed on over 60 species of plants with a preference for grasses such as maize and sorghum. It feeds on all growth stages of maize but most frequently in the whorl of young plants. The adult female lays eggs in clusters of up to hundreds of eggs which, during summer, hatch in two to four days. The life cycle of *S. frugiperda*, including six larval instars, requires four weeks under optimal conditions (21-27 °C). Cool, wet spring seasons followed by warm, humid weather are favorable to propagation of the fall armyworm. Larvae of *S. frugiperda* usually consume a large amount of foliage and especially later instars also infest maize ears, leading to severe agricultural losses. Maize yield reduction due to feeding of the fall armyworm have been reported as high as 34% [32]. Only recently, *Nature News* reported a rapid propagation of *S. frugiperda* throughout the African continent where it was first identified in January 2016 [34]. With increasing global trade and climate change it is reasonable to expect the migration of this pest to Europe and Asia, making it to a serious threat for global maize production.

Understanding of the detoxifying mechanisms which cause the tolerance of *S. frugiperda* towards BXDs would facilitate an efficient management of this cosmopolitan pest, and therefore is subject of many studies. When fed on artificial diet containing DIMBOA, *S. frugiperda* larvae excreted large amounts of DIMBOA-Glc, HMBOA-Glc and MBOA-Glc in the frass. In

contrast, *S. littoralis* accumulated higher amounts of free DIMBOA in the frass, indicating that it is less efficient in glucosylating this compound [30]. Interestingly, no DIMBOA-Glc was detected in the frass of more BXD-susceptible species, *Mamestra brassicae* and *Helicoverpa armigera*, suggesting that glycosyltransferase activity towards BXDs may cause the increased tolerance of the genus *Spodoptera* [35]. Similar findings were reported for a comparison between *S. frugiperda*, *S. littoralis* and *O. nubilalis* feeding on MBOA-supplemented artificial diet [31]. Whereas *S. frugiperda* and *S. littoralis* almost quantitatively transformed MBOA to MBOA-*N*-Glc, *O. nubilalis* predominantly accumulated MBOA in the frass, in parallel to the toxic effect of MBOA towards this species discussed before. *In vitro* assays confirmed that DIMBOA and MBOA are glucosylated by *S. frugiperda* gut homogenate in presence of UDP-glucose [31, 35]. Interestingly, the metabolite excreted after DIMBOA ingestion, identified as (2*S*)-DIMBOA-Glc by NMR analysis, is an epimer of the (2*R*)-DIMBOA-Glc produced by the plant. This change in stereochemistry in the glucoside hinders the re-activation by plant β-glucosidases which are still active in the gut lumen [35]. Since the formation of toxic aglucones is blocked via this transformation, it represents an efficient detoxification mechanism towards BXDs. As glucoside formation was shown to be the main detoxification mechanism in *S. frugiperda*, the involvement of UDP-glucosyltransferases (UGTs) in BXD metabolism was suggested.

3.4 UDP-Glucosyltransferases in insects

During larval feeding, insect herbivores are often faced with a large diversity of toxic secondary metabolites produced by their host plant. Besides other strategies, insects possess a diverse spectrum of enzymatic conjugation capabilities to circumvent the toxicity of plant metabolites, pesticides and other xenobiotics (metabolic detoxification) [36, 37].

Glycosyltransferases (GTs), besides glutathione-*S*-transferases (GSTs) and other conjugating enzyme families, are a major member of detoxifying enzymes in phase II of the xenobiotic metabolism in organisms, producing hydrophilic, less toxic metabolites that can be easily excreted via multidrug-transporters. Members of these enzyme families often have broad, overlapping substrate selectivities to ensure that few small organic xenobiotic compounds escape detoxification metabolism [38].

GTs catalyze the transfer of a sugar residue from an activated sugar donor to a specific acceptor molecule, forming glycosidic bonds [39]. Currently this class of enzymes consists of 103 families, classified according to the degree of primary sequence identity [40], and can be found at the Carbohydrate-Active enZYme (CAZy) database (www.cazy.org). In contrast to the primary structure, GTs show a highly conserved secondary and tertiary structure, and adopt characteristic folds referred to as GT-A and GT-B fold [39]. Furthermore, GTs can be categorized according to the catalytic mechanism, into either inverting or retaining enzymes [39, 40]. This categorization is associated with the catalytic outcome: inversion or retention of the anomeric configuration of the sugar donor in the newly formed glycosidic bond. UDP-dependend glucosyltransferases (UGTs) belong to the CAZy family GT1 which adopt the GT-B fold and act as inverting enzymes [41]. UGTs are found in all free-living organisms from bacteria to

fungi, plants and animals [42]. They utilize an uridine diphosphate (UDP)-activated sugar for the glycosylation reaction, mostly UDP-glucuronic acid or UDP-glucose, but also UDP-xylose, UDP-galactose and UDP-*N*-acetylglucosamine [38]. All members of the UGT superfamily contain a highly conserved C-terminal UGT signature motif that consists of 44 amino acids and is involved in binding of the nucleotide-activated sugar donor [38, 43]. It is important to note that UGTs catalyze the sugar conjugation to small lipophilic molecules (aglycones), as for instance hormones, secondary metabolites and xenobiotics, possessing single or multiple glycosylation sites: functional groups, such as –OH, –COOH, $–NH_2$, –SH, and C–C groups [44]. Due to high diversity of potential substrates, the N-terminal domain, responsible for aglycone binding, is highly variable [38]. Enzymes which conjugate sugars to macromolecules, such as proteins, peptides, lipids or polysaccharides, are not included in the UGT superfamily [38].

In insects, UGTs have functions in both, endogenous metabolism and in detoxification [38]. UGT activity was shown towards various endogenous compounds, including catechols or ecdysteroid hormones, suggesting a role in cuticle sclerotization and pigmentation, as well as in the regulation of embryonic and larval development [45–47]. Also a role in olfaction is proposed, as UGTs specifically expressed in antenna, the insect olfaction organ, have been reported [48, 49]. However, a major function of insect UGTs is the detoxification of xenobiotics, mostly pesticides and plant allelochemicals. UGT activities have been reported towards several plant phenolics [50–53]. These studies have shown that insect UGTs typically use UDP-glucose as sugar donor, unlike mammalian UGTs which conjugate UDP-glucuronic acid.

Despite various reactions having linked to UGTs, the molecular identity of insect UGTs was relatively unknown compared to the well-studied mammalian UGTs. Only recently, a comparative analysis of the UGT multigene family reported the identification of over 310 putative UGT genes from genomic databases of eight different insect species [42]. Sequence alignments, conducted in this study, confirmed that insect UGTs, as vertebrate UGTs, are membrane-bound proteins located in the endoplasmic reticulum (ER) and share all conserved UGT domains and catalytic residues. The structural knowledge of insect UGTs and the organization of their encoding gene sequences in the genome, together with rising numbers of published genomes and transcriptomes, facilitates the identification and functional characterization of UGTs with potential function in detoxification.

Based on *in vivo* and *in vitro* studies of BXD detoxification in *S. frugiperda* described in paragraph 3.3, the involvement of UGTs was suggested. However, the enzymes and encoding genes potentially responsible for the conjugation have not been investigated. Only recently, Wouters et al. [54] reported the identification of 39 putative UGT genes retrieved from generated transciptome sequence data of *S. frugiperda* and comparison with other available public databases of this species, and other insect species (further referred to as SfUGTs). Out of the 39 sequences, 25 have been successfully expressed in insect cells and functionally characterized via *in vitro* enzymatic assays towards the abundant BXD DIMBOA and its degradation product MBOA [54]. Five candidates were able to glycosylate either DIMBOA or MBOA, or both. Three candidates (SfUGTs 14, 20, 29, referred to as SfUGTs 32, 22 and 35 in the original publication) were able to form MBOA-*N*-glucoside, the major detoxification product found in the frass of

several lepidopteran species when feeding on maize [31]. One candidate (SfUGT11, referred to as SfUGT3) was able to conjugate both, DIMBOA and MBOA, but formed the plant-derived (2*R*)-DIMBOA-Glc. However, only SfUGT5 (referred to as SfUGT6) specifically formed (2*S*)-DIMBOA-Glc, the major detoxification product found in the frass of *S. frugiperda* after feeding on maize [35], thus further supporting the role of UGTs in BXD detoxification in *S. frugiperda*.

4 Aim of the study

The fall army worm, *Spodoptera frugiperda*, is a cosmopolitan agricultural pest which is known to feed on over 60 species of plants with a strong preference for grasses such as maize. Benzoxazinoids (BXDs), a group of nitrogen-containing secondary metabolites are suggested to be the key denfense compounds of maize, and mediate resistance towards a variety of potential predators, inluding insects. Unlike other generalist herbivores, *S. frugiperda* tolerates high amounts of ingested BXDs, without showing indication of toxicity. Feeding experiments revealed that *S. frugiperda* is very efficient in detoxifying BXDs by reglucosylation of toxic benzoxazinone aglucones and their benzoxazinoline degradation products. The involvement of UDP-glycosyltransferases (UGTs), known for their importance in xenobiotic metabolism in vertebrates, was suggested and confirmed by the identification, heterologous expression and functional characterization of five putative UGT candidates from *S. frugiperda* (SfUGTs) which were capable of conjugating either DIMBOA or MBOA, or both.

To assess the potential importance and contribution of these UGT candidates in the metabolism of BXDs and other xenobiotics, as well as endogenous compounds in *S. frugiperda*, this study aims to further characterize these enzymes. In a broad substrate screening, the five candidates are tested towards various, structurally diverse compounds, mostly plant allelochemicals. The evaluation of their substrate specificities towards various potential compounds, that might be ingested during larval feeding, allows an assessment of the potential contribution of the individual enzymes to the overall xenobiotic metabolism. On the transcriptional level, the relative expression levels of the corresponding SfUGT-encoding genes are compared among five different larval tissues to investigate the distribution of BXD-detoxifying UGTs in the insect body. In a previous study, 39 putative UGT candidates were identified in *S. frugiperda* out of which only 25 had been successfully expressed. Therefore, this study further aims to clone and heterologously express the remaining UGT candidates and to analyze the resulting proteins for potential UGT activity towards benzoxazinoids. In summary, the general aim of the study is to expand the knowledge about BXD metabolism and the responsible detoxifying enzymes in this maize pest.

5 Materials and methods

5.1 Used donor and recipient organisms

Spodoptera frugiperda (maize strain)	obtained from colonies at the Max Planck Institute for Chemical Ecology, Department of Entomology (Jena, Germany)
Escherichia coli	NEB® 10-beta Competent *E. coli* (High Efficiency), New England Biolabs® Inc.
Trichoplusia ni	High Five™ cells in Express Five® SFM, Gibco® by Life Technologies (Darmstadt, Germany)

5.2 Chemicals

All chemicals used in this work are listed in the Supplement, paragraph 9.1. MilliQ grade water (ddH_2O) was obtained using the Milli-Q® Integral Water Purification System (Merck Millipore, Darmstadt, Germany).

5.3 Primers

All primers were ordered from Sigma-Aldrich and 100 μM stock solutions in ddH_2O were prepared according to the manufacturer's manual. Working solutions of primers were prepared by diluting the stocks to a final concentration of 10 μM. All primers used are summarized in paragraph 9.2.

5.4 Insects

Larvae of *Spodoptera frugiperda* were obtained from colonies at the Max Planck Institute for Chemical Ecology and were maintained by the Department of Entomology under controlled light and temperature conditions (16:8 h light/dark photoperiod, 20 °C) on artificial diet based on white beans [55].

5.5 Insect cell culture

Spodoptera frugiperda Sf9 cells and *Trichoplusia ni* High Five® cells (Gibco® by Life Technologies, Darmstadt, Germany) were cultured in Sf- 900 II serum-free medium and in Express-Five Serum-Free Medium, respectively. Express Five medium was supplemented with 16 mM L-Glutamine (Gibco®) and 50 μg/ml Gentamicin, prior to use. The adherent cultures were maintained at 27 °C and subcultured every 3 to 4 days.

5.6 RNA isolation from tissues of *Spodoptera frugiperda*

For the amplification of putative UDP-glycosyltransferase-encoding genes from *Spodoptera frugiperda* (SfUGTs), third to fourth instar larvae of *S. frugiperda* were allowed to feed on maize leaf pieces (2 weeks old plants, L4 stage) for 48 h and dissected on ice-cold 10 mM phosphate buffer (10 mM KH_2PO_4, 10 mM K_2HPO_4, pH 7.0). Their guts and integuments were collected seperately and stored in RNAlater (Sigma-Aldrich, Steinheim, Germany) at -20 °C until RNA extraction. Confluent Sf9 cell cultures were harvested shortly prior to RNA extraction. The feeding and dissection of the insects as well as the total RNA extraction from gut, integument and Sf9 cells were performed by Felipe Wouters.
For quantitative real-time PCR analysis (qPCR), nine third to fourth instar *S. frugiperda* larvae were allowed to feed on artificial diet [55]. After 48 h the insects were dissected and five different tissues were collected separately: gut, malpighian tubules, fat bodies, testes and cuticle. Each tissue was pooled from three individuals, resulting in three biological replicates per tissue, and stored in RNAlater at -20 °C until RNA extraction.
For RNA extraction the tissue samples were weighed, an appropriate volume of RL buffer (Jena Analytik, Jena, Germany) and 2.4 mm metal beads were added and the tissues were homogenized in a TissueLyser II bead mill (Qiagen, Hilden, Germany) at 40 Hz for 1 min. The homogenate was centrifuged at 10,000 x g at room temperature in an Eppendorf Centrifuge 5424R (Eppendorf, Hamburg, Germany). The supernatant was used for RNA isolation performed according to the protocol of the innuPREP RNA Mini Kit (Jena Analytik, Jena, Germany).
Obtained RNA concentrations were determined using a NanoDrop 2000c Spectrometer (Thermo Scientific, Schwerte, Germany). In order to eliminate genomic DNA, $\leq$10 μg of isolated RNA were mixed with 1 μl of TurboDNase enzyme (2 U/μl) and 5 μl 10x DNase buffer (Thermo Scientific, Schwerte, Germany). The total volume was adjusted to 50 μl with RNase-free water (Jena Analytik) and the reaction mixture was incubated at 30 °C for 30 min. The DNase-treated RNA was subsequently isolated from the reaction mixture using the RNeasy MiniElute Kit (Qiagen, Hilden, Germany) and final RNA concentrations were determined as described in paragraph 5.7.

5.7 Determination of RNA and DNA concentrations

RNA and DNA concentrations were determined by measuring the absorbance at 260 nm of 1 μl of RNA or DNA samples using a NanoDrop 2000c Spectrometer. The NanoDrop 2000c Operating Software (version 1.6) subsequently calculated the concentration automatically ($A_{260\ nm}$ (absorbance unit) = 1 corresponds to 50 ng/μl of DNA and 40 ng/μl of RNA). To evaluate the purity of the samples the absorption at 230 and 280 nm were measured and the 260/230 and 260/280 ratios were determined.

5.8 Reverse transcription (RT)

For Reverse Transcription of RNA into cDNA the SuperScript™ III Reverse Transcriptase Kit was used (all components were purchased from Invitrogen™, Darmstadt, Germany). To 500 - 1000 ng of the isolated RNA 1 μl of oligo(dT) primers and 1 μl of dNTPs (2.5 mM each) were added. The total volume was adjusted to 11 μl using RNase-free water. The RNA was denatured at 65 °C for 5 min, cooled down to 4 °C and subsequently mixed with 4 μl of 5x First-Strand buffer, 1 μl DTT (0.1 M), 1 μl RNaseOUT inhibitor and 1 μl SuperScript™ III Reverse Transcriptase (200U/ μl). The reverse transcription was conducted at 50 °C for 60 min, followed by incubation at 70 °C for 15 min in a Biometra Thermocycler TPersonal (Biometra, Goettingen, Germany). The obtained cDNA was stored at -20 °C until further use.

5.9 Quantitative real-time PCR (qPCR) analysis

Five benzoxazinoid-glucosylating enzymes (SfUGTs 5, 11, 14, 20 and 29), expressed and tested by Felipe Wouters [54], were further characterized by the determination of their expression levels among five different *S. frugiperda* larval tissues: gut, Malpighian tubules, testes, fat bodies and cuticle. From every tissue, three biological replicates were collected, resulting in 15 samples in total. Total RNA from the mentioned tissues was extracted as described in paragraph 5.6, followed by DNase treatment to eliminate genomic DNA and reverse transcription to cDNA using 500 ng of RNA (see paragraph 5.8). In order to prepare the cDNA samples for qPCR analysis an aliquot of 10 μl of the cDNA samples was diluted to a final cDNA concentration of 5 ng/μl and stored at -20 °C until qPCR analysis. The remaining 10 μl of the cDNA were left undiluted.

5.9.1 Primer design

Primers used for qPCR analysis of the five SfUGTs as well as five reference genes were designed using the online tool Primer3Plus [56]. To achieve high specifity and efficiency, short primers (optimum 20 bp) with a resulting amplicon size of maximal 150 bp and an optimal melting temperature of 60 °C were designed. To avoid amplification of contaminating genomic DNA, only primers that span an exon-exon junction were selected. The obtained primer pairs were subsequently blasted (Primer-BLAST) against the published *S. frugiperda* genome [57] and transcriptome [58–60] databases in order to verifiy their specificity for their respective target genes. The resulting qPCR primer pairs are listed in table S1.

5.9.2 Verification of primer specificity by sequencing and melting curve analysis

For the verification of the target specifity of the designed primer pairs the sequence of the amplified PCR products were determined and an analysis of their respective melting curves was included. Therefore, the undiluted cDNA samples from all tissues were pooled by mixing of 50 ng of every cDNA sample. The general qPCR reaction was conducted as triplicate determination using the CFX Connect™ Real-Time PCR Detection System (BioRad, Munich, Germany) as followed:

Table 1: Composition and conditions of the qPCR reaction.

Component	**Volume**	**PCR conditions**	
2x Brilliant® III SYBRR Master Mix	10 μl	1. Initial Denaturation (95 °C)	3 min
cDNA (5 ng/μl)	1 μl	2. Denaturation (95 °C)	10 s
Forward primer (10 μM)	1 μl	3. Primer annealing/ extension (60 °C)	20 s
Reverse primer (10 μM)	1 μl	4. Plate read (fluorescence detection)	
sterile water	7 μl	**Cycle: repeat steps 2.-4.**	**39x**
total	20 μl	5. Denaturation	10 s
		Melt Curve (60 - 95 °C, increment 0.5 °C)	5 s

To exclude genomic DNA contaminations in the cDNA samples or primer solutions, a non-template control (no cDNA added to reaction) and -RT control (pooled RNA samples were used as template) were included. In the end of each PCR run a melting curve was determined by slowly heating the PCR reaction from 50 to 95 °C. To confirm that the PCR amplification resulted in only one specific PCR product, the qPCR amplicons were analyzed by agarose gel electrophoresis and cloned into the pCR™4-TOPO® sequencing vector (Invitrogen™), *Escherichia coli* NEB10-beta cells were transformed with the resulting plasmids as described in paragraph 5.12. The transfomants were screened for positive colonies containing the desired insert via colony PCR (see paragraph 5.14), plasmids were isolated and the sequence of the vector insert was determined by Sanger sequencing (see paragraph 5.15).

5.9.3 Determination of amplification efficiency

Subsequently, the amplification efficiency of the qPCR reaction was determined for every primer pair, separately. Therefore, a dilution series of the cDNA pool was prepared: 0.05, 0.1, 0.5, 1, 5, 10 and 25 ng/μl. After performing of the PCR under the conditions shown in table 1, the CP values were plotted against the log-transformed concentrations and the primer amplification efficiencies were calculated based on the slope of the linear regression curve (Efficiency = – $1+10^{(-1/slope)}$) [61].

5.9.4 Relative quantification of SfUGTs using $2^{\Delta\Delta CP}$

After confirmation of the primer pairs in terms of specificity and efficiency, the expression levels of the respective target genes were quantified relatively to a housekeeping gene using the $2^{\Delta\Delta CP}$ method described by Livak et al. [62]. The qPCR was conducted for every tissue cDNA sample seperately in triplicate determination using the Brilliant III SYBR® Master Mix (Agilent Technologies, Waldbronn, Germany) based on the fluorescent dye SYBR Green.
In this study, five candidate housekeeping genes previously used for *Spodoptera* spp. [63], the elongation factor 1 alpha (EF1α), glyceraldehyde-3-phosphate dehydrogenase (GAPDH), ribosomal protein L10 (RPL10), ubiquinol-cytochrome c reductase (UCCR), and arginine kinase (AK), were evaluated for their suitability as normalization genes for the comparison of expression levels among tissues. Housekeeping gene selection was performed based on the comparative ΔCt method [64]. After the selection of the best reference gene, the expression levels of the genes of interest (GOI) relative to the reference gene (Ref) were calculated, based on its real-time PCR efficiencies (E), and the crossing point difference (ΔCP) of one unknown sample (treatment) versus one control [62] (see equation below). For the comparison of the five tissues examined in this work, the cuticle tissue was set as control.

$$ratio = \frac{(E_{GOI})^{\Delta CP_{GOI}(control-sample)}}{(E_{Ref})^{\Delta CP_{Ref}(control-sample)}}$$

Expression values of the biological replicates were averaged and standard error was calculated. Differences in expression levels between tissues were determined by statistical analysis.

5.10 Design for the amplification of putative SfUGT genes

For the identification of putative UGT-encoding genes, contigs obtained from Illumina sequencing of the transcriptomes from *S. frugiperda* larval gut and integument tissues and Sf9 cells (D. G. Vassão, unpublished results) were compared to the sequence and domain structure of published *Helicoverpa armigera* UDP-glucosyltransferases [42]. The contig assembly, performed by Felipe Wouters, resulted in 36 full coding sequences of putative *S. frugiperda* UGTs [54]. These coding sequences were confirmed with the published *S. frugiperda* draft genome [57] and transcriptome databases [58–60] and were used for the design of full sequence primers used for the amplification of the respective genes. Twenty-five of these SfUGT candidates were successfully expressed and tested for glucosylation activity by Felipe Wouters [54]. For the amplification of ten additional putative UDP-glucosyltransferases, full sequence primers were designed (see supplement, paragraph 9.2.2).
Designed reverse primers were lacking the stop codon to enable the expression of fusion proteins with a V5 epitope and His-tag using the pIB/V5-His TOPO ® TA vector system (Invitrogen™). Forward primers included the start codon as well as bases surrounding the start codon upstream and downstream.

5.11 Polymerase chain reaction and agarose gel electrophoresis

For the amplification of putative UDP-glucosyltransferases (SfUGTs), total RNA was extracted from the guts and integuments of *S. frugiperda* larvae and from Sf9 cells as described in paragraph 5.6. The obtained RNA was reverse transcribed to cDNA (see paragraph 5.8) and cDNA samples of all tissues were pooled and diluted to a concentration of 100 ng/μl. PCR amplification using Phusion HF Polymerase (Thermo Scientific, Schwerte, Germany) was conducted under following conditions:

Component	**Volume**
5 x Phusion HF Buffer	5 μl
cDNA mix(100 ng/μl)	1 μl
Forward primer (10 μM)	2.5 μl
Reverse primer (10 μM)	2.5 μl
dNTP mix (2.5 mM each)	0.5 μl
DMSO	0.5 μl
Phusion HF Polymerase (2U/μl)	0.25 μl
ddH_2O	12.75 μl
total	25 μl

PCR conditions	
1. Initial Denaturation (98 °C)	30 s
2. Denaturation (98 °C)	10 s
3. Primer annealing (52-62 °C)	30 sec
4. Extension (72 °C)	1 min
Cycle: repeat steps 2.-4.	**35x**
5. Final Extension (72 °C)	5 min
store at 4 °C	

To determine if the desired product was amplified, 5 μl of the PCR reaction were mixed with 6x DNA loading buffer (30% glycerol, 0.25% Bromphenol Blue in ddH_2O) and applied into slots of an 1% (w/v) agarose gel in 1x TAE buffer (40 mM Tris, 150 mM EDTA, 20 mM glacial acetic acid), containing 0.005% (v/v) Midori Green (Nippon Genetics Europe GmbH, Dueren, Germany). Agarose gel electrophoresis was performed in an electrophoresis chamber (Mupid®-One, Nippon Genetics Europe GmbH) filled with 0.5x TAE buffer at a constant voltage of 135 V for 20 min. As nucleotide size standard 3 μl of 1 kb Plus DNA Ladder Mix (Fermentas by Thermo Scientific, Schwerte, Germany) were used. Due to the intercalating character of Midori Green, separated PCR products could be visualized by UV excitation at 254 nm using the GeneGenius Bio-Imaging System (Syngene, Cambridge, UK).

5.12 Cloning of putative UDP-Glycosyltransferase genes (SfUGTs) and qPCR fragments

After amplification of the full coding sequences of the SfUGTs and separation by agarose gel electrophoresis, PCR products of the expected length (1500 - 1600 bp) were purified using the QIAquick PCR Purification Kit (Qiagen) or the Zymoclean™ Gel DNA Recovery Kit (ZymoResearch, Freiburg im Breisgau, Germany), depending on the purity of the PCR product and DNA concentration was determined (see paragraph 5.7).

Due to its proof-reading activity, Phusion HF polymerase generates double-stranded DNA with blunt ends. Before cloning into the pIB/V5-His TOPO® TA vector, first 3' A-overhangs were attached using GoTaq® DNA Polymerase (Promega, Mannheim, Germany). Therefore, to 15 μl of the purified PCR product, 4 μl of 5x GoTaq Colourless® Reaction Buffer, 0.6 μl dNTP mix (2.5 mM each) and 0.4 μl GoTaq® polymerase were added. After incubation at 72 °C for 20 min, the double-stranded DNA product with 3' A overhangs was purified according to the protocol of the DNA Clean & Concentrator™ S Kit (ZymoResearch), followed by the determination of the DNA concentration (see paragraph 5.7).
For ligation of the amplified SfUGT genes into the pIB/V5-His TOPO® TA expression vector (Invitrogen™), 10 ng of the respective PCR products, 0.5 μl of salt solution and 0.5 μl of the expression vector were mixed and the total volume was adjusted to 3 μl with ddH_2O. After 30 min incubation at room temperature, the reaction mixture was added to 50 μl of NEB 10-beta Competent *Escherichia coli* cells. After transformation of the chemically competent cells via heat shock, performed according to the manufacturer's protocol, aliquots of 50 to 100 μl were plated on LB_{amp} agar plates (10 g tryptone, 5 g, yeast extract, 5 g NaCl in 1 L ddH_2O, containing 1.2% agar and 50 μg/ml ampicillin) using sterile ColiRollers® Plating Beads (Merck Millipore) for even distribution. The plates were incubated overnight at 37°C and then stored at 4°C until further use.
Cloning of PCR products into the pCR™4-TOPO® sequencing vector (Invitrogen™) was performed as described for the pIB/V5-His TOPO® TA expression vector) with few variations. After the ligation reaction was incubated for 5 min, transformed NEB-10 beta cells were plated on LB_{kan} agar plates (LB-agar, containing 50 μg/ml kanamycin).

5.13 Site-directed mutagenesis in the coding sequence for the catalytic amino acid histidine

Structure analyses of human UGTs have shown that an N-terminal domain histidine (H), conserved in all members of the human UGT families UGT1A and UGT2B, is crucial for the catalytic activity of these enzymes towards phenolics and primary amines [65]. However, in UGT2B10 this residue is substituted by a leucine (L) because of which it lacks activity towards phenolics. Interestingly, UGT2B10 glucuronidates tertiary amines as nicotine, a property that seems to be exclusive for only few UGTs [66]. In another study [67], a UGT2B10 L to H substitution mutant was shown to gain activity towards phenolics indicating that these N-terminal residues were important for selective glycosylation of particular heteroatoms in a given substrate.
As the N-terminal H is also highly conserved in insects [42] and UGT activity was mostly observed for phenolic compunds [53], it might play a similar role in insects. To analyze the role of N-terminal histidine and leucine for UGTs from *S. frugiperda* in benozoxazinoid glucosylation as well as for potential tertiary amine or thiol substrates, mutants were generated which substitute the conserved catalytic histidine by a leucine. For point mutations in the His-coding triplets, primers containing the desired mutation surrounded by 15 DNA bases upstream and downstream, each, were used. The resulting forward and reverse primer were complementary to

each other (see paragraph 9.2.3, tableS3).
As template for site-directed mutagenesis, non-linearized pIB/V5-His TOPO® TA vectors containing genes encoding the DIMBOA-glucosylating enzyme SfUGT5 and the MBOA-glucosylating enzyme SfUGT29, replicated in *E. coli* (see paragraph5.12), were used. The PCR reaction, amplifiying the whole plasmid, was conducted using a gradient Phusion PCR (Thermo Scientific) in a Biometra Thermocycler T-gradient (Biometra, Goettingen, Germany) as followed:

Component	**Volume**	**PCR conditions**	
5 x Phusion HF Buffer	10 μl	1. Initial Denaturation (98 °C)	1 min
plasmid(100 ng/μl)	0.7 μl	2. Denaturation (98 °C)	10 s
Forward primer (10 μM)	2.5 μl	3. Primer annealing (60-72 °C)	30 sec
Reverse primer (10 μM)	2.5 μl	4. Extension (72 °C)	4.5 min
dNTP mix (2.5 mM each)	0.5 μl	**Cycle: repeat steps 2.-4.**	**18x**
DMSO	1.5 μl	5. Final Extension (72 °C)	10 min
Phusion HF Polymerase (2U/μl)	0.5 μl	store at 4 °C	
ddH_2O	31.3 μl		
total	50 μl		

Successful amplification was confirmed via agarose gel electrophoresis as described in paragraph 5.11. As the template plasmid DNA was methylated during replication in *E. coli*, the plasmids containing the wild type gene sequences were removed by incubation with the methylation-specific restriction enzyme DpnI (Thermo Scientific). Therefore, 1 μl of DpnI was added to 10 μl of the PCR reaction mixture. After incubation at 37 °C for 1 h the enzyme was inactivated by heating to 80 °C for 10 min. To re-obtain circular plasmid from the linear PCR products, 1 μl T4 ligase enzyme and 2 μl 5x T4 ligase buffer were added (Thermo Scientific). The total volume was adjusted to 20 μl by adding 5 μl of ddH_2O and the reaction mixture was incubated at 25°C for 1 h. After inactivating the enzyme at 70°C for 10 min, *E. coli* NEB-10 beta cells were transformed with the resulting plasmid as described in paragraph 5.12. Transformants, containing the desired mutation were screened by colony PCR (see paragraph 5.14), positive plasmids were isolated and the sequences were confirmed by Sanger Sequencing (see paragraph 5.15).
To study the influence of the mutation on the enzyme activity, *Trichoplusia ni* High Five™ cells (Gibco®) were transfected with the verified plasmids as well as their respective wild-types, separately (see paragraph 5.16). After successful transfection and selection of stably transfected cells (see paragraph 5.17), the microsomal fractions were extracted (see paragraph 5.18) and the protein expression was analyzed via western blot as described in paragraph 5.20. After adjustment of the relative amounts of the heterologously expressed SfUGTs by western blot analysis (see paragraph 5.21), *in vitro* enzyme assays were performed (see paragraph 5.22).

Differences of glucosylation activity between missense mutants and their respective wild types were compared by LC-MS/MS analysis (see paragraph 5.23).

5.14 Colony PCR

To verify if the *E. coli* colonies contained the expression vector with the desired SfUGT insert or qPCR product, single colonies were picked via a sterile pipette tip, suspended in 10 μl of water and used as templates for colony PCR. For amplification, vector-specific sequencing primers were used (see paragraph 9.2.4, paragraph S4). The colony PCR was conducted using GoTaq® DNA Polymerase (Promega, Mannheim, Germany) under following conditions:

Component	**Volume**	**PCR conditions**	
5x GoTaq Green® Reaction Buffer	5 μl	1. Initial Denaturation (95 °C)	10 min
E. coli colonies in water	2 μl	2. Denaturation (95 °C)	30 s
OpIE2 fwd primer (10 μM)	2.5 μl	3. Primer annealing (55 °C)	30 sec
OpIE2 rev primer (10 μM)	2.5 μl	4. Extension (72 °C)	1 min/kb
dNTP mix (2.5 mM each)	0.5 μl	**Cycle: repeat steps 2.-4.**	**35x**
GoTaq® DNA Polymerase	0.2 μl	5. Final Extension (72 °C)	5 min
ddH_2O	12.3 μl	store at 4 °C	
total	25 μl		

Afterwards, samples were run on an 1% agarose gel as described in paragraph 5.11 and gels were documented using the GeneGenius Bio-Imaging System (Syngene).

5.15 Plasmid isolation and Sanger sequencing

After the verification of successfully transformed *E. coli* colonies via colony PCR, 4 ml of LB_{amp} or LB_{kan} liquid medium (10 g tryptone, 5 g, yeast extract, 5 g NaCl in 1 L ddH_2O, containing 50 μg/ml ampicillin or kanamycin) were inoculated with bacteria and incubated overnight at 37 °C and 250 rpm in an Certomat® BS-1 incubation shaker (B. Braun Biotech International, Melsungen, Germany). Plasmid isolation was performed according to the protocol of the NucleoSpin® Plasmid DNA Purification Kit (Macherey-Nagel, Dueren, Germany) and the plasmid DNA concentration was determined using a NanoDrop 2000c Spectrometer (see paragraph 5.7).

Afterwards, sequences of the vector insert were determined by Sanger sequencing [68] using fluorescence-marked chain-terminating didesoxynucleotides (ddNTPs). Therefore, a PCR reaction using the BigDye™ Terminator v3.1 Sequencing Kit (Thermo Scientific, Schwerte, Germany) was conducted as followed:

Component	**Volume**	**PCR conditions**	
200 ng plasmid DNA Reaction Buffer	x μl	1. Initial Denaturation (96 °C)	5 min
BigDye™ Terminator v3.1 Ready Reaction Mix	4 μl	2. Denaturation (96 °C)	30 s
BigDye™ Terminator v3.1 5x Sequencing Buffer	4 μl	3. Primer annealing (55 °C)	30 sec
OpIE2 fwd or rev primer (10 μM)	1 μl	4. Extension (60 °C)	4 min
ddH_2O	(11-x) μl	**Cycle: repeat steps 2.-4.**	35x
total	20 μl	store at 4 °C	

The incorporation of ddNTPs aborted the elongation process and led to the enrichment of DNA fragments of different length and varying fluorescence-marked 3' ends which were isolated according to the protocol of the DyeEx® Spin Column Kit (Qiagen, Hilden, Germany). The DNA fragments of different length were separated by capillary electrophoresis followed by flourescence detection of the 3'-terminal ddNTP using the ABI PrismDyeEx® Genetic Analyzer 3130xl (Applied Biosystems™ by Thermo Scientific, Schwerte, Germany).

5.16 Transient transfection of insect cells

For the heterologous expression of the putative SfUGT genes, *Trichoplusia ni* High Five™ cells were transfected with recombinant expression vectors, verified by Sanger sequencing. One day before transfection, confluent High Five™ cells from a T-75 flask (Greiner Bio-One, Kremsmünster, Austria) were split and 500 μl of the culture were transferred into one well of a Corning® CellBIND® 6-Well culture plate (Corning Inc., Corning, USA), containing 2.5 ml fresh Express Five® SFM supplemented with 16 mM *L*-Glutamine and 50 μl/ml Gentamicin. After overnight incubation at 27 °C, the medium was replaced by 2.85 ml fresh medium. The transfection mixture was prepared by mixing 1.7 μg of recombinant plasmids with 5 μl of FuGENE® Transfection Reagent (Promega, Mannheim, Germany). The total volume was adjusted to 150 μl with fresh medium, the transfection mixture was mixed by vortexing and incubated at room temperature for 10 min. The entire mixture was then added to one well of the 6-well culture plate. The procedure was performed for each plasmid seperately. After gently shaking the plates horizontally, the cells were incubated at 27 °C for 72 h. Nontransfected High Five™ cells served as negative control.

Seventy-two hours posttransfection, transiently transfected cells were harvested and 1 ml of each culture was transfered into the wells of a new 6-well culture plate, containing 2 ml of fresh medium per well (1 : 3 dilution, 20% confluency).

5.17 Selection of stably transfected cell lines

After overnight incubation at 27 °C, the medium of the 20% confluent transient cells was replaced by fresh medium. Blasticidin (Sigma-Aldrich, Steinheim, Germany) was added to a final concentration of 50 μg/ml. The cells were incubated at 27 °C and the medium containing 50 μg/ml blasticidin was replaced every 3 - 4 days until the cells had grown to 100% confluency. The selection procedure took 2 - 3 weeks, depending on the transfection efficiency. The medium of the selected cell lines was replaced by fresh medium without blasticidin and split 1 : 2 into the wells of a new 6-well cell culture plate. The cells were incubated at 27 °C overnight and the medium was replaced by fresh medium, containing 10 μg/ml blasticidin. The cells were then left to grow to 100% confluency, changing the medium containing 10 μg/ml blasticidin every 3 - 4 days. To expand the volume of the stably transfected cell lines, the entire 3 ml cell culture from one well of the 6-well plate was transferred into a T-75 flask, containing 7 ml fresh medium. The stable cell lines were maintained in medium containing 10μg/ml blasticidin and subcultured every 3 - 4 days. To obtain a higher culture volume for membrane extraction the stable cell lines were distributed into five T-75 flasks per transfected recombinant plasmid.

5.18 Extraction of the microsomal fraction

For microsome extraction confluent, stably transfected cells from five T-75 flasks (10 ml culture) per recombinant plasmid were harvested by scraping the cells off the bottom using a sterile cell scraper (Sarstedt AG, Nuembrecht, Germany). The obtained cell suspensions were combined into a 50 ml falcon tube and centrifuged at 1,000 x g for 15 min at 4 °C (Avanti™ J-20 XP Centrifuge, Beckman Coulter, Krefeld, Germany). The supernatant was discarded, the cells were washed twice with ice-cold PBS buffer (137 mM NaCl, 2.7 mM KCl, 10 mM Na_2HPO_4, 1.8 mM KH_2PO_4, pH 7.4) and centrifuged at 1,000 x g for 15 min.
The resulting cell pellet was resuspended in 10 ml hypotonic buffer (20 mM Tris, 5 mM EDTA, 1 mM DTT, 20% glycerol, pH 7.5), containing 0.1% Benzonase® nuclease and 1x cOmplete™, EDTA-free Protease Inhibitor Cocktail (Roche, Basel, Switzerland), followed by incubation on ice for 30 min. After cell lysis, the cells were homogenized by 30 strokes in a Potter-Elvehjem tissue grinder (Kontes Glass Co., Vineland, USA) and were subsequently mixed with an equal volume of sucrose buffer (20 mM Tris, 5 mM EDTA, 1 mM DTT, 500 mM sucrose, 20% glycerol, pH 7.5). The homogenate was centrifuged at 1,200 x g and 4 °C for 10 min (Avanti™ J-20 XP Centrifuge, Beckman Coulter), the supernatant was transferred into Beckman polycarbonate ultracentrifugation bottles (25 x 89 mm) (Beckman Coulter) and centrifuged at 100,000 x g and 4 °C for 1.5 h in a fixed angle Type 70 Ti rotor (Optima™ L-90K Ultracentrifuge, Beckman Coulter).
After ultracentrifugation, the clear supernatant, containing the cytosolic fraction, was aliquoted into 1.5 ml eppendorf tubes. The pellet, containing the microsomal fractions, was resuspended in 1 ml of phosphate buffer (100 mM KH_2PO_4, 100 mM K_2HPO_4, pH 7.0), containing 1x cOmplete™, EDTA-free Protease Inhibitor Cocktail. After homogenization by 30 strokes in a Potter-Elvehjem tissue grinder the microsomal fraction was aliquoted into 1.5 ml eppendorf

tubes and snap frozen in liquid nitrogen. The aliquots were stored at -80 °C until further use. To verify the enrichment of membrane-bound heterologously expressed UGTs, the protein concentrations of the cytosolic and microsomal fractions were determined using the Bradford assay (see paragraph 5.19) and equal amounts of both fractions were applied on a SDS polyacrylamide gel. After SDS polyacrylamide electrophoresis (SDS-PAGE), expression of recombinant proteins, possessing a V5 epitope, was analyzed via western blot (see paragraph 5.20).

5.19 Bradford assay for protein concentration determination

Determination of protein concentrations in the microsomal and cytosolic fractions were determined via Bradford Assay [69]. To create a calibration curve bovine serum albumin(BSA) (SERVA, Heidelberg, Germany) was used as reference protein. BSA was diluted as followed: 12.5, 25, 50, 100, 250, 500, 750 and 1000μg/ml. The dilutions were prepared in the same buffer that was used to resuspend the protein samples. The assay was performed as triplicate determination in a 96-well microplate. Therefore, 5 μl of the protein samples were mixed with 200 μl of Bradford Reagent (SERVA) (freshly diluted 1 : 5 with water) and then incubated at room temperature for 5 min. Absorption was measured at 595 nm using the Molecular Devices SpectraMAX 250 Plate Reader (Marshall Scientific LLC, California, USA).

5.20 SDS-PAGE and enhanced chemiluminescent (ECL) western blot

To verify the successful heterologous expression and the enrichment of membrane-bound UGTs in the microsomal fraction, western blot was performed. For that purpose, equal amounts of the extracted cytosolic and microsomal fractions were separated by SDS-PAGE and the recombinant UGTs, possessing a V5 epitope, were detected by western blot via binding of a specific anti-V5-antibody, coupled to the horseradish peroxidase (HRP) enzyme, and subsequent chemiluminescence protein detection using the substrate luminol.

Cytosolic and microsomal protein samples (10 μg each) were mixed with an appropriate amount of 5x Laemmli Sample Buffer (0.25 M Tris, pH 6.8, 10% SDS, 50% glycerol, 5% β-mercaptoethanol, 0.02% bromphenol blue) and denatured at 95 °C for 10 min. The samples were applied into the slots of a Mini-PROTEAN® (any kD) Precast Gels and were run at 120 V for 1 h 15 min in a Mini-PROTEAN® Tetra Cell (BioRad, Munich, Germany) filled with 1x Tris/Glycine Buffer (25 mM Tris, 192 mM Glycine, 0.1% SDS in ddH_2O, pH 8.3). For higher sample numbers 26-well Criterion™ TGX™ (any kD) Precast Gels in combination with a Criterion™ Cell (BioRad) were used. Standard PageRuler Plus Prestained Protein Ladder (Thermo Scientific) served as protein size standard.

After SDS-PAGE, an Immun-Blot® PVDF membrane (BioRad) was activated in 100% methanol and subsequently membrane and gel were incubated in 1x Towbin Transfer Buffer (25 mM Tris, 192 mM Glycine, 20% MeOH in ddH_2O, pH 8.3) for 15 min under continuous shaking, separately. The transfer of proteins from gel to PVDF membrane was performed by semi-dry blotting. Therefore, the gel on top of the membrane was arranged between two sheets of Extra Thick Blot Paper (BioRad) presoaked in 1x Towbin Transfer Buffer (sandwich assembly) and

positioned between the electrode plates of a Trans-Blot® SD Semi-Dry Electrophoretic Transfer Cell (BioRad). During electrophoretic transfer, the negatively charged SDS-protein complex migrated out of the gel and moved towards the positive electrode, where they were deposited on the membrane. Transfer was performed at constant voltage of 15 V for 30 min for Mini-PROTEAN® Precast Gels and 25 V for 30 min for Criterion™ gels, respectively.
After blotting, the membrane was incubated in blocking buffer (1x TBST, containing 5% (w/v) skim-milk powder) for at least 1 h under continuous shaking to reduce unspecific interactions of the antibody with proteins on the membrane. The membrane was washed twice with 1x TBST (20 mM Tris, 150 mM NaCl, 0.1% Tween® 20, pH 7.4) for 10 min followed by overnight incubation in blocking buffer containing the Anti-V5-HRP antibody (1 : 5.000 (v/v)) (Novex® by Life Technologies, Darmstadt, Germany) at 4 °C under continuous shaking. On the next day the membrane was washed twice with 1x TBST and once with 1x TBS (20 mM Tris, 150 mM NaCl, pH 7.4) for 10 min, each.
For the dectection of V5-tagged recombinant UGTs, the membrane was incubated in a mixture of ECL solutions A (22 μl *p*-coumaric acid (90 mM in DMSO) and 50 μl luminol (250 mM in DMSO) in 5 ml of 100 mM Tris-HCl, pH 8.5) and B (4 μl H_2O_2 30% (w/w) in 5 ml of 100 mM Tris-HCl, pH 8.5) for one minute. Afterwards the membrane was placed between transparent foil in an Amersham™ Hypercassette™ and an Amersham™ Hyperfilm™ (GE Healthcare, Freiburg, Germany) was placed on top of the membrane. The oxidation of luminol catalyzed by the HRP enzyme with hydrogen peroxide as cofactor led to the formation of an dianionic excited state that releases energy as photons while dropping to its energy ground state.
This light emission led to the formation of black protein bands on a photographic film after developing in Carestream® autoradiography GBX developer and fixer (Sigma-Aldrich). Western blot results were documented by scanning the photographic film using a GS-900^{TM} Calibrated Densitometer with ImageLab^{TM} 5.1 Software (Bio-Rad).

5.21 Adjustment of SfUGT amounts for enzymatic assays by western blot quantification

In order to estimate the relative amounts of heterologously expressed UGTs, a western blot approach according to Krempl et al. (2015) was performed [70]. Therefore, four to five increasing amounts of microsomal total protein, determined via Bradford assay (paragraph 5.19), were separated by SDS-PAGE using 26-well Criterion™ TGX™ (any kD) Precast Gels and recombinant UGTs were detected by ECL western blot (see paragraph 5.20). Due to the linear correlation of applied protein amounts to the chemiluminescent signal, the relative protein amounts of recombinant proteins were estimated by determining the band intensities on a scanned photographic film.
Using the gel analysis software ImageLab™ 5.1., band intensities (represented by peak areas) were determined and the corresponding protein amounts of all proteins were normalized to each other. Therefore, the protein showing the lowest signal in western blot was used as reference and set to a factor of one. If different protein amounts of total proteins were applied to avoid

saturation of the chemiluminescent signal for high abundant UGTs, the peak areas obtained for each protein were extrapolated to the total protein amounts used for the reference protein. The peak areas of the reference protein bands were divided by the peak areas of the other proteins, and the obtained factors were averaged over all total protein amounts applied for western blot. The averaged factors correspond to the x-fold amount of total protein needed, to equalize the amounts of heterologously expressed SfUGTs used for enzymatic assays (paragraph 5.22).

5.22 *In vitro* enzymatic assays

For verification of the glycosylation activity of the heterologously expressed SfUGTs and further characterization of benzoxazinoid-glycosylating SfUGTs, *in vitro* enzymatic assays were performed. The general composition of the assays is listed in table 2.

Table 2: Composition of UGT enzyme assays with crude microsomal extracts.

Assay component	**Volume**	**Final amount/ concentrations**
12.5 mM UDP-Glucose (in ddH_2O)	4 μl	1 mM
12.5 mM substrate (in DMSO)	2 μl	0.5 mM
crude microsomal extract (1 mg/ml in potassium phosphate buffer	x μl (up to 25 μl)	up to 25 μg
potassium phosphate buffer (100 mM)	(50-x) μl	100 mM

In all enzymatic assays uridine 5'-diphospho(UDP)-α-*D*-glucose (UDP-glucose) served as sugar donor. The substrates and amounts of crude microsomal extracts added varied depending on the experiment. Potassium phosphate buffer (100 mM, pH 7.0) was added to reach a final reaction volume of 50 μl. Assays were performed in tubes of 96-well PCR plates. First, all components except the microsomal extract were mixed on ice. Reactions were started by adding the microsomal extract and incubated at 30 °C for 1 h in a Biometra Thermocycler T-gradient (Biometra, Goettingen, Germany) (lid temperature set to 30 °C). By addition of an equal volume of methanol/ formic acid (1 : 1) the reactions were stopped and centrifuged at 13,000 x g for 5 min at 4 °C. The supernatant was transferred into 0.3 ml polypropylene micro-vials N9 (Macherey-Nagel, Dueren, Germany). Samples were stored at -20 °C until further analysis by LC-MS (see paragraph 5.22). All enzymatic assays were performed as triplicates. A list of all substrates tested in this work can be found in paragraph 9.4. Most of the substrates were obtained commercially; DIMBOA and HMBOA were supplied by Felipe Wouters [35, 54]

5.22.1 Enzymatic assay to test the glucosylation activity of heterologously expressed SfUGTs

In order to test the glycosylation activity of seven succesfully expressed SfUGTs, 1-naphthol and 4-nitrophenol were used as general substrates. Additionally, all enzymes were tested for activity towards the main benzoxazinoid defense compounds from maize: DIMBOA, MBOA and HMBOA. Twenty-five μg of total protein from each crude microsomal extracts were used. The same amount of total protein from microsomal extracts from nontransfected High Five™ cells (NTC) served as control for endogenous glycosylation activity. To see possible non-enzymatic conversions of the substrates, a no-enzyme control was included. Therefore, the microsomal extracts were denatured by boiling at 95°C for 10 min before adding to the reaction mixture.

5.22.2 Substrate screening of five BXD-glucosylating enzymes

To further characterize five SfUGTs (SfUGT5, 11, 14, 20 and 29) which show glycosylation activity towards the benzoxazinoids DIMBOA, MBOA and HMBOA [54], the enzymes were screened for their specificity towards various compounds. Tested substrates are listed in table S5. In order to guarantee comparability between the tested SfUGTs, the total protein amounts from each microsomal extract were adjusted according to the calculated protein levels determined by western blot analysis (see paragraph 5.21). Twenty μg of total protein from the microsomal extract containing the reference protein were used. A control consisting of the same protein amount of a crude microsomal extract from nontransfected cells was prepared for each UGT. Boiled microsomes served as negative control.

5.22.3 Enzymatic assays of missense mutants of the catalytic His residue

In order to determine the importance of the catalytic histidine residue, substitution mutants of the SfUGTs 5 and 29 were generated which possess a leucine instead of a histidine at the catalytic site (paragraph 5.13). The glycosylation activity of these missense mutants against the general substrates 1-naphthol and 4-nitrophenol, the benzoxazinoids DIMBOA, MBOA and HMBOA, the thio-compound thiophenol and the alkaloid quinine were compared to their respective wildtype proteins. As for the substrate screening described above, comparability was achieved by adjusting the amounts of total protein used in the enzymatic assays based on their calculated expression levels determined by western blot (see paragraph 5.21). Twenty μg of total protein from microsomal extract from the reference protein were used. A control consisting of the same protein amount of a crude microsomal extract from nontransfected cells was prepared for each UGT. Boiled microsomes served as negative control.

5.23 Liquid chromatography-mass spectrometry and -tandem mass spectrometry (LC-MS and LC-MS/MS)

For the analysis of the enzymatic assays, glycosylated metabolites were detected using LC-MS and LC-MS/MS. Analytical chromatography procedures were performed on an Agilent 1200 coupled to a triple-quadrupole MS for metabolites with available standards or previously optimized multiple reaction monitoring (MRM) parameters. For all compounds with no available standard or MRM parameters, HPLC-MS experiments to assess MS spectra of the respective analyte were performed on the Agilent 1100 HPLC system coupled to an Esquire ESI-Iontrap mass spectrometer (Bruker Daltonics, Bremen, Germany). Different chromatographic gradients were used depending on the character of the tested metabolite (see paragraph 9.5).
For the 1200 HPLC system a sample volume of 5 μl was applied and separated using a Zorbax Eclipse XDB-C18 column (4.6 x 50 mm, 1.8 μm) (Agilent) in combination with 0.05% formic acid in water and acetonitrile as mobile phases A and B. The flow rate was 1.1 ml/min. LC-MS/MS analyses were performed on an API3200 tandem mass spectrometer (MS/MS) (Applied Biosystems, MDS Sciex, Darmstadt, Germany) equipped with a turbospray ion source operating in negative ionization mode. The ionization voltage was maintained at -4500 eV. Turbo gas temperature was 700 °C, collision gas 5 psi, nebulizing gas and heating gas 60 psi and curtain gas 25 psi. Multiple reaction monitoring (MRM) was used to monitor parent ion to fragment ion conversion with parameters from the literature for the glucosides of DIMBOA, MBOA, HMBOA [35,54], gossypol, 1-naphthol [70] and helicin [71]. MRM parameters used for the glucosides of thiophenol, 4-nitrophenol and esculetin were optimized from infusion experiments (compound optimization) with authentic standards obtained commercially. Parameters for MRM analysis of different analytes are listed in paragraph 9.6. Both Q1 and Q3 quadrupoles were maintained at unit resolution. Absolute concentrations (in μM) of the formed glucosides were determined by the normalization to an external standard curve of the respective standards. Standards for phenyl-β-*D*-thioglucopyranoside, esculin, helicin, salicylic acid 2-*O*-beta-*D*-glucoside and 4-nitrophenyl-β-*D*-glucopyranoside were commercially available, whereas standards for MBOA-Glc, (*2R*)-DIMBOA-Glc and (*2S*)-HMBOA-Glc were obtained from purified samples supplied by Felipe Wouters [35, 54]. Due to missing reference compounds, gossypol and 1-naphthol were relatively quantified by the integration of the respective peak areas and comparison between the samples. Analyst 1.5 software (Applied Biosystems, Darmstadt, Germany) was used for data acquisition and processing.
For the 1100 HPLC system (Agilent) mobile phase A was substituted by 0.2% formic acid and the EC 250/4.6 Nucleodur Sphinx RP 5 column (250 x 4.6 mm, 5 μm) (Macherey-Nagel) served as stationary phase. A sample volume of 10 μl was applied and separated using a flow rate of 1 ml/min. The mass spectrometer was operated in both, positive and negative mode over the range of m/z 60 - 1200. The electrospray ionisation (ESI) parameters were set as followed: skimmer voltage 40 V, capillary exit voltage 113.5 V, capillary voltage 4000 V, nebulizer pressure 35 psi, drying gas 11 L/min and gas temperature 330 °C. Chromatograms were analyzed with the DataAnalysis software and extracted ion chromatogram(s) (EIC) within a signal intensity

range suitable for quantification were selected (see paragraph 9.4). Using one or more EICs, analytes were quantified relatively by the peak areas using the QuantAnalysis software from Bruker Daltonics.

5.24 Protein sequence alignment and phylogenetic analysis of SfUGT candidates

For protein structure analysis, obtained DNA sequences from successfully cloned and expressed *S. frugiperda* UGT (SfUGT) candidates were translated to their respective protein sequence and were included in a multiple sequence alignment with the human UGT2B7 and *H. armigera* UGT HaUGT47A2. Five SfUGTs with previously reported potential function in benzoxazinoid detoxification (SfUGT5, 11, 14, 20 and 29) [54] were also included. Multiple sequence alignment was performed using the ClustalW algorithm [72] in Geneious software ® 6.0.5 (Biomatters Ltd., Auckland, New Zealand).
Seven newly expressed SfUGT candidates were assigned to their corresponding insect UGT families by phylogenetic analysis. Therefore, phylogentic trees were generated based on a multiple sequence alignment of the seven UGT candidates with 25 previously expressed and assigned SfUGTs [54] using the ClustalW algorithm in MEGA6 [73]. For the prediction of the three-dimensional structure of SfUGTs the protein sequences were analyzed for similarities to other proteins published in the Uni-Prot database [74] using the Basic Local Alignment Search Tool (BLAST) for proteins (BlastP) (https://blast.ncbi.nlm.nih.gov/Blast.cgi).

5.25 Statistical analysis

After quantification of the glucosides formed during the enzymatic assays of three independent experiments, the means and standard errors were calculated for every triplicate determination. Student's t-test was performed to analyze if the observed UGT activity in transfected microsomal fractions is significantly higher compared to the endogenous activity of non-transfected High Five^{TM} microsomes (NTC). To test the differences in UGT activities towards one substrate among the tested SfUGTs, an one-way analysis of variance (ANOVA) was performed for the net amount of glucosylation products formed by the recombinant UGTs. Therefore, for each substrate, the average of the amount of formed product calculated for the NTC was substracted from the product amount formed by SfUGT-containing microsomes (UGT) in each independent experiment. For substrate screenings where the NTC exceeded the activity of UGT-containing microsomes, substraction led to negative values. In these cases, the enzyme was considered as not active against the tested substrate and thus was excluded from the ANOVA analysis. Accordingly, for illustration of the net product formation in a bar chart using the mean of the substracted data (UGT-NTC), negative values were set to 0, as no enzyme activity was considered. Differences in the net glucoside amounts formed by each enzyme observed in ANOVA analysis were indicated by small letters over the respective bar.

6 Results

6.1 Expression and functional characterization of seven UGT candidates from *Spodoptera frugiperda*

6.1.1 Expression of seven UGT candidates in insect cells

UGT candidates from *S.frugiperda* were identified on the basis of transcriptome analysis of larval gut and integument tissues and Sf9 cells [54]. Full length coding sequences were assembled due to their similarity to UGT-encoding genes identified in other insect species and also by manually assembling the 5' and 3' ends from the raw transcriptome data, as well as RACE-PCR [42]. From the 36 full UGT sequences retrieved, 25 had been previously expressed in insect cells and screened for UGT activity towards the benzoxazinoids MBOA and DIMBOA revealing five UGTs with potential function in benzoxazinoid detoxification [54].
In this study, it was aimed to amplify the remaining UGT candidates and to test them for UGT activity towards benzoxazinoids. From the 11 sequences, 9 UGT candidates were successfully amplified from mixed cDNA from *S. frugiperda* larval gut and integument tissues and cloned into the pIB/V5-His-TOPO® TA expression vector. The obtained DNA sequences from Sanger sequencing, translated protein sequences and more information to sequence lengths and protein molecular weight can be found in the supplement, paragraph 9.3. Subsequently, *Trichoplusia ni* High Five™ cells were transfected with recombinant expression vectors. Transfected cell cultures were harvested at confluency and the microsomal fraction was extracted. Expression of recombinant UGT proteins fused to a V5-epitope at the C-terminus was analyzed by SDS-PAGE and subsequent western blot using a V5-specific antibody. Protein expression was analyzed in both, microsomal and cytosolic fractions. Figure 3 shows that all SfUGTs have been successfully expressed in the microsomes of High Five™ cells, with exception of SfUGTs 41 and 43. In contrast, no recombinant protein was detected in the cytosolic fraction, confirming that SfUGTs, as other insect UGTs [42] are located in the endoplasmatic reticulum. As SfUGTs 41 and 43 were not expressed in High Five^{TM} cells, they were excluded from further analysis.

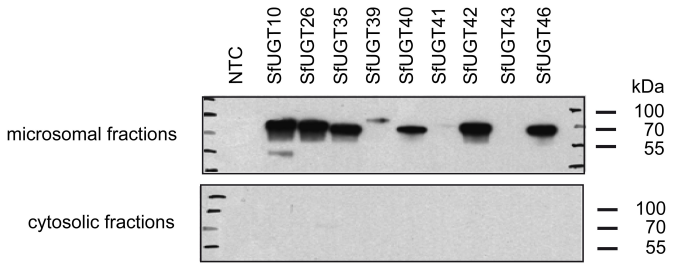

Figure 3: Western blot analysis of the successful expression of new SfUGTs candidates in High Five™ cells. Equal amounts of total protein (10 μg from cytosolic and microsomal extracts of SfUGT-transfected cells were analyzed by SDS-PAGE and recombinant proteins possessing the V5 epitope were detected by western blot using a V5-specific antibody. PageRuler Plus Prestained Protein Ladder (Thermo Scientific) served as protein molecular weight standard.

When using the pIB/V5-His-TOPO® TA cloning system, recombinant fusion proteins with C-terminal V5-epitope and His-tag are produced. Hence, expected protein molecular weights for all expressed UGTs including the tags are between 63 and 65 kDa. The observed protein bands were between 60 and 80 kDa. Higher molecular weights compared to the calculated values might be a result of posttranslational modifications of the proteins during protein expression in the ER lumen of the eukaryotic host.
To enforce this suggestion, NetGlyc 1.0 Server was used to analyze the protein sequences for potential asparagine *N*-glycosylation sites. One *N*-glucosylation site was predicted for SfUGTs 35, 40 and 46, two for SfUGTs 26 and 42, three for SfUGT10 and five sites for SfUGT39. Thus, the higher observed molecular weights are likely to be due to postranslational modifications in the ER lumen.

6.1.2 Enzymatic assays for the functional characterization of new UGT candidates

To test the functionality and importance for benzoxazinoid detoxification of the seven successfully expressed UGT candidates *in vitro*, microsomes were extracted from stably transfected *Trichoplusia ni* High Five^{TM} cell cultures and used for enzymatic assays. UDP-glucosyltransferase activity towards two simple phenolic compounds, 4-nitrophenol and 1-naphthol, and the benzoxazinoids MBOA, DIMBOA and HMBOA was tested. As previously observed in different studies, the xenobiotics 4-nitrophenol and 1-naphthol are glycosylated by a wide range of human, plant and insect UGTs [50, 67, 75]. Due to their broad acceptance as substrates, they were chosen as general UGT substrates to confirm the functionality of the expressed UGTs. Enzymatic assays were conducted using equal total protein amounts (25 μg) from microsomal fractions expressing the respective UGTs and from non-transfected cells as control (NTC).
All microsomal extracts from UGT-transfected cells were able to glucosylate 1-naphthol (figure 4, B). Also in non-transfected microsomes glucosylation activity was observed. However, 1-naphthyl-glucoside formation was significantly higher in microsomes containing recombinant UGTs. Only SfUGT26-transfected microsomes did not show significant difference to the control, suggesting that SfUGT26 is not active towards 1-naphthol. Similarly, all UGTs except SfUGTs 10 and 26 showed significantly higher glucosylation activity towards 4-nitrophenol (figure 4, A). Enzymatic assays with MBOA (figure 4, C) as substrate revealed three enzymes, SfUGTs 39, 40 and 46 which are capable of glucosylating MBOA. However, the observed glucoside amounts were low. SfUGTs 39 and 40 and additionally SfUGT42 showed similarly low activity towards HMBOA (figure 4, E). In contrast, SfUGT26 which did not show activity towards the general substrates, glucosylated HMBOA and DIMBOA in high amounts (55 μM of HMBOA-glucoside and 120 μM of DIMBOA-glucoside) (figure 4, D). This activity is similar to the previously reported enzyme SfUGT5 (referred to as SfUGT6 in the original publication) [54]. It was shown, that the third enzyme glucosylating DIMBOA, SfUGT11 (referred to as SfUGT3 in [54]) forms a (2*R*)-epimer of DIMBOA-glucoside, the original plant defense compound, whereas SfUGT5 formed the opposite (2*S*)-epimer, the detoxification metabolite detected in *S. frugiperda* frass [35]. Comparison of the retention times of the DIMBOA-glucosides formed by SfUGTs 5, 11 and 26 with

an authentic plant-derived (2*R*)-DIMBOA-glucoside standard shows that SfUGT26 formed the (2*S*)-epimer of DIMBOA-glucoside (figure 5).

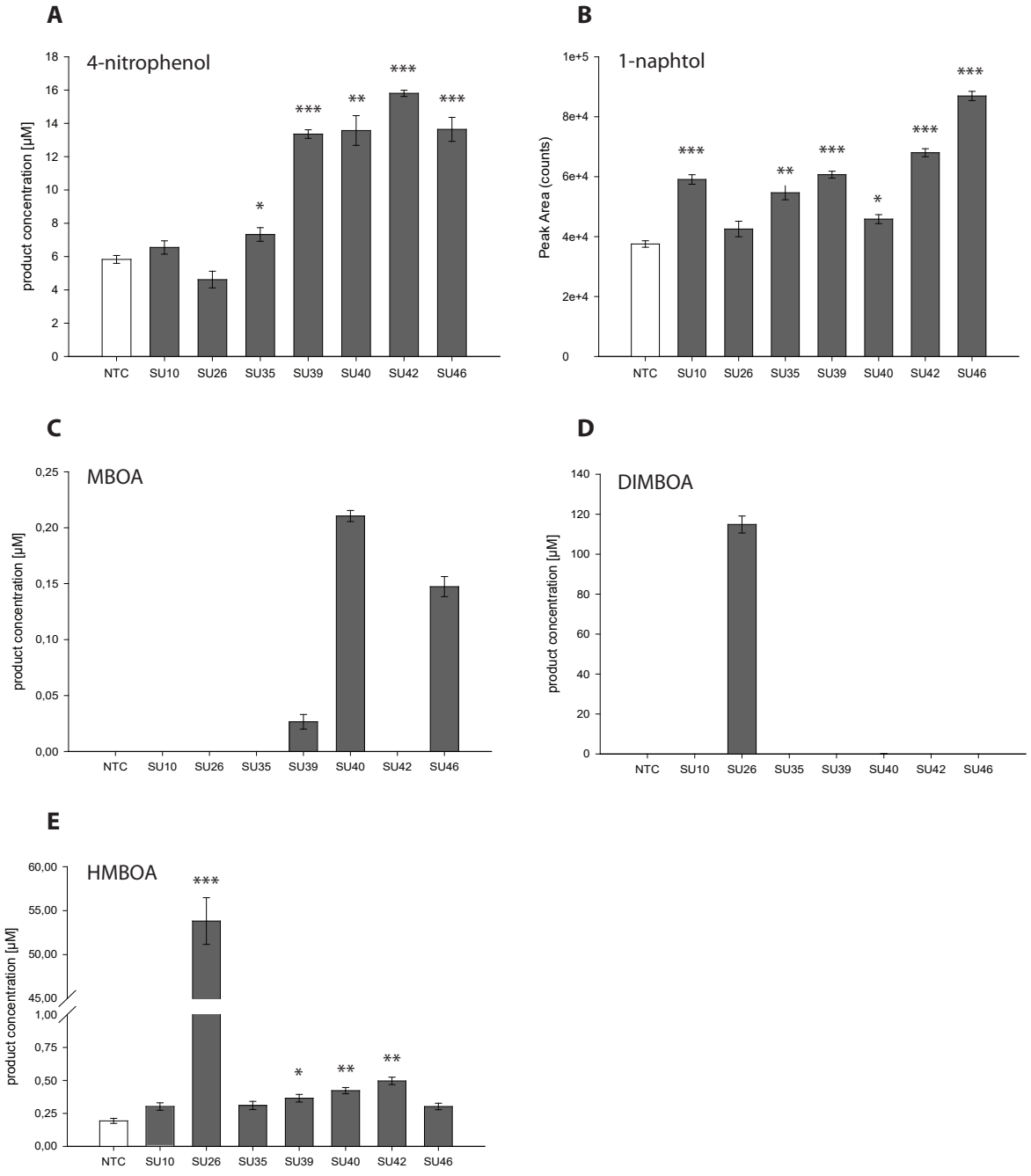

Figure 4: Functional analysis of newly expressed SfUGTs towards benzoxazinoids and exogenous phenolics. The amounts of glucosides formed by 25 μg of SfUGT-containing microsomes (gray bars) extracted from transfected insect cells are illustrated as mean ± standard error of three replicate determinations. The same amount of total protein from microsomes of non-transfected cells served as control (white bars). Differences between the glucoside formation of UGT-transfected microsomes and the non-transfected control (NTC) were analyzed via Student's t-test. Results are indicated by asterisks (* - $P < 0.05$, **- $P < 0.01$, *** - $P < 0.001$).

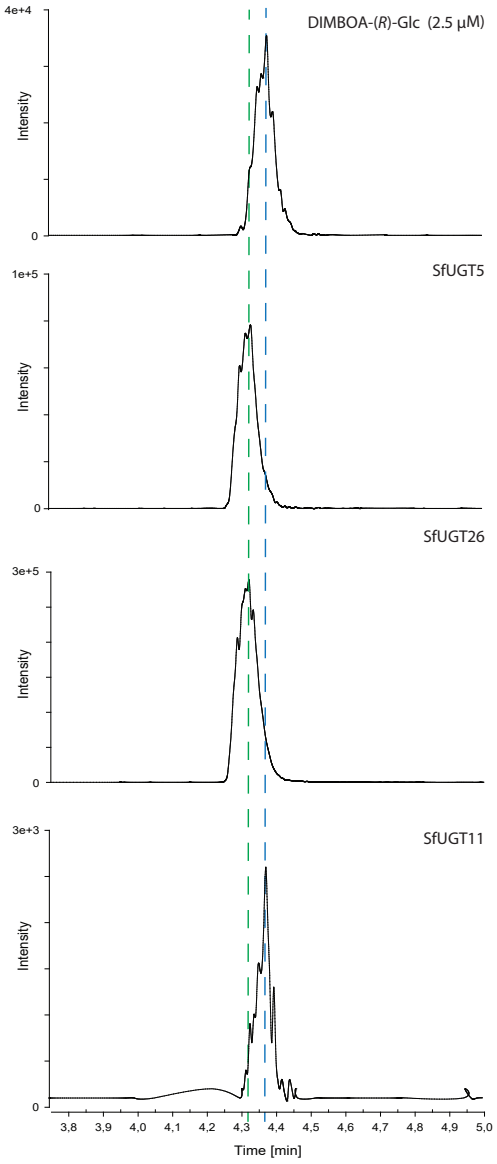

Figure 5: Comparison of the retention times of DIMBOA-glucoside formed by SfUGT 5, 11 and 26. Extracted ion chromatograms from MRM analysis of DIMBOA-glucoside (418/372) formed in enzymatic assays with DIMBOA as substrate are illustrated. Whereas the peak of DIMBOA-glucoside formed by SfUGT11 aligns with that from the plant-derived (2R)-DIMBOA-glucoside, SfUGT26 and SfUGT5 form a product with a slightly shifted retention time. This product was previously shown to be the epimer (2S)-DIMBOA-glucoside [35, 54].

6.1.3 Phylogenetic analysis and protein sequence analysis of newly expressed SfUGTs

To determine if the expressed UGTs show the typical protein structure of animal UGTs, the obtained DNA sequences from Sanger Sequencing were translated and resulting amino acid sequences were analyzed. The seven newly expressed SfUGTs together with the five SfUGTs with previously demonstrated activity towards BXDs were aligned and compared to the insect UGT HaUGT47A2 from *H. armigera* and the human UGT2B7 (figure 6). Multiple alignment of these 14 UGT sequences based on the ClustalW algorithm [72] revealed that all expressed UGTs consist of two major domains: a highly variable N-terminal substrate binding domain and a conserved C-terminal sugar-donor binding domain, connected through a short interdomain linker [42]. All *S. frugiperda* UGTs contain a 16 - 22 amino acid-long N-terminal signal peptide which directs the translocation of the protein to the ER and is probably cleaved off by a signal peptidase after integration into the ER membrane [76]. Signal peptide cleavage sites, predicted by SignalP4.1 Server [76], are shown in figure 6. The comparison with other animal UGTs showed that SfUGTs share all important domains and UGT motifs. Close to the C-terminal end of the proteins, a short transmembrane domain consisting of 16, mainly hydrophobic amino acids is identified. The membrane domain is followed by a highly variable cytoplasmic tail showing varying lengths from 9 - 46 amino acids. Comparison of UGT sequences from different insect species revealed that cytoplasmic tail lengths, ranging from 4 - 51 amino acids with a modal value of 23 amino acids, are common in insect UGTs [42]. Unlike the other SfUGTs, SfUGT39 shows a relatively long cytoplasmic tail (46 aa) with high similarity to UGT47A2 from *H. armigera*. Directly in front of the transmembrane domain a negatively charged amino acid (mainly Asp or Glu) is highly conserved, suggesting its importance for positioning and orientation of the membrane domain [42].

Crystal structure data and mutational analysis of the C-terminal domain of human UGT2B7 [65, 77] gave insight about crucial protein regions and amino acids for sugar-donor binding. The UDP-glucuronic acid binding regions predicted for UGT2A7 (donor binding regions, DBR1 and 2) are also conserved in SfUGTs. Since the specific amino acids which are predicted to interact with the components of UDP-glucuronic acid (6) are also conserved in *S. furgiperda* UGTs, it is likely that these residues are also important for binding UDP-glucose.

Regarding the three-dimensional structure of expressed UGTs, blastP searches in the UniProtKB Swiss-Prot database using the expressed SfUGT as query revealed that they are similar to UGTs which belong to the GT1 family and are predicted to adopt a GT-B fold [40]. These enzymes are known to use an inverting mechanism for catalysis of the sugar transfer to the substrate.

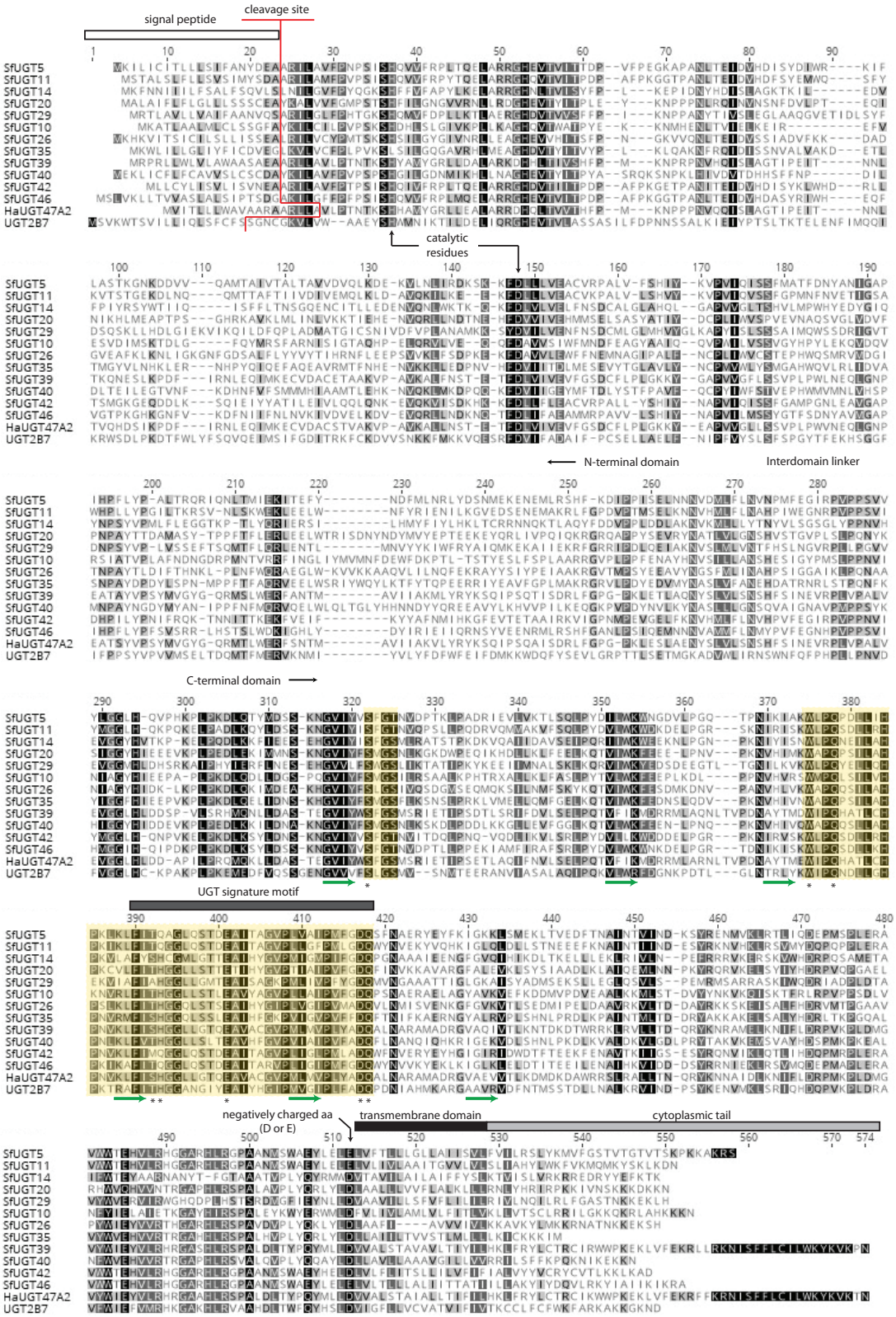

Figure 6: Multiple alignment of twelve heterologously expressed and functionally characterized UGTs from *S. frugiperda*. The primary protein structure of five previously characterized SfUGTs with potential function in benzoxazinoid detoxification and seven newly expressed UGT candidates in this study are compared to the human UGT2B7 and the insect UGT47A2 from *H. armigera*. The predicted signal peptide, UGT signature motif, transmembrane domain and cytoplasmic tail are shown as bars on top of the alignment. The catalytic residues H35 (H37 in the alignment) and D151 (D148), putative β-sheets as well as responsible regions (DBR1 and 2, highlighted in yellow) and residues (*) for sugar-donor binding in the C-terminal domain were predicted based on the crystal structure and mutational analsis reported for UGT2B7 [65].

Based on phylogenetic analysis of 25 SfUGTs, expressed and tested by Felipe Wouters [54], the seven newly expressed UGTs were assigned to insect UGT families (figure 7). SfUGTs with detected activity towards the benzoxazinoids DIMBOA and MBOA (higlighted in green) are distributed among five insect UGT families: UGT33, 40, 42, 46 and 47. DIMBOA-conjugating SfUGTs 5 and 26 belong to the two largest families UGT33 and UGT40, respectively. SfUGTs with activity towards MBOA are present in all five families. SfUGTs 10, 35 and 42 (highlighted in orange) did not show activity towards DIMBOA and MBOA.

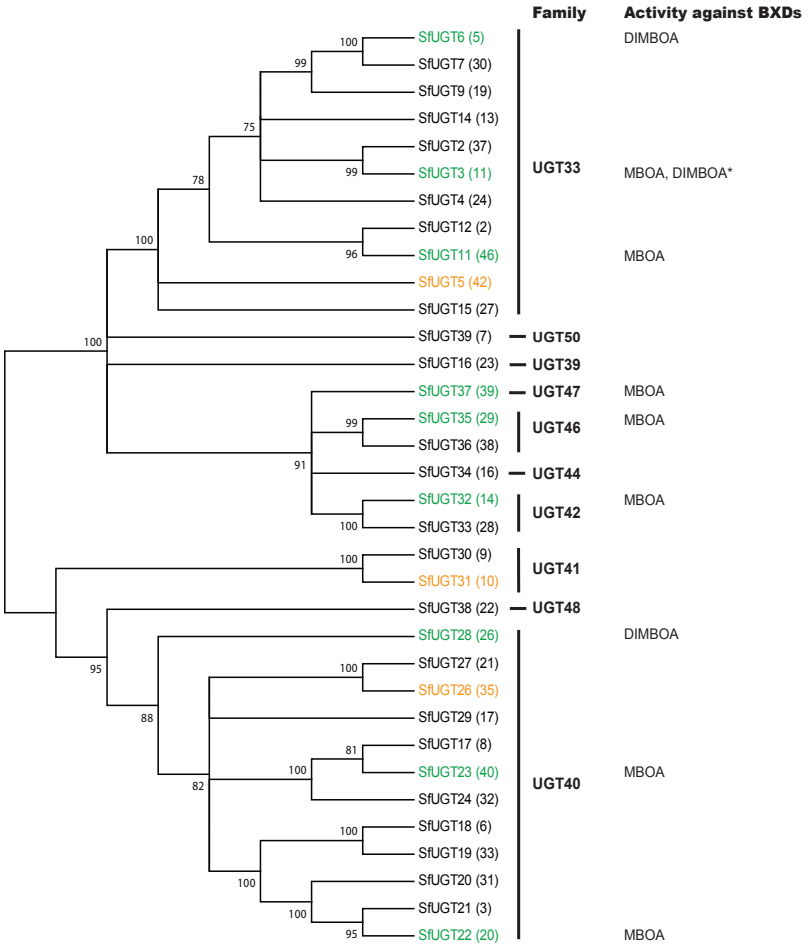

Figure 7: Phylogenetic tree of heterologously expressed and functionally characterized *S. frugiperda* UGTs. Based on phylogenetic studies previously performed for SfUGTs [54], the seven UGT candidates, expressed and functionally characterized in this study, were assigned to their corresponding UGT families. Official SfUGT nomenclature was adopted from [54] and the nomenclature used in this study are shown in parenthesis. Protein sequences were aligned using the ClustalW algorithm [72] a consensus phylogenetic tree was constructed using the Neighbor-joining method [78]. Distance calculation were performed using p-distance method [79] and bootstrap analysis (1000 replicates) [80]. Branches corresponding to partitions reproduced in less than 70% bootstrap replicates are collapsed. The percentage of replicate trees in which the associated taxa clustered together are shown next to the branches. All SfUGTs with ability to glucosylate DIMBOA and/ or its major degradation product MBOA are highlighted in green. Newly expressed proteins with no detected BXD activity are highlighted in orange. * - Unlike other DIMBOA-conjugating enzymes, this enzyme forms the plant-derived (2*R*)-DIMBOA-Glc.

6.2 Comparison of the relative expression of five bezoxazinoid-glucosylating SfUGTs among five different tissues

To determine the relative expression levels of five previously characterized BXD-conjugating glycosyltransferases (SfUGTs 5, 11, 14, 20 and 29) [54] in five different *S. frugiperda* larval tissues (gut, Malpighian tubules, testes, fat bodies and cuticle), quantitative real-time PCR (qPCR) analysis was performed. The Brilliant III SYBR® qPCR system (Agilent Technologies) used in this study includes the fluorescent dye SYBR Green that specifically intercalates between the DNA bases of double-stranded DNA that is formed during PCR amplification on the single-stranded cDNA template [81]. By measuring the fluorescence at the end of each amplification cycle the amount of PCR product that had been amplified in each cycle can be determined. As mean for quantification of the starting target concentration the CP value, also referred to as Ct value (crossing point or threshold cycle, respectively) is used. This value represents the number of PCR cycles needed to reach a defined fluorescence signal. At the crossing point the same amount of synthesized DNA is present in all reaction tubes. As during a PCR reaction DNA is doubled after every PCR cycle, higher starting concentrations of cDNAs encoding the gene of interest lead to lower CP values [61].
As the intercalating dye interacts with any double-stranded DNA it is necessary to use highly specific and efficient primers. For this reason all primers were tested prior to use for the actual qPCR analysis.

6.2.1 Validation of the designed qPCR primers

Primers were designed according to the requirements for quantitative PCR analysis [82] (see paragraph 5.9.1). To confirm the specificity to their respective target gene, melting curves and sequence of the respective amplicons were analyzed and the amplification efficiencies were determined, for every primer pair separately. Therefore, a qPCR reaction was conducted using a pool of all cDNA samples from all tissues as template (see paragraph 5.9.2, table 1).
Melting curve analysis was conducted in the end of each qPCR run by slowly heating the PCR reaction from 50 to 95 °C. During the denaturation of the double-stranded PCR products SYBR Green is released what leads to reduction of the fluorescence signal which is detected [61]. The resulting melting temperature depends on the length and base composition of the PCR product and hence can detect potential issues, as the formation of primer dimers, genomic DNA contamination or mis-annealling of the primers. Additionally, the PCR products were analyzed by agarose gel electrophoresis, isolated and cloned into the pCR^{TM}4-TOPO® sequencing vector for subsequent Sanger sequencing.
Both, melting curve analysis and gel electrophoresis confirmed the formation of only one PCR product with expected amplicon sizes between 100 and 150 bp (see paragraph 9.2.1, table S1), indicating that the designed primers were specific for their respective target gene. Analysis of the amplicon sequences obtained by Sanger sequencing of up to 15 colonies per amplicon confirmed these results.

All analyzed sequences were identical to the expected amplicons, only for SfUGT11 one SNP was observed, a transition of T(83)C which did not change the encoded amino acid.
To exclude potential contamination of the cDNA samples or primer stocks with genomic DNA, a no reverse transcription (-RT) control using pooled RNA samples was analyzed under equal qPCR conditions. As no amplification was observed, the absence of genomic DNA was confirmed.
Another parameter influencing qPCR analysis is the amplification efficiency of the primers. A PCR reaction with an ideal effiency of 100% leads to the exact doubling of the starting template concentration after every cycle ($c = c_0 \cdot 2^n$). Inhibitory effects (contaminants in the cDNA samples) or unspecific binding and the formation of primer dimers lead to the decrease or increase of amplification efficiency and thus to less reliable qPCR results [61]. For this reason the efficiencies of the used primer pairs were determined as described in paragraph 5.9.3. All determined amplification efficiencies were between 99 and 109%. To ensure comparability between PCR assays, the calculated amplification effiencies were subsequently included in the calculation of the relative expression of the target genes using the $2^{\Delta\Delta CP}$ method [62].

6.2.2 Selection of the best housekeeping gene

When comparing the gene expression between different cDNA samples it is important to consider experimental variations, such as the amount and quality of the starting material, and the efficiencies of RNA extraction and reverse transcription. For this reason, accuracy of qPCR analysis relies on the normalization to an internal control RNA, the housekeeping gene [64]. Requirements for a suitable housekeeping gene are that it should be stably expressed in all analyzed tissues showing minimal variability in the expression between samples. As the expression of commonly used internal standards can vary due to various factors depending on the experimental conditions [83], appropriate validation of housekeeping genes in any new experimental system is necessary. Various comparative approaches for housekeeping gene validation have been developed, including the statistical algorithms of BestKeeper [84], geNorm [85] and Normfinder [86], and the comparative ΔCt method [64].
In this study, five candidate reference genes previously used for *Spodoptera spp.* [63], the elongation factor 1 alpha (EF1α), glyceraldehyde-3-phosphate dehydrogenase (GAPDH), ribosomal protein L10 (RPL10), ubiquinol-cytochrome c reductase (UCCR), and arginine kinase (AK), were evaluated for their suitability as normalization genes. Using the comparative ΔCt method [64], the stability of expression values of the tested candidate genes was analyzed among 15 cDNA samples. This approach compares the relative expression of 'pairs of genes' within each sample. If the ΔCt value between the two genes remains constant in different samples, both genes are assumed to be stable. If the ΔCt fluctuates, one or both genes are variably expressed. Pairwise comparison of the ΔCt values of all putative housekeeping genes reveals which pairs show less variability and thus which genes are stably expressed among the tested samples. In this way, the examined genes can be ranked by their stability and the best suitable housekeeping gene(s) showing the lowest standard deviation of ΔCt values can be selected.
In figure 8 the pairwise comparisons of the complete set of the five housekeeping genes tested

among 15 different cDNA samples are shown. It is clearly visible that comparisons including the genes UCCR and AK led to high standard deviations of the expression among all tissue samples (average StdDev 3.29 and 3.50 respectively), whereas GAPDH, RPL10 and EF1α showed decreased variability (average StdDev of 1.91, 2.09 and 2.13, respectively), indicating that expression of these genes is more stable. Finally, rankings (from most to least stable gene) are as followed: GAPDH > RPL10 > EF1α > UCCR > AK. As GAPDH showed the least variability among all 15 cDNA samples tested, it was selected as reference gene to normalize the expression levels of the SfUGTs.

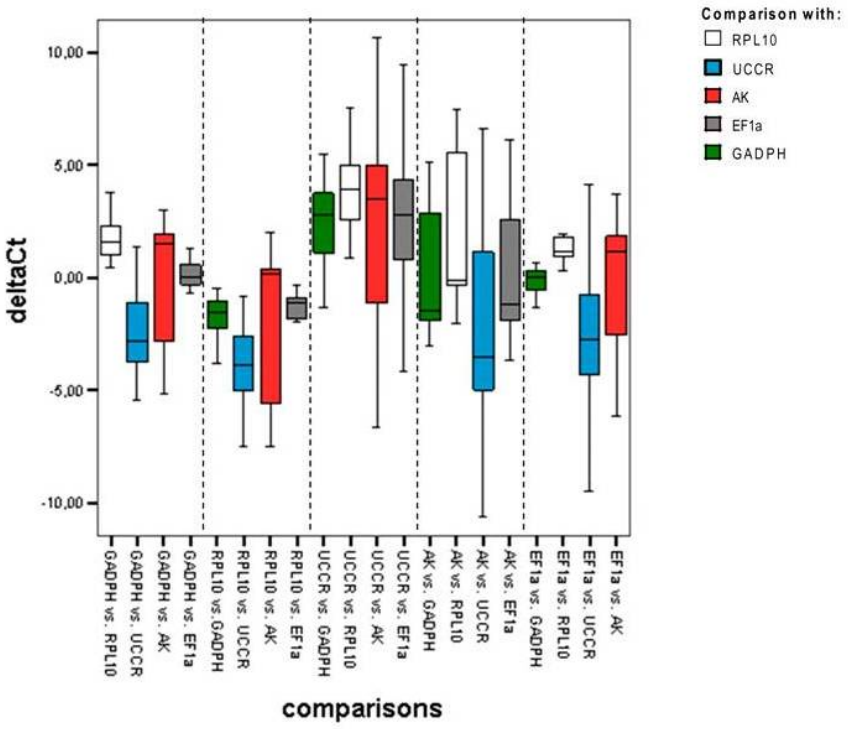

Figure 8: $\triangle$Ct method for housekeeping gene selection. [64]
Boxplot chart for the demonstration of the variability of $\triangle$Ct values in housekeeping gene comparisons among 15 *S. frugiperda* tissue-specific cDNA samples. Illustrated are the median (lines), 25^{th} to 75^{th} percentiles (boxes) and the data range from minimum to maximum (whiskers).

6.2.3 Relative quantification of the expression using the $\Delta\Delta$Cp method

After primer validation, expression levels of the respective target genes were relatively quantified using the $2^{\Delta\Delta CP}$ method described by Livak et al. [62]. In this method the quantification of gene expression is determined by normalization of the expression of the gene of interest to a stably expressed housekeeping gene. The expression levels of five SfUGTs among five tissues were calculated relative to the previously selected reference gene GAPDH as described in paragraph 5.9.4. The obtained expression levels were then compared to specific glucosylation activities towards DIMBOA and MBOA observed among the five tissues in enzyme activity assays performed by Felipe Wouters [54].

For the gene encoding the DIMBOA-glucosylating enzyme SfUGT5 highest expression was observed in the gut tissue, followed by intermediate expression in Malpighian tubules and low expression in fat bodies, cuticle and testes. The same pattern was observed for DIMBOA-UGT activities detected in the respective samples (figure 9, A). Since the obtained expression data for SfUGT5 did not meet the prerequisites for a variance analysis (ANOVA) (variance equality), a Friedman variance analysis on ranks was performed, revealing a statistical difference in the expression levels among tissues (see paragraph 9.9.4). Due to the low replicate number (N = 3), it was not possible to determine which specific tissues differ from each other, using a post hoc test. However, the considerably higher values for median and 75% percentile in the gut compared to other tissues suggest that this tissue is responsible for the difference observed in the variance analysis on ranks.

The four genes encoding for MBOA-glucosylating enzymes SfUGTs 11, 14, 20 and 29 (figure 9, B 2 - 5) show different expression patterns. All four genes showed expression in fat bodies. However, whereas SfUGTs 14 and 20 showed highest expression in fat bodies, SfUGTs 11 and 29 were most highly expressed in the testes. For all genes very low expression in both cuticle and gut tissue were observed. Intermediate expression in Malpighian tubules was detected for SfUGT20. Accordingly, also the tissue-specific UGT activity towards MBOA was distributed among the five tissues (figure 9, B 1), indicating that different enzymes contribute to overall MBOA metabolism in the insect. The highest activity was observed in fat bodies which was only slightly higher compared to testes and Malpighian tubules. Lower activity was detected for cuticle and gut. However, the observed differences in the activities towards MBOA among tissues were not statistically significant (see paragraph 9.9.4).

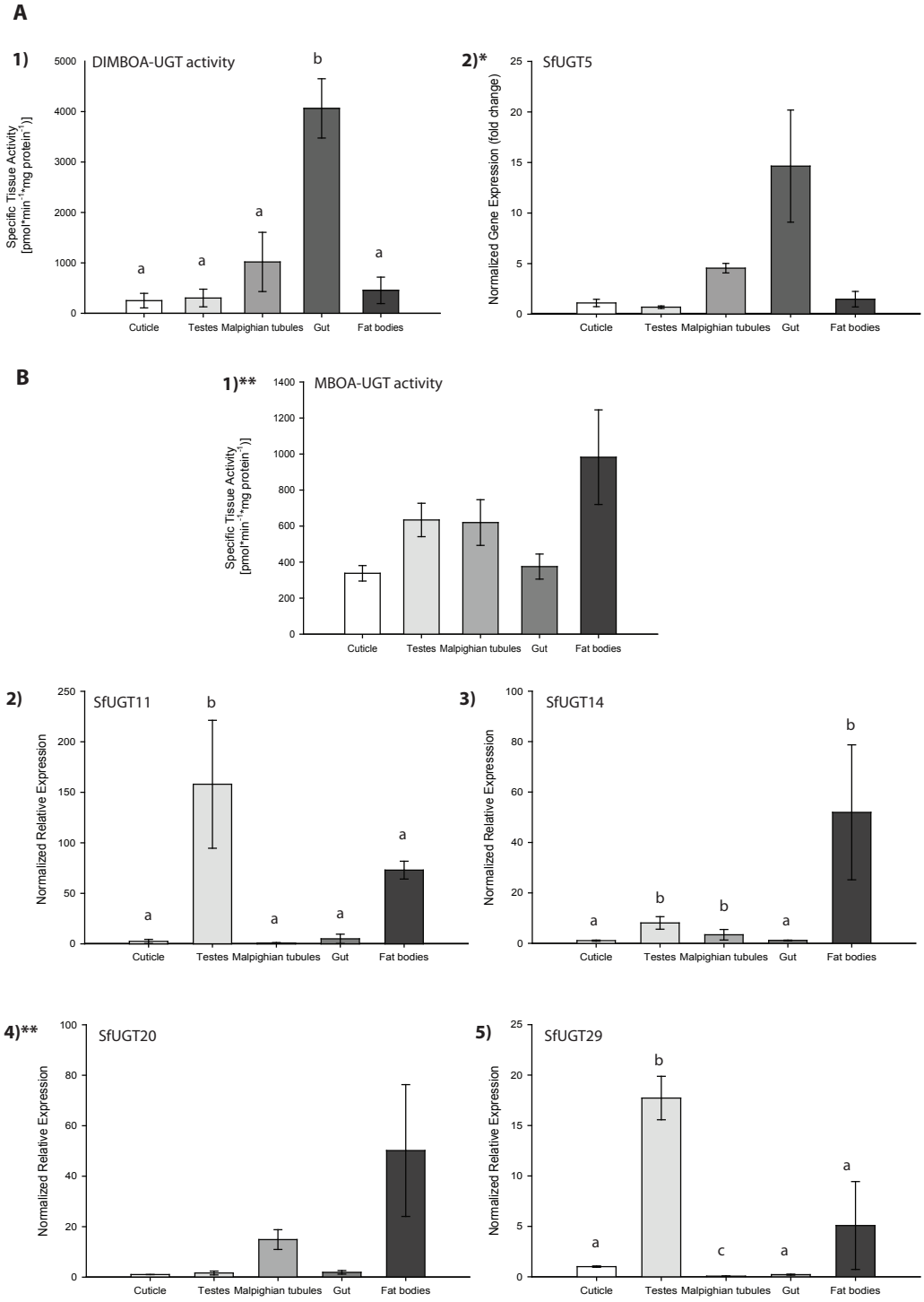

Figure 9: Relative expression of five SfUGTs and specific tissue glucosyltransferase activity against BXDs among five different *S. frugiperda* tissues.

A - shows the tissue-specific glucosyltransferase (UGT) activity towards DIMBOA (**1**) and relative expression levels of the corresponding gene encoding the DIMBOA-glucosylating enzyme SfUGT5 (**2**). **B** - shows the expression levels of four genes encoding MBOA-glucosylating SfUGTs 11, 14, 20 and 29 (**2**-**5**) and summarizes tissue-specific activities observed against MBOA (**1**). Statistical differences shown by variance analysis (ANOVA) and subsequent post hoc test are incated as small letters (a - c). * - Friedman Repeated Measures Analysis of Variance (ANOVA) on Ranks shows a significant difference in the expression levels between different tissues (P = 0.043). ** - One-way Repeated Measures ANOVA shows no significant difference in expression levels among tissues.

6.3 Substrate screening for the evaluation of substrate specificities for five BXD-glucosylating SfUGTs

6.3.1 Microsome extraction and adjustment of SfUGT amounts used for enzymatic assays

To evaluate the substrate specificities of benzoxazinoid-conjugating SfUGTs, stably transfected High Five™ cells expressing DIMBOA-glucosylating SfUGT5 or MBOA-glucosylating SfUGTs 11, 14, 20, 29, provided as frozen DMSO stocks by Felipe Wouters [54], were resurrected and cultured in Express Five® SFM containing 10 μg/ml blasticidin. As insect glucosyltransferases are known to be membrane-bound ER proteins [38,42], the microsomal fractions were extracted to enrich the UGT contents of protein extracts. Equal amounts of total protein of both, microsomal and cytosolic fractions were analyzed by SDS-PAGE following western blot. As described in paragraph 5.20, detection of recombinant UGTs, possessing a V5 epitope, were detected via binding of a specific V5-antibody, coupled to the horseradish peroxidase (HRP) enzyme, and subsequent chemiluminescence protein detection using the substrate luminol. Whereas the cytosolic fractions showed very low to no recombinant protein, high amounts of the expressed recombinant SfUGTs were present in the microsomal fractions, confirming their localization in the ER (figure 10). As the luminescence signal can be correlated to the amount of expressed protein, expression levels of recombinant UGTs can be estimated. Comparing the signal intensities, SfUGT5 showed highest expression, followed by SfUGTs 14, 20 and 29 with intermediate expression levels and SfUGT11 with the lowest expression in High Five™ cells. As expected, no protein was detected in non-transfected cells (NTC).

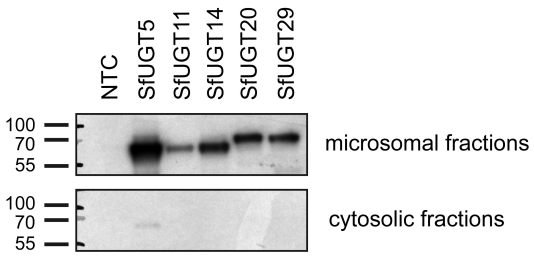

Figure 10: Western blot analysis of the successful expression of SfUGTs in High Five™ cells.
Equal amounts of total protein (10 μg from cytosolic and microsomal extracts of SfUGT-transfected cells were analyzed by SDS-PAGE and recombinant proteins possessing the V5 epitope were detected by western blot using a V5-specific antibody. PageRuler Plus Prestained Protein Ladder (Thermo Scientific) served as protein molecular weight standard.

To compare the activity of SfUGTs in the microsomal extracts, it was crucial to equalize the amounts of heterologously expressed SfUGTs used for subsequent enzymatic assays. Therefore, protein amounts of all UGTs were normalized to the protein showing the lowest signal in western blot, SfUGT11. Following the approach of Krempl et al. [70], different total protein amounts from microsomal extracts were analyzed by SDS-PAGE and subsequent western blot, the signal intensities of all proteins were determined and extrapolated to the protein amounts applied for SfUGT11. Factors were calculated which correspond to the x-fold amount of total protein needed to obtain the same amount of recombinant protein as for the reference protein SfUGT 11. The factor for the reference protein was set to 1. Applied total protein amounts and calculated factors are shown in figure 11.

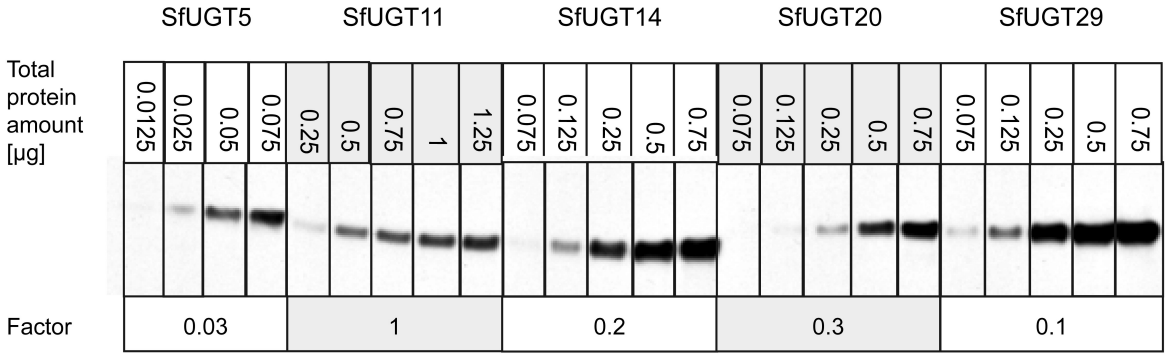

Figure 11: Estimation of the amounts of recombinant SfUGTs in microsomal fractions from transfected insect cells. Using ImageLab^{TM} software band intensities on the western blot were measured and resulting peak areas were extrapolated to the total protein amounts used for the reference protein SfUGT11, as different amounts of total protein amounts were used for the different SfUGTs to avoid saturation of the luminescence signal. The area of the reference protein was divided by the area of all other SfUGTs and obtained factors were averaged over all protein amounts used. The resulting factors represent the estimated expression levels relative to each other, with the reference protein set to 1.

6.3.2 Screening of SfUGTs against 20 different substrates

To further characterize the BXD-conjugating SfUGTs 5, 11, 14, 20 and 29 regarding substrate specificity, these enzymes were screened for their activity towards 20 structurally diverse substrates. The tested substrates belong to various chemical groups, including benzoxazinoids, mono-, di and trisubstituted phenolic compounds, terpenoids, flavonoids and coumarins and were chosen on the basis of previously reported glycosylation activities in other insect species. In order to guarantee comparability between the tested SfUGTs, the used total protein amounts of microsomal extracts were adjusted according to their calculated relative expression levels determined by western blot (praragraph 6.3.1). As observed in previous studies [38, 70], working with insect cultures for the expression of recombinant UGTs led to a considerable amount of glucosylation activity by endogenous glucosyltransferases. For this reason, a control consisting of a crude microsomal extract from non-transfected cells with the same total protein amount was prepared for each UGT, separately.

Results of the substrate screening are illustrated in two bar charts per tested substrate (see supplement, paragraph 9.7, figure S1). The first chart (left) compares the product formation of each UGT-transfected microsomal fraction (UGT, gray bars) to the UGT activity observed for the corresponding total protein amount of the non-transfected control (NTC, white bars), based on Student's t-test. The second chart (right) shows the net amounts of glucosides formed by the recombinant UGT, resulting from the subtraction of the NTC activity (UGT-NTC). An approach to rank SfUGTs by activity based on variance analysis (ANOVA) of the net amounts of glucosides formed by UGT-transfected microsomal extracts is summarized in table 3. For a comparison of substrate specificities within one enzyme a subset of the substrates which could be directly quantified by external standard curve was analyzed (table 4).

The five tested SfUGTs catalyzed the glucosylation of a wide range of compounds, belonging to all chemical groups included in the analyses. The four SfUGTs known for their capability to conjugate MBOA, showed activity towards diverse compounds, mostly phenol-derived compounds and benzoxazinoid-related compounds. SfUGT 11 catalyzed the glucosylation of a total number of 16 substrates, showing moderate to high activity towards 12 compounds. Similarly, SfUGT20, SfUGT29 and SfUGT14 showed moderate to high activities towards 4, 8 and 9 aglucones among their total accepted substrates (7, 10 and 9), respectively. In contrast, SfUGT 5 catalyzed the glucosylation of 6 compounds in total, showing moderate to high activity towards only three BXD-related compounds, IAA, DIMBOA and HMBOA. This indicates that SfUGT5 is more specific towards BXDs compared to the other enzymes. Comparing the substrate specificity within one enzyme for a subset of substrates confirms the latter. SfUGT5 produced major amounts of BXD-glucoside, and only minor amounts of phenolic glucosides. In contrast, SfUGTs 11, 14, 20 and 29 show higher selectivity for phenolic compounds, even though they show differences in their main products. The best tested substrates for each enzyme were: 4-nitrophenol for SfUGTs 11 and 20, salicyl aldehyde for SfUGT14, and esculetin for SfUGT29. The amounts of MBOA-glucoside were comparably low for all four SfUGTs. However, SfUGT14 seems to be more selective for MBOA than the other enzymes (MBOA-glucoside amounts represented 25% of the most efficiently formed product). None of the enzymes was able to conjugate *L*-tyrosine, *L*-DOPA and dopamine under our assay conditions. On the other hand, esculetin and *p*-nitrophenol were conjugated by all enzymes.

Table 3: Comparison of the glucosylation activities among five benzoxazinoid-conjugating SfUGTs towards 20 substrates of various chemical structures. SfUGTs were ranked based on ANOVA analysis of the net amounts of glucosides produced by UGT-containing microsomal extracts (UGT) after subtraction of the amount produced by corresponding amounts of non-transfected controls (NTC). When glucoside formation of the UGT did not differ from the NTC, according to the significance level obtained from Student's t-test, the UGT was considered as not active (-), even if a low net glucoside amount remained after subtraction. Low activity (1) was related to the enzyme(s) showing the lowest net amounts of glucosides formed, whereas highest activity (3) corresponds to the enzyme(s) forming the highest net amounts. Moderate glucosylation activity (2) was considered for all enzymes forming an intermediate amount of glucosides in between the highest and lowest amounts observed.

	SfUGT5	**SfUGT11**	**SfUGT14**	**SfUGT20**	**SfUGT29**
Benzoxazinoid-related					
Indole	-	3	-	-	-
IAA	3	1	-	-	-
BOA	-	2	3	-	2
6-OH-BOA	-	2	2	-	3
MBOA	-	1	3	1	2
DIMBOA	3	1	-	-	-
HMBOA	3	1	-	-	-
Phenolic compounds					
4-nitrophenol	1	3	2	2	2
1-naphthol	-	2	2	1	-
Salicyl aldehyde	-	-	3	-	-
Vanillin	1	3	-	-	2
Catechol	-	2	3	-	2
L-Tyrosine	-	-	-	-	-
L-DOPA	-	-	-	-	-
Dopamine	-	-	-	-	-
Flavonoids					
Quercetin	-	3	2	1	1
Terpenoids					
Menthol	-	3	-	2	1
Gossypol	-	2	-	2	-
Coumarins					
Esculetin	1	2	3	1	2
Alkaloids					
Capsaicin	-	3	-	2	2
Active against x substrates	6	16	9	7	10

Table 4: Comparison of substrate specificities for a subset of compounds with available external standards. Product formation was quantified using an external standard curve using authentic glucoside standards. Observed product formation (in %) for one substrate was determined relative to the main product of the respective enzyme (100%).

	SfUGT5	**SfUGT11**	**SfUGT14**	**SfUGT20**	**SfUGT29**
MBOA	-	0.2%	25%	3%	4%
DIMBOA	71%	2%	-	-	-
HMBOA	100%	4%	-	-	-
4-nitrophenol	2%	100%	12%	100%	56%
Salicyl aldehyde	-	-	100%	-	-
Esculetin	1%	14%	58%	90%	100%

6.3.2.1 *In vitro* assays with substrates possessing multiple potential glucosylation sites

For some substrates which possess several putative glucosylation sites, the formation of more than one glucosylation products was observed, namely for 6-OH-BOA, quercetin and gossypol. These products were considered as monoglucoside isomers as they showed the same mass but different retention times. Diglucoside formation was not detected (see paragraph 9.4, table S5). For 6-OH-BOA two products (a and b) were detected, possibly one *N*- and one *O*-glucoside (see figure 12). However, product a (white bars) was formed in equal amounts by non-transfected controls and UGT-containing microsome fraction (confirmed by t-test), suggesting that it is produced by endogenous UGTs of the host insect cells. In contrast, the second glucoside (product b, gray bars) seems to be formed by the expressed SfUGTs as low to no activity was observed for the NTC (depending on the used total protein amount).

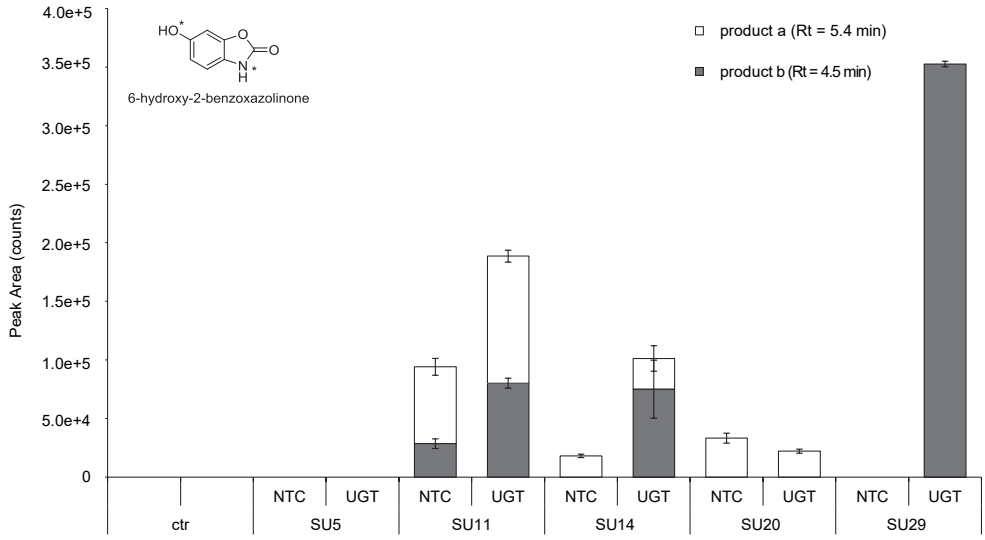

Figure 12: Comparison of the formation of isomers formed during the glucosylation of 6-OH-BOA.

For quercetin, 3 products were detected, the isomers 1 to 3 (see figure S2). As standards for two potential glucosylation products, the 3-*O*-glucoside isoquercitrin (1) and 4'-*O*-glucoside spiraeoside (2) were available, their retention times were compared to the products formed during enzymatic assays (see figure S2). Using this approach, it was shown that all SfUGTs and non-transfected controls (NTC) formed isoquercitrin. When comparing the amounts of each glucoside isomer formed (see figure 13), SfUGT5 formed equal amounts of isoquercitrin as its NTC. Student's t-test analysis confirmed that SfUGT5 is not active towards quercetin ($P = 0.068$). All other enzymes formed considerably higher amounts of isoquercitrin compared to their control (confirmed by t-test, $P < 0.001$ for SfUGTs 11 and 14, $P = 0.011$ for SfUGT20, $P = 0.003$ for SfUGT29) with SfUGT11 showing the highest activity. Spiraeoside was produced by SfUGTs 11 and 20, whereby higher amounts were formed by SfUGT11. In addition, one more isomer was detected, isomer 3, formed by SfUGTs 14 and 29 with SfUGT14 showing higher activity. Moreover, when analyzing the peak corresponding to isoquercitrin in the assays (figure

S2), it was observed that two peaks might be present (for instance in assays of SfUGT11) that might be the result of two overlapping structures with similar polarity. The peak corresponding to the product of SfUGT29 is also slightly different compared to the isoquercitrin standard indicating that it might be in fact another isomer.

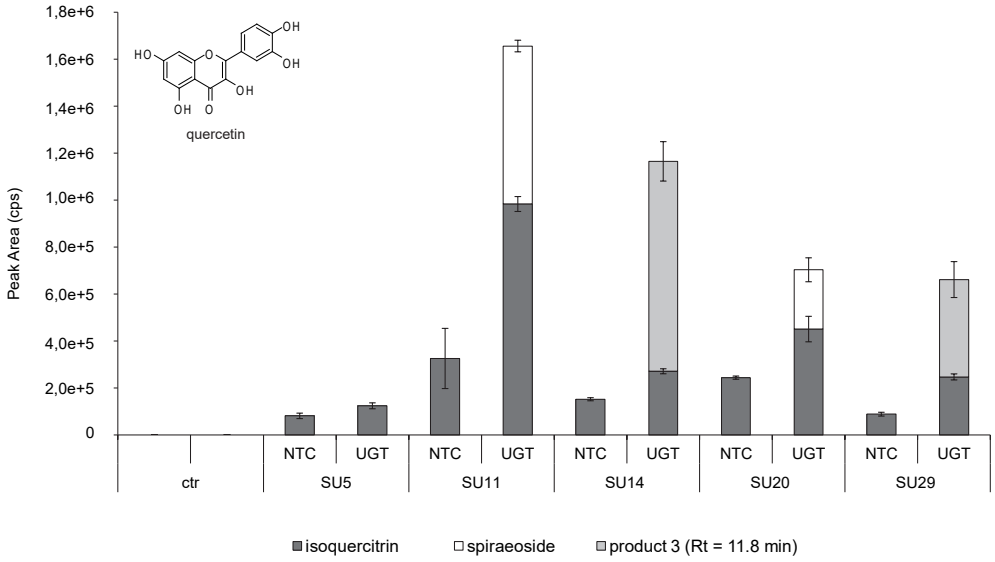

Figure 13: Comparison of the formation of isomers formed during the glucosylation of quercetin.

For gossypol, the formation of 3 different monoglucosides was observed (see figure S3). Two enzymes, SfUGT11 and SfUGT20, showed activity towards gossypol but slightly different specificities. SfUGT11 formed 2 products, isomers 2 and 3 with 96% of the total glucoside amount formed represented by isomer 3 and only approx. 4% by isomer 2. However, as the signal to noise (S/N) ratio was at the detection limit (S/N = 3), no accurate quantification of isomer 2 was possible. SfUGT20 also formed isomer 3 however the amount formed was $\sim$ 4-fold lower compared to SfUGT11. The main product of SfUGT20 was isomer 1 which represented 60% of the glucoside amount formed by this enzyme. No endogenous activity towards gossypol in non-transfected cells was detected.

6.4 Studies of the importance of catalytic histidine H35 for the substrate specificity of SfUGTs

Based on the comparison to reported crystal structures of plant UGTs [87, 88] it is suggested that two highly conserved residues in the N-terminal domain of the protein, H35 and D151, are involved in catalysis of sugar conjugation with an aglycone [77]. Interestingly, UGT2B10 where H35 is substituted with a leucine, unlike other human UGTs, lacks the ability to glucuronidate phenolic compounds and, in contrast, seems to be selective for the conjugation of tertiary amines [66]. Mutational analyses of UGT2B10 have shown that by substituting L35 (L34 in the respective protein sequence) with a histidine, the *N*-glucuronidation activity towards nicotine and cotinine is completely abolished whereas *O*-glucuronidation activity is gained to-

wards phenolics as 1-naphthol and 4-methylumbelliferone [67].
Multiple alignment (see figure 6) of the protein sequences of SfUGTs 5, 11, 14, 20 and 29 revealed that also the studied SfUGTs possess the catalytic H35 (H37 in the alignment) and D151(D149 in the alignment). To study the importance of histidine for catalysis of *O*- and *N*- and putative *S*-glucosylation we performed site-directed mutagenesis of the catalytic residue H35 in SfUGTs 5 and 29, known for their capability to glucosylate DIMBOA or MBOA. Wild-type and mutant enzymes were tested for their activity towards the simple exogenous phenolics 4-nitrophenol and 1-naphthol, the thiol thiophenol as well as the benzoxazinoids DIMBOA, MBOA and HMBOA. In addition quinine, an alkaloid that contains two tertiary amines, was tested to analyze if the substitution of H35 by leucine has an effect on the selectivity of the enzyme for tertiary amines as observed for human UGT2B10.
To compare the activity of the wild type enzymes (SfUGT5 and 29) to their respective site-directed mutants (SfUGTs 5_mut and 29_mut) in enzymatic assays the total protein amounts of micorosomal fractions had to be adjusted as already described in paragraph 6.3.1. In a first SDS-PAGE equal amounts of all proteins were applied and SfUGT5_mut was determined as the protein showing the lowest expression (data not shown). Thus, factors were calculated to normalize all total protein amounts to SfUGT5_mut. The protein amounts applied in western blot and relative expression levels calculated after the determination of the peak intensitites are shown in figure 14. Crude microsomal extracts from non-transfected cells with the same total protein amount were prepared for each UGT.

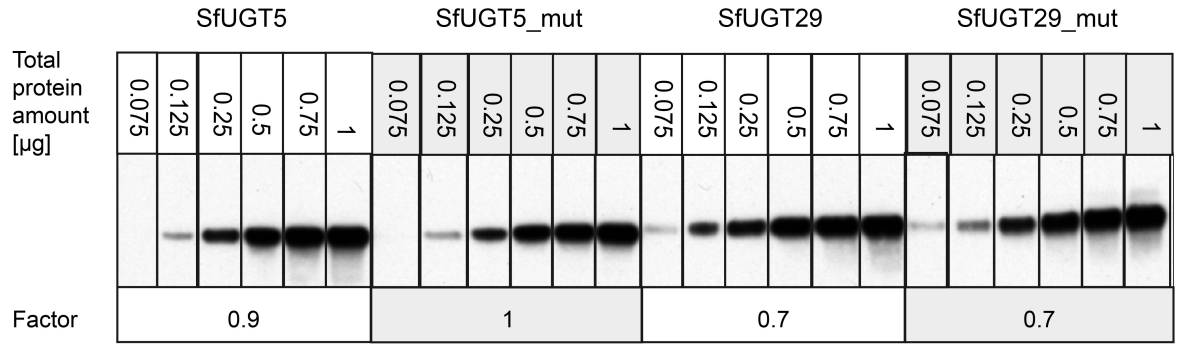

Figure 14: Estimation of the amounts of recombinant SfUGTs in microsomal fractions from transfected insect cells for two SfUGTs and their respective H35L mutants. Using ImageLab^{TM} software band intensities on the western blot were measured and resulting peak areas of the reference protein were divided by the area of all other SfUGTs. The averaged factors over all protein amounts used represent the estimated expression levels of the SfUGTs relative to each other, with the reference protein set to 1.

Glucoside formation was observed for all tested substrates, except of the tertiary amine quinine which was conjugated by none of the enzymes (data not shown). To compare the glucosylation activity towards the other substrates between the different enzymes, the net glucoside formation was calculated by subtracting the glucoside amount formed by endogenous UGTs from the host strain from the total glucoside amount formed by the UGT-transfected cells (see figure 15). The raw data, including the total amounts of glucosides formed by UGT-containing microsomes

and their respective NTC are shown in the supplement, paragraph 9.8, figure S4. Differences between NTC and UGT activity were tested using Student's t-test. Figure 15 clearly shows that the high activity towards DIMBOA and HMBOA observed for wild type SfUGT5 was completely abolished in the H35L mutant SfUGT5_mut. The same effect was observed for SfUGT29 towards MBOA and thiophenol. SfUGT5 did not lose activity towards 4-nitrophenol after mutation whereas SfUGT29 activity towards 4-nitrophenol was abolished. However, activity of SfUGT5 was already very low in the wild type showing that the enzyme has only low specificity for this substrate. The H35L mutant of SfUGT5 produced 80% more 1-naphthylglucoside than the respective wild type. Also the SfUGT29 mutant activity towards naphthol was not completely abolished, but the mutant enzyme retained an activity of 25% of the respective wild-type activity.

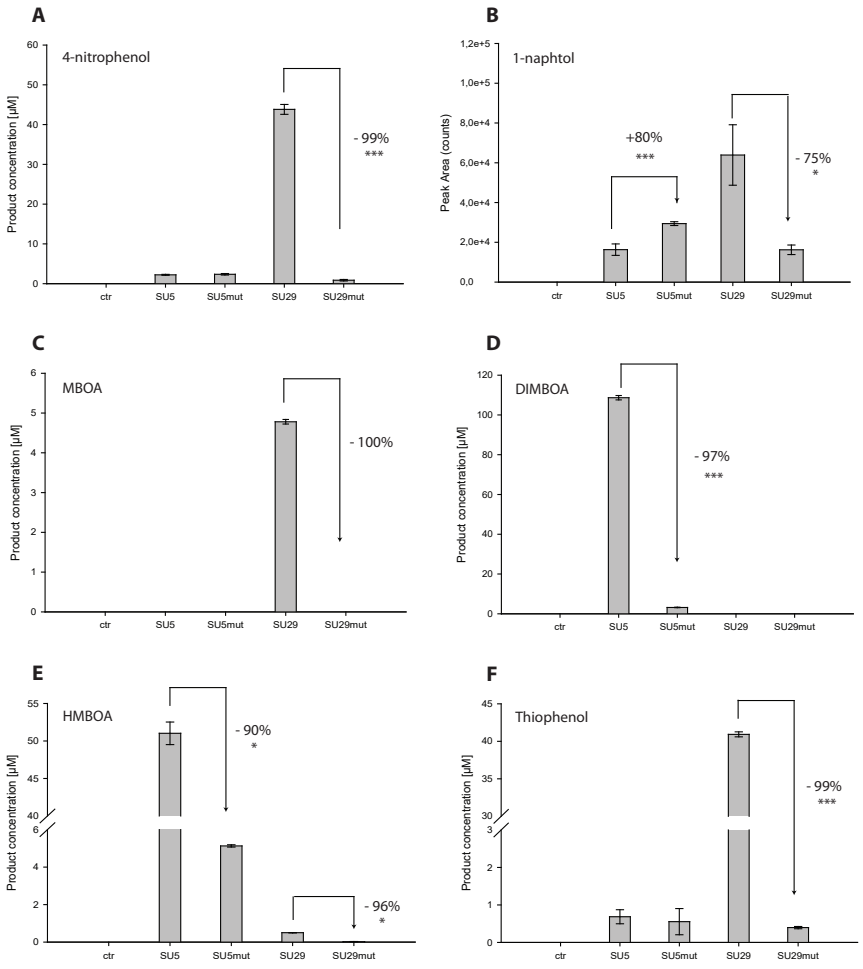

Figure 15: Mutational analysis of the importance of the catalytic H35 in UGTs from *S. frugiperda*. The net amounts of glucosides formed by SfUGT-containing microsomes extracted from transfected insect cells are illustrated as mean ± standard error of three replicate determinations. Net glucoside amounts were calculated via subtraction of the glucoside amounts formed by non-transfected controls from the total amount of glucosides formed by UGT-transfected cells. Total protein amounts were adjusted according to the calculated relative expression levels via western blot. Differences between the net glucoside formation of mutant UGTs (SfUGT_*mut*) and their corresponding wild type (SfUGT) were analyzed via Student's t-test. Results are indicated by asterisks (* - $P < 0.05$, **- $P < 0.01$, *** - $P < 0.001$). Gain or loss of activity in the mutant protein compared to the wild type is given in %.

7 Discussion

7.1 SfUGTs are widely expressed among *S. frugiperda* larval tissues

Previous analysis of tissue-specific activities towards DIMBOA and MBOA suggested that there is no difference in the expression levels of genes encoding DIMBOA or MBOA-detoxifying enzymes between larvae feeding on artificial diet and on maize leaves [54]. Recent studies comparing the transcriptome levels in the midgut of *Spodoptera* spp. 3rd instar larvae feeding on artificial diet and on maize leaves enforced this observation: the expression levels of UGT-encoding genes were not altered considerably between the two treatments [89]. Accordingly, UGTs are not induced upon toxin ingestion when feeding on maize leaves but are suggested to be expressed constantly in the insect.

As no diet-dependent induction of UGTs was observed in previous studies, we decided to analyze if there are differences in basal UGT expression levels between larval tissues. Therefore, we compared the tissue-specific expression levels of five reported DIMBOA- and MBOA-conjugating SfUGTs [54] in *S. frugiperda* larvae feeding on artificial diet.

Expression analysis by quantitative real-time PCR of SfUGT5 to 29 suggested that these enzymes are widely expressed in 3rd to 4th instar *S. frugiperda* larvae (figure 9). However, there are differences in the expression profiles of individual UGTs: SfUGT5, known for its ability to glucosylate DIMBOA, is predominantly expressed in the gut tissue with moderate expression in Malpighian tubules whereas the four MBOA-glucosylating enzymes SfUGTs 11, 14, 20 and 29 are mainly expressed in fat bodies and testes. In contrast, very low to no expression is observed in the cuticle. The expression profile of SfUGT5 (figure 9, A) strongly supports its potential function in detoxification, since the gut tissue and Malpighian tubules (plus fat bodies) are the main detoxification-related tissues [42]. This expression profile is also consistent with the observed tissue-specific activities towards DIMBOA where the highest glucosylation rate was found in the gut, followed by Malpighian tubules.

Activity towards MBOA was similar among all five tested tissues, suggesting that expression of the four MBOA-detoxifying UGTs is distributed throughout the insect body. This is consistent with the differential expression profile obtained for MBOA-glucosylating SfUGTs (figure 9, B). Although all these four SfUGTs were expressed in the fat bodies, only SfUGT14 and 20 showed highest expression in this tissue. SfUGT20 was also moderately expressed in Malpighian tubules. However, very low expression was observed in gut and cuticle suggesting that the activity towards MBOA seen in these tissues might be provoked by other, not yet characterized UGTs. Interestingly, SfUGT11 and 29 were highly expressed in testes. Little is known about the role of insect UGTs in reproductive organs. In *M. sexta* ovaries and eggs, glucosyltransferase activity was observed towards the ecdysteroid 26-hydroxy-ecdysone (26E), which plays an important role in embryonic development [47]. In newly hatched eggs the 26E-glucose-conjugate was the major detectable ecdysteroid suggesting that glucosylation might play a role in the regulation of ecdysteroid hormone activity during and after embryogenesis. *In vitro* assays of SfUGTs 11 and 29 towards ecdysteroids might shed more light on the potential role in embryogenesis and is worthy of further study.

The observed tissue-specific activities towards MBOA can not be fully correlated to one specific enzyme which indicates that MBOA-detoxification is the result of the cooperation of several different UGTs widely expressed throughout larval tissues. In contrast, DIMBOA detoxification in gut and Malpighian tubules can be correlated to SfUGT5 expression levels detected in these tissues. In this study, three more MBOA-glucosylating SfUGTs and one additional DIMBOA-conjugating enzyme were expressed and functionally characterized (paragraph 6.1.2). Expression analysis of these enzymes might help to complete the picture of DIMBOA- and MBOA-metabolism in *S. frugiperda*.

7.2 SfUGTs show a broad substrate specificity towards xenobiotics and plant allelochemicals

To assess the potential importance and contribution of UGTs in the metabolism of exogenous as well as endogenous compounds in *S. frugiperda*, previously characterized, heterologously expressed BXD-conjugating SfUGTs were screened for their selectivities towards 20 structurally diverse compounds, mostly plant allelochemicals (paragraph 6.3.2). The *in vitro* screening revealed that the tested SfUGTs show a wide substrate specificity. Simple phenols, as e.g. nitrophenol and naphthol, a coumarin (esculetin) and flavonoid (quercetin), an alkaloid (capsaicin) and all tested benzoxazinoids were glucosylated by at least one of the tested enzymes. In contrast, there was no detectable conjugation of *L*-tyrosine, *L*-DOPA and dopamine, which are involved for example in cuticle melanization.

This capacity to bind and conjugate many different aglucones is also true for other insect UGTs: in *D. melanogaster* UGT activity towards the xenobiotics 4-nitrophenol and 1-naphthol as well as endogenous xanthurenic acid has been reported [90, 91]. Glucosylation of simple mono-, di-, and triphenols; phenolic acids, aldehydes and alcohols; and coumarins and flavonoids was observed in enzyme preparations of different tissues from *Manduca sexta* and four other insect species [51, 52]. Similar findings were reported for a previously performed screening of heterologously expressed *Bombyx mori* UGT BmUGT1 towards 38 diverse substrates revealing its capability to conjugate a total number of 16 different compounds, mainly phenol-derived compounds, including flavonoids (naringenin and quercetin), terpenoids (e. g. *S*-(-)-β-citronellol and (+)-isomenthol) and simple phenolic compounds (e. g. 4-nitrophenol and 1-naphthol) [53]. Beyond the acceptance of substrates from diverse structural groups, the size of tolerated substrates ranged from small compounds (as e.g. indole and 4-nitrophenol) to more complex structures as the sesquiterpene dimer gossypol. Only recently, Krempl et al. reported the heterologous expression and functional characterization of UGTs from two Heliothine moth species with ability to conjugate both, the simple phenol 1-naphthol and gossypol [70]. Also in various studies on human UGTs, the glycosylation of complex compounds, as the tetrapyrrole bilirubin, steroids and alkaloids was observed [92–94].

This broad substrate specificity might be due to the flexible three-dimensional structure of UGTs. It is well known, that human UGTs belong to the GT-B fold family [65, 77]. These enzymes consist of two $\beta/\alpha/\beta$ Rossmann-like domains which are connected by a short linker region. In

contrast to the GT-A fold, the two domains are less tightly associated and face each other to form a catalytical cleft [39]. In parallel, whereas the C-terminal UDP-sugar binding domain is conserved among UGTs, the N-terminal domain which is responsible for aglucone substrate binding, is highly flexible, especially in areas adjacent to the cleft formed by the two domains. This flexibility in the substrate-binding domain and the wide catalytic cleft formed in the GT-B fold may facilitate binding of various aglycones in orientation conducive to catalysis [38].
Moreover, the capability of both, *O*- and *N*-glucosylation and the formation of various isomers for substrates with several potential glucosylation sites was also observed. To my knowledge, the recently reported purification of MBOA-*N*-glucoside from the faeces [31] of *S. frugiperda* and identification of potential UGT enzymes responsible for its formation [54] is the only example for small molecule *N*-glucosylation observed in insects. However, studies on human UGTs reported the conjugation of primary, secondary and tertiary amines [95]; *in vitro* assays of heterologously expressed UDP-glucuronosyltransferase 1A3 showed that it is capable of both, *N*- and *O*-glycosylation [96].
Taking all results together, the *S. frugiperda* UGTs screened in this study are likely to be involved in detoxification responses upon ingestion of xenobiotics and plant allelochemicals, as they were able to conjugate a variety of phenolic compounds but did not show activity towards endogenous compounds, as described below. This is consistent with the expression of these enzymes in detoxification-relevant tissues.

7.3 SfUGTs form monoglucosides rather than diglucosides

During screenings of substrates with several potential glucosylation sites the formation of multiple products was observed (paragraph 6.3.2.1). After close examination of the analyte masses obtained by Iontrap-MS or MRM-analysis, these products were identified as monoglucoside isomers, mostly likely with the attached sugar on different positions. In contrast, no formation of diglucosides was detected. However, identification of diglucosides has already been reported for both, human and insect UGTs.
Heterologously expressed UGTs from the cotton bollworm *H. armigera* and tobacco budworm *H. virescens* formed mono- and diglucosides of gossypol [70]. The 3 observed monoglucosides were also detected in assays with SfUGTs 11 and 20 whereas no diglucoside formation was observed. Interestingly, Krempl et al. [70] reported the formation of gossypol diglucosides by endogenous UGTs of Sf9 cells. As this cell line was originally established from *S. frugiperda* [97], it seems reasonable to suggest that SfUGTs might also be able to catalyze this reaction. However, the amount of monoglucosides formed by SfUGTs 11 and 20 were comparably low in contrast to the remaining unconjugated gossypol (data not shown), suggesting that they are not very efficient in glucosylating gossypol. Also our assay conditions were slightly different, as we used a higher substrate to enzyme ratio and did not add metal ions as cofactor. In addition, we used a less sensitive mass spectrometer for detection (triple-quad MS API3200, compared to API5000) so small diglucoside amounts might have been missed due to the detection limit of the detection method.

Also in the metabolism of flavonoids, conjugation to glucose is known to be the predominant pathway in insects [98]. In previous studies, mostly monoglucosides have been observed [99,100] but also di- and tri glucosides of quercetin have been isolated from the cocoon shell of the silkworm *B. mori* [101]. In our experiments, the formation of 3 monoglucoside isomers of quercetin has been observed and two isomers were identified as the 3-*O*-glucoside isoquercitrin and 4'-*O*-glucoside spiraeoside by the comparison with authentic standards. Both are already reported plant metabolites: isoquercitrin is very abundant in many fruits and vegetables, and spiraeoside is found in high amounts in onions [102]. Both, flavonols and their respective glucosides widely occur in plants and play an important role as antioxidants and feeding deterrents towards insects [103]. In insects, flavonoids are reported to be sequestered to increase their fitness [104]. For example, various butterfly species, especially females, sequester flavonoids from their larval host plants to increase attractiveness to mate-searching males [105]. In grasshoppers, isoquercitrin, as a hydrolysis product of the diglucoside rutin, was shown to be excreted but also partly sequestered in the cuticle and is believed to provide protection against fungal infections [106]. Possibly, the glucosylation of quercetin by *S. frugiperda* UGTs might have a similar importance for sequestration or excretion of the flavonoid.

7.4 SfUGT5 seems to be specific for DIMBOA and HMBOA detoxifcation

Although all tested SfUGTs conjugate a variety of compounds, they seem to differ in their activity towards benzoxazinoids (BXDs). This was shown by the comparison of glucoside amounts formed for a subset of substrates which could be quantified using an external standard curve (paragraph 6.3.2, table 4). The SfUGTs known for their capability to glucosylate MBOA (SfUGTs 11, 14, 20 and 29) show higher activity towards phenolic compounds whereas the formed MBOA-glucoside amounts are comparably low for all UGTs. Additionally, these enzymes seem to have a flexible substrate binding site as they can form multiple isomers of substrates with several potential glucosylation sites (paragraph 7.3).
In contrast, SfUGT5 produces major amounts of BXD-glucosides (DIMBOA- and HMBOA-glucoside) but only minor amounts of phenolic glucosides. Comparing the total number of substrates conjugated (table 3), SfUGT5 is also the enzyme that accepts the least number of substrates. These results, along with its expression predominantly in the gut tissue of *S. frugiperda* larvae, indicate its potential importance for DIMBOA and HMBOA detoxification. Additionally, this enzyme stereoselectively glucosylates DIMBOA and HMBOA, forming the (2*S*)-*O*-glucosides [54]. This epimer of the plant-derived (2*R*)-*O*-glucoside was shown to be a major detoxification metabolite of DIMBOA in maize-fed *S. frugiperda* larvae, specially due to the altered stereochemistry of C2 [35].
DIMBOA is one of the most abundant and most toxic BXDs in aerial parts of maize, being the predominant BXD in young maize leaves, while HMBOA is predominant in older leaves [13]. Therefore, having a UGT with high specificity towards DIMBOA and HMBOA might be advantageous for the insect because other exogenous compounds, especially phenolics, may be abundant during feeding. If the enzyme had a broad specificity, the ingestion of various phe-

nolic compounds would interfere with BXD glucosylation. To analyze if the rate of DIMBOA or HMBOA glucosylation could be affected by ingested plant phenolics, further kinetics and inhibition studies are necessary. However, as SfUGTs 11, 14, 20 and 29 conjugate a wide range of plant phenolics, these enzymes might help to minimize the inhibition of SfUGT5 activity by dietary phenolics. MBOA is a product of spontaneous degradation of the two most abundant BXDs DIMBOA and HDMBOA [107]. This degradation is facilitated by the alkaline pH [16] which is common in the gut of most lepidopteran species [17]. MBOA was shown to be less toxic towards chewing herbivores [108]. Having several UGTs, distributed throughout larval tissues, that are able to conjugate MBOA might be enough to cope with the constantly formed MBOA during DIMBOA metabolism.

7.5 Mutation of the catalytic residue H35 in SfUGTs leads to complete loss of UGT activity towards BXDs

Structure analyses of human UGTs have shown that an N-terminal histidine (H), conserved in all members of the human UGT families UGT1A and UGT2B, is crucial for the catalytic activity of these enzymes towards phenolics and primary amines [65]. However, in UGT2B10 this residue is substituted by a leucine (L) because of which it lacks activity towards phenolics. Interestingly, UGT2B10 glucuronidates tertiary amines as nicotine, a property that seems to be exclusive for only few UGTs [66]. In insects tertiary-*N*-glucosylation has not been reported yet. In a mutational study it was shown that by substituting L35 (L34 in the respective protein sequence) in UGT2B10 by a histidine, the *N*-glucuronidation activity towards tertiary amines is completely abolished whereas *O*-glucuronidation activity is gained towards phenolics [67], indicating that these N-terminal residues were important for selective glycosylation of particular heteroatoms in a given substrate.

As the N-terminal H35 is also highly conserved in insects [42] and UGT activity was mostly observed for phenolic compounds [53], it might play a similar role in insects. In the present study, multiple sequence alignment of BXD-conjugating SfUGTs with other animal UGTs showed that H35 (H37 in the alignment) and D151 (D149) are also conserved in *S. frugiperda* UGTs. To analyze the role of N-terminal histidine and leucine for UGTs from *S. frugiperda* in benozoxazinoid glucosylation as well as for potential tertiary amine or thiol substrates, H35L substitution mutants were generated which substitute the conserved catalytic histidine by a leucine. We have chosen to compare the effects on two different enzymes: SfUGT5, known for DIMBOA-*O*-glucosylation, and SfUGT29 which forms MBOA-*N*-glucoside. After expression in HighFive^{TM} cells, we compared their activity to their respective wild type towards several substrates: the BXDs MBOA, DIMBOA and HMBOA, the simple phenolics 4-nitrophenol and 1-naphthol, the thiol thiophenol and the alkaloid quinine which contains two tertiary amine moieties.

Glucoside formation was observed for all tested substrates, except of quinine indicating that the substitution of histidine by leucine in the human UGT2B10 may not be the leading factor for tertiary amine glucuronidation and that the full explanation for the *N*-glucuronidation preference for tertiary amines is probably more complex. However, as quinine was the only tertiary

amine tested, it is not excluded that glucosylation of other substrates may be possible. Therefore, screening of other potential substrates with tertiary amine moiety need to be conducted.
The activity towards benzoxazinoids was abolished in the mutants, suggesting that H35 might play an important role in catalysis of both, *N*-glucosylation of MBOA and *O*-glycosylation of DIMBOA and HMBOA. However, when testing simple phenolics, the H35L mutant of SfUGT5 produced 80% more 1-naphthyl-*O*-glucoside than the respective wild type. Also the SfUGT29 mutation did not completely abolish activity towards naphthol, but lowered the activity to 25% of the respective wild-type activity. For 4-nitrophenol, a differential profile was observed: whereas the actvity of the SfUGT5 mutant did not significantly differ from its wild type, mutation of SfUGT29 resulted in the loss of catalytic activity. Additionally, 1-naphthol and 4-nitrophenol glucosylation were also observed for the newly expressed SfUGT35 which naturally shows a leucine instead of H35. These results suggest that histidine as general base is not crucial for the glucosylation of these compounds.
Depending on the substrate tested, the substitution of H35 to leucine had a activity-diminishing or -increasing effect. This leads to the suggestion that the amino acid at position 35 is not the leading factor for catalysis but other factors seem to be important, depending on the chemical nature of the substrate. Due to the lack of crystal structures of the highly variable N-terminus of animal UGTs, it is not easy to predict which amino acids might be important for efficient substrate binding and catalysis. Hence, structure-activity studies may be an important topic for future research.

7.6 Four newly expressed SfUGTs show activity towards DIMBOA and MBOA

Transcriptional analysis of larval gut and integument tissues, and Sf9 cells retrieved 36 UGT-encoding genes in *S. frugiperda* out of which 25 were successfully expressed and functionally characterized in a previous study [54]. Five candidates (SfUGTs 5, 11, 14, 20, 29) were shown to have activity towards either DIMBOA or MBOA and were subject of further characterization regarding substrate specificity and tissue-specific expression in the present study.
In this work, we also aimed to express and functionally characterize the remaining genes retrieved from transcriptome analysis, and to assess their potential contribution to BXD detoxification. From the 11 remaining genes, 7 UGT candidate genes were successfully expressed in insect cells which was confirmed via western blot (figure 3). A multiple sequence alignment of the respective protein sequences with already characterized animal UGTs revealed that they share all conserved domains and residues of UGTs (figure 6). They consist of two major domains: a highly variable N-terminal aglucone binding domain and a more conserved C-terminal domain responsible for binding of the sugar donor [42]. As mammalian UGTs they possess a C-terminal transmembrane domain followed by a short cytoplasmic tail and an N-terminal signal peptide which directs the translocation of the protein to the ER. Therefore, unlike soluble plant UGTs [41], SfUGTs are membrane-anchored proteins located in the ER membrane [109]. This was also consistent with the detection of the recombinant UGT expression in microsomal extracts but not in the cytosolic fraction by western blot (figure 3). Unlike the other SfUGTs, SfUGT39

shows a relatively long cytoplasmic tail (46 aa) which might be important for interactions with other proteins as observed for example for human UGT2B7 which interacts with CYP3A4 on the cytosolic side of the ER for efficient subsequent metabolism of ingested drugs [110]. Possible interaction of SfUGT39 with other detoxification enzymes may be analyzed for instance by co-immunoprecipitation [111].

In order to test if the expressed recombinant SfUGTs might be involved in BXD metabolism in *S. frugiperda*, they were tested towards the general substrates 4-nitrophenol and 1-naphthol as well as the BXDs DIMBOA, HMBOA and MBOA. All enzymes were active towards 1-naphthol confirming that they were enzymatically active (figure 4). All microsomal extracts containing one of the seven UGTs produced significantly more 1-naphthyl-glucoside than the respective non-transfected control microsomes. Using DIMBOA as substrate, out of the seven expressed UGTs, only SfUGT26 formed DIMBOA-glucoside. Moreover, it showed high activity towards HMBOA. By comparison of the retention times of the DIMBOA-glucosides formed by SfUGT26 and SfUGT5, respectively, it was shown that SfUGT26 is also forming the (2S)-epimer (figure 5). The activity of SfUGT26 is similar to the previously reported SfUGT5 which is known to form (2S)-DIMBOA-glucoside, an epimer of the plant derived 2(R)-glucoside and main detoxification product of DIMBOA detected in high amounts in the frass of *S. frugiperda* larvae, feeding on maize leaves [35, 54]. This indicates that it might have a similar importance for DIMBOA and HMBOA detoxification in *S. frugiperda*. As mentioned above, DIMBOA and HMBOA glucosides are the most abundant aerial parts of young and old maize leaves, respectively [13]. Although SfUGT5 was shown to be specific for DIMBOA and HMBOA, it might not be sufficient to cope with the large amounts of ingested BXDs during larval feeding. Therefore, having a second enzyme with similar activity might be beneficial for the insect. As SfUGT26 forms similarly low amounts of simple phenolic glucosides, compared to its high activity towards DIMBOA and HMBOA (table 5), it is suggested that it may be also specific for these BXDs. However, kinetic studies for both enzymes may give more information about which enzyme is more specific and active towards DIMBOA and HMBOA and thus has a higher impact for their detoxification. SfUGTs 26 and 5 might co-exist in one tissue where they both contribute equally to BXD detoxification or might act in separate tissues. In this study, SfUGT5 was shown to be predominantly expressed in the gut of *S. frugiperda* larvae. To answer, if the two enzymes co-exist in the same tissue or are expressed in different tissues, quantitative real-time PCR analysis may be performed in the future to determine the tissue-specific expression of SfUGT26.

Table 5: Comparison of the glycosylation activity of *S. frugiperda* UGTs towards BXDs and phenolic compounds. Product formation was quantified using a external standard curve using authentic glucoside standards. Observed product formation (in %) for one substrate was determined relative to the main product of the respective enzyme (100%). Abbreviations: n.t. - not tested

SfUGT#	**5**	**11**	**14**	**20**	**29**	**26**	**39**	**40**	**42**	**46**
MBOA	-	0.2%	25%	3%	4%	-	0.4%	3%	-	2%
DIMBOA	71%	2%	-	-	-	100%	-	-	-	-
HMBOA	100%	4%	-	-	-	47%	1%	2%	2%	-
4-NP	2%	100%	12%	100%	56%	-	100%	100%	100%	100%
SAld	-	-	100%	-	-	n.t.	n.t.	n.t.	n.t.	n.t.
Esculetin	1%	14%	58%	90%	100%	n.t.	n.t.	n.t.	n.t.	n.t.

Additionaly, three UGT candidates, SfUGTs 39, 40 and 46, were able to glucosylate MBOA. However, MBOA-*N*-glucoside was only the minor product of these enzymes whereas the activity towards phenolic compounds was higher (table 5). This is consistent with the observations in the substrate specificity screening where MBOA-glucosylating enzymes showed a broad substrate specificity towards many plant allelochemicals, especially phenolic compounds (table 3). Tissue-specific expression analysis of the newly characterized enzymes may help to complete the picture of MBOA metabolism. As it was shown in this study, MBOA-conjugating UGTs are present in various tissues of the insect, suggesting that several UGTs with low specificity towards MBOA contribute to the overall MBOA detoxification. As explained before, MBOA is a less toxic degradation product of DIMBOA which is produced constantly and spontaneously during DIMBOA metabolism. Therefore, having a specific enzyme for MBOA detoxification might not be as crucial as for DIMBOA. In addition, three enzymes with minor activity towards HMBOA, SfUGTs 39, 40 and 42, were identified which may have only a minor role in HMBOA detoxification.

In summary, ten SfUGTs with potential contribution to BXD metabolism in *S. frugiperda* have been successfully expressed and characterized; out of these enzymes, two were shown to stereoselectively glucosylate DIMBOA to form (2*S*)-DIMBOA-glucoside, four were able to conjugate MBOA, three catalyzed the glycosylation of both, MBOA and HMBOA and one enzyme was conjugating each of the three compounds, forming the plant-derived (2*R*)-DIMBOA-glucoside. It is important to mention that all SfUGTs, characterized previously and in this study, were heterologously expressed as recombinant proteins to which tags were attached to enable western blot detection and purification of the enzymes. These modifications lead to the production of an artificial enzyme that does not exist in this form *in vivo* and may alter the catalytic activity compared to the native enzyme. To give the evidence that the BXD-detoxifying enzymes, identified through *in vitro* enzymatic assays in this study, contribute to BXD-detoxifcation *in vivo*, the generation of knockout or RNAi-mediated knockdown mutants of the respective genes is necessary.

8 Conclusion

Benzoxazinoids belong to a group of two-component defenses in plants and are the major chemical defensive compounds against herbivores in maize. These secondary metabolites are stored as stable non-toxic glucosides in the plant cell and are activated by specific glucosidases upon herbivory, releasing toxic aglucones. This defense mechanism is very efficient towards a wide range of generalist herbivores, including several lepidopteran larvae. However, the fall armyworm *Spodoptera frugiperda* is able to detoxify BXDs efficiently by conjugation of glucose to the small lipohilic aglucones and their degradation products, making them less toxic and facilitating their fast excretion. The enzymes that catalyze this reaction are UDP-glucosyltransferases (UGTs) which are known to have a major role in the detoxifying metabolism of xenobiotics.
In this study, five UGT candidates from *S. frugiperda* with previously reported glycosylation activity towards BXDs have been further characterized to evaluate their importance in BXD and overall xenobiotic metabolism of this insect. A previous comparison of tissue-specific glucosylation activity towards the benzoxazinone aglucone DIMBOA and its benzoxazolinone degradation product MBOA among five different tissues revealed that the highest glucosylation rates for DIMBOA were found in the gut tissue, whereas activity towards MBOA is distributed among tissues, with slightly higher glucosylation rates in fat bodies. Relative expression analysis of the five candidates among the same tissues confirmed that the gene encoding for DIMBOA-glycosylating SfUGT5 is highly expressed in the gut, indicating that SfUGT5 is most likely involved in the detoxification of DIMBOA. However, the observed tissue-specific activities towards MBOA could not be fully correlated to one specific enzyme suggesting that MBOA detoxification is the result of the cooperation of several different enzymes which are highly distributed in the insect body. These findings were enforced by the results of a substrate screening of the heterologously expressed enzymes towards a range of structurally diverse compounds.
The expressed enzymes generally had a wide substrate specificity towards xenobiotic and plant alleochemicals but did not conjugate endogenous compounds. However, whereas the UGT candidates known for their capability towards MBOA show higher activities towards phenolic compounds and form MBOA-*N*-Glc only to a minor extent, DIMBOA-conjugating SfUGT5 shows a clear preference for BXDs, especially DIMBOA and HMBOA. In addition, we were able to heterologously express and assess the contribution of seven additional UGT candidates in BXD metabolism of *S. frugiperda* via *in vitro* enzymatic assays. Among them, four enzymes were able to conjugate either MBOA or HMBOA, or both. However, similarly to the previously reported MBOA-UGTs, they seem more efficiently conjugate phenolic compounds. Interestingly, we identified one enzyme, SfUGT26, that glucosylates DIMBOA with simlilar stereochemical specificity and acitvity as the previously identified SfUGT5. Also this enzyme conjugates phenolics only to a low extent. As the formation of MBOA-*N*-Glc formation has been also observed in insect species susceptible to BXDs, whereas no DIMBOA-Glc formation was detected, the conjugation of MBOA seems to be a general mechanism in lepidopteran species. DIMBOA-glucosylation, on the other hand, appears to be a detoxification mechanism which is specific for the genus *Spodoptera* where it might underlie these species' success as pests on grass crops.

References

[1] J. Doebley. The genetics of maize evolution. *Annual Review of Genetics*, 38:37–59, 2004.

[2] E. S. de Lange, D. Balmer, B. Mauch-Mani, and T. C. J. Turlings. Insect and pathogen attack and resistance in maize and its wild ancestors, the teosintes. *New Phytologist*, 204:329–341, 2014.

[3] B. Shiferaw, B. M. Prasanna, J. Hellin, and M. Bänziger. Crops that feed the world 6. Past successes and future challenges to the role played by maize in global food security. *Food Security*, 3:307, 2011.

[4] S. Machado, E. D. Bynum, T. L. Archer, R. J. Lascano, L. T. Wilson, J. Bordovsky, E. Segarra, K. Bronson, D. M. Nesmith, and W. Xu. Spatial and temporal variability of corn growth and grain yield. *Crop Science*, 42:1564–1576, 2002.

[5] D. N. Duvick. Biotechnology in the 1930s: the development of hybrid maize. *Nature Reviews Genetics*, 2:69–74, 2001.

[6] Y. H. Chen, R. Gols, and B. Benrey. Crop domestication and its impact on naturally selected trophic interactions. *Annual Review of Entomology*, 60:35–58, 2015.

[7] E. C. Oerke. Crop losses to pests. *The Journal of Agricultural Science*, 144:31–43, 2005.

[8] L. N. Meihls, H. Kaur, and G. Jander. Natural variation in maize defense against insect herbivores. *Cold Spring Harbor Symposia Quantitative Biology*, 77:269–283, 2012.

[9] A. Djamin and M. D. Pathak. Role of Silica in Resistance to Asiatic Rice Borer, *Chilo suppressalis* (Walker), in Rice Varieties. *Journal of Economic Entomology*, 60:347–351, 1967.

[10] D. J. Bergvinson, J. T. Arnason, R. Hamilton, J. A. Mihm, and D. C. Jewell. Determining leaf toughness and its role in maize resistance to the European com borer (Lepidoptera: Pyralidae). *Journal of Economic Entomology*, 87:1743–1748, 1994.

[11] A. Mithöfer and W. Boland. Plant defense against herbivores: chemical aspects. *Annual Review of Plant Biology*, 63:431–450, 2012.

[12] H. M. Niemeyer. Hydroxamic Acids Derived from 2-Hydroxy-2H-1,4-Benzoxazin-3(4H)-one: Key Defense Chemicals of Cereals. *Journal of Agricultural and Food Chemistry*, 57:1677–1696, 2009.

[13] A. Kohler, D. Maag, N. Veyrat, G. Glauser, J. L. Wolfender, T. C. Turlings, and M. Erb. Within-plant distribution of 1,4-benzoxazin-3-ones contributes to herbivore niche differentiation in maize. *Plant Cell and Environment*, 38:1081–1093, 2015.

[14] S. Pentzold, M. Zagrobelny, F. Rook, and S. Bak. How insects overcome two-component plant chemical defence: plant beta-glucosidases as the main target for herbivore adaptation. *Biological Reviews Cambridge Philosophical Society*, 89:531–551, 2014.

[15] H. Hartenstein, D. Sicker, and J. Klein. Efficient isolation procedure for (2R-β-D-glucopyranosyloxy-4-hydroxy-2H-1,4-benzoxazin-3(4H)-one from maize. *Indian Journal of Heterocyclic Chemistry*, 3:151–153, 1993.

[16] H. M. Niemeyer, H. R. Bravo, G. F. Penã, and L. J. Corcuera. Decomposition of 2,4-Dihydroxy-7methoxy-2H-1,4-benzoxazin-3-(4H)-one, a Hydroxamic Acid From Gramineae. In H. Kehl, editor, *Chemistry and Biology of Hydroxamic Acids*, pages 22–28. Basel Karger, 1982.

[17] M. Berenbaum. Adaptive Significance of Midgut pH in Larval Lepidoptera. *The American Naturalist*, 115:138–146, 1980.

[18] F. C. Wouters, B. Blanchette, J. Gershenzon, and D. G. Vassão. Plant defense and herbivore counter-defense: benzoxazinoids and insect herbivores. *Phytochemistry Reviews*, 15:1127–1151, 2016.

[19] A. Kohler, D. Maag, N. Veyrat, G. Glauser, J. L. Wolfender, T. C. Turlings, and M. Erb. Within-plant distribution of 1,4-benzoxazin-3-ones contributes to herbivore niche differentiation in maize. *Plant, Cell and Environment*, 38:1081–1093, 2015.

[20] A. Oikawa, A. Ishihara, M. Hasegawa, O. Kodama, and H. Iwamura. Induced accumulation of 2-hydroxy-4,7-dimethoxy-1,4-benzoxazin-3-one glucoside (HDMBOA-Glc) in maize leaves. *Phytochemistry*, 56:669–675, 2001.

[21] Y. Hashimoto and K. Shudo. Chemistry of biologically active benzoxazinoids. *Phytochemistry*, 43:551–559, 1996.

[22] T. Ishizaki, Y. Hashimoto, K. Shudo, and T. Okamoto. Reaction of 4-acetoxy-1,4-benzoxazin-3-one with DNA. A possible chemical mechanism for the antifungal and mutagenic activities. *Tetrahedron Letters*, 23:4055–4056, 1982.

[23] F. C. Wouters, J. Gershenzon, and D. G. Vassão. Benzoxazinoids: Reactivity and Modes of Action of a Versatile Class of Plant Chemical Defenses. *Journal of the Brazilian Chemical Society*, 27:1379–1397, 2016.

[24] D. Sicker and M. Schulz. Benzoxazinones in plants: Occrurence, Synthetic Access, and Biological Activity. In Atta ur Rahman, editor, *Studies in Natural Products Chemistry*, pages 185–232. Elsevier Science Ltd., 27 edition, 2002.

[25] F. J. Pérez and H. M. Niemeyer. Reaction of DIMBOA, a resistance factor from cereals, with papain. *Phytochemistry*, 28:1597–1600, 1989.

[26] J. G. Houseman, F. Campos, N. M. R. Thie, B. J. R. Philogène, J. Atkinson, P. Morand, and J. T. Arnason. Effect of the Maize-Derived Compounds DIMBOA and MBOA on Growth and Digestive Processes of European Corn Borer (Lepidoptera: Pyralidae). *Journal of Economic Entomology*, 85:669–674, 1992.

[27] F. Campos, J. Atkinson, J. T. Arnason, B. J. Philogene, P. Morand, N. H. Werstiuk, and G. Timmins. Toxicokinetics of 2,4-dihydroxy-7-methoxy-1,4-benzoxazin-3-one (DIMBOA) in the European corn borer, *Ostrinia nubilalis* (Hübner). *Journal of Chemical Ecology*, 15:1989–2001, 1989.

[28] F. Campos, J. Atkinson, J. T. Arnason, B. J. Philogene, P. Morand, N. H. Werstiuk, and G. Timmins. Toxicity and toxicokinetics of 6-methoxybenzoxazolinone (MBOA) in the european corn borer, *Ostrinia nubilalis* (Hübner). *Journal of Chemical Ecology*, 14:989–1002, 1988.

[29] J. Atkinson, J. Arnason, F. Campos, H. M. Niemeyer, and H. R. Bravo. Synthesis and Reactivity of Cyclic Hydroxamic Acids. In *Synthesis and Chemistry of Agrochemicals III*, volume 504 of *ACS Symposium Series*, pages 349–360. American Chemical Society, 1992.

[30] G. Glauser, G. Marti, N. Villard, G. A. Doyen, J. L. Wolfender, T. C. Turlings, and M. Erb. Induction and detoxification of maize 1,4-benzoxazin-3-ones by insect herbivores. *The Plant Journal*, 68:901–911, 2011.

[31] D. Maag, C. Dalvit, D. Thevenet, A. Kohler, F. C. Wouters, D. G. Vassao, J. Gershenzon, J. L. Wolfender, T. C. Turlings, M. Erb, and G. Glauser. 3-beta-*D*-Glucopyranosyl-6-methoxy-2-benzoxazolinone (MBOA-*N*-Glc) is an insect detoxification product of maize 1,4-benzoxazin-3-ones. *Phytochemistry*, 102:97–105, 2014.

[32] I. Cruz, M. L. C. Figueiredo, A. C. Oliveira, and C. A. Vasconcelos. Damage of *Spodoptera frugiperda* (Smith) in different maize genotypes cultivated in soil under three levels of aluminium saturation. *International Journal of Pest Management*, 45:293–296, 1999.

[33] A. N. Sparks. A Review of the Biology of Fall Armyworm. *The Florida Entomologist*, 62:82–87, 1979.

[34] S. Wild. Invasive pest hits Africa. *Nature*, 543:13–14, March 2017. doi:10.10.38/nature.2017.21527.

[35] F. C. Wouters, M. Reichelt, G. Glauser, E. Bauer, M. Erb, J. Gershenzon, and D. G. Vassao. Reglucosylation of the benzoxazinoid DIMBOA with inversion of stereochemical configuration is a detoxification strategy in lepidopteran herbivores. *Angewandte Chemie International Edition*, 53:11320–11324, 2014.

[36] C. F. Wilkinson. Xenobiotic Conjugation in Insects. In *Xenobiotic Conjugation Chemistry*, volume 299 of *ACS Symposium Series*, pages 48–61. American Chemical Society, 1986.

[37] C. J. Kennedy and K. B. Tierney. Xenobiotic Protection xenobiotic protection /Resistance Mechanisms in Organisms. In R. A. Meyers, editor, *Encyclopedia of Sustainability Science and Technology*, pages 12293–12314. Springer New York, New York, NY, 2012.

[38] R. Meech, J. O. Miners, B. C. Lewis, and P. I. Mackenzie. The glycosidation of xenobiotics and endogenous compounds: versatility and redundancy in the UDP glycosyltransferase superfamily. *Pharmacoly and Therapeutics*, 134:200–218, 2012.

[39] L. L. Lairson, B. Henrissat, G. J. Davies, and S. G. Withers. Glycosyltransferases: structures, functions, and mechanisms. *Annual Review of Biochemistry*, 77:521–555, 2008.

[40] P. M. Coutinho, E. Deleury, G. J. Davies, and B. Henrissat. An Evolving Hierarchical Family Classification for Glycosyltransferases. *Journal of Molecular Biology*, 328:307–317, 2003.

[41] S. A. Osmani, S. Bak, and B. L. Moller. Substrate specificity of plant UDP-dependent glycosyltransferases predicted from crystal structures and homology modeling. *Phytochemistry*, 70:325–347, 2009.

[42] S.-J. Ahn, H. Vogel, and D. G. Heckel. Comparative analysis of the UDP-glycosyltransferase multigene family in insects. *Insect Biochemistry and Molecular Biology*, 42:133–147, 2012.

[43] P. I. Mackenzie, I. S. Owens, B. Burchell, K. W. Bock, A. Bairoch, A. Belanger, S. Fournel-Gigleux, M. Green, D. W. Hum, T. Iyanagi, D. Lancet, P. Louisot, J. Magdalou, J. R. Chowdhury, J. K. Ritter, H. Schachter, T. R. Tephly, K. F. Tipton, and D. W. Nebert. The udp glycosyltransferase gene superfamily: recommended nomenclature update based on evolutionary divergence. *Pharmacogenetics*, 7:255–69, 1997.

[44] E.-K. Lim and D. J. Bowles. A class of plant glycosyltransferases involved in cellular homeostasis. *The EMBO Journal*, 23:2915, 2004.

[45] Saad A. Ahmad, Theodore L. Hopkins, and Karl J. Kramer. Tyrosine β-Glucosyltransferase in the tobacco hornworm, Manduca sexta (L.): properties, tissue localization, and developmental profile. *Insect Biochemistry and Molecular Biology*, 26:49–57, 1996.

[46] K. J. Kramer and T. L. Hopkins. Tyrosine metabolism for insect cuticle tanning. *Archives of Insect Biochemistry and Physiology*, 6:279–301, 1987.

[47] J. T. Warren, B. Steiner, A. Dorn, M. Pak, and L. I. Gilbert. Metabolism of Ecdysteroids During Embryogenesis of *Manduca Sexta*. *Journal of Liquid Chromatography*, 9:1759–1782, 1986.

[48] Q. Wang, G. Hasan, and C. W. Pikielny. Preferential expression of biotransformation enzymes in the olfactory organs of *Drosophila melanogaster*, the antennae. *Journal of Biological Chemistry*, 274:10309–15, 1999.

[49] F. Bozzolan, D. Siaussat, A. Maria, N. Durand, M. A. Pottier, T. Chertemps, and M. Maibeche-Coisne. Antennal uridine diphosphate (UDP)-glycosyltransferases in a pest insect: diversity and putative function in odorant and xenobiotics clearance. *Insect Molecular Biology*, 23:539–549, 2014.

[50] M. D. Real, J. Ferre, and F. J. Chapa. UDP-glucosyltransferase activity toward exogenous substrates in Drosophila melanogaster. *Analytical Biochemistry*, 194:349–352, 1991.

[51] S. Ahmad and T. Hopkins. β-Glucosylation of plant phenolics by phenol β-glucosyltransferase in larval tissues of the tobacco hornworm, *Manduca sexta* (L.). *Insect Biochemistry and Molecular Biology*, 23:581–589, 1993.

[52] S. Ahmad and T. Hopkins. Phenol beta-glucosyltransferases in six species of insects: properties and tissue localization. *Comparative Biochemistry and Physiology B*, 104:515–519, 1993.

[53] T. Luque, K. Okano, and D. R. O'Reilly. Characterization of a novel silkworm (Bombyx mori) phenol UDP-glucosyltransferase. *European Journal of Biochemistry*, 269:819–825, 2002.

[54] F. C. Wouters. *Detoxification and metabolism of maize benzoxazinoids by lepidopteran herbivores*. PhD thesis, Friedrich-Schiller-Universität Jena, 2016.

[55] R. Bergomaz and M. Boppré. A simple instant diet for rearing arctiidae and other moths. *Journal of the Lepidopterists' Society*, 40:131–137, 1986.

[56] A. Untergasser, H. Nijveen, X. Rao, T. Bisseling, R. Geurts, and J. A. M. Leunissen. Primer3Plus, an enhanced web interface to Primer3. *Nucleic Acids Research*, 35:W71–W74, 2007.

[57] P. K. Kakumani, P. Malhotra, S. K. Mukherjee, and R. K. Bhatnagar. A draft genome assembly of the army worm,*Spodoptera frugiperda*. *Genomics*, 104:134–143, 2014.

[58] P. K. Kakumani, R. Shukla, V. N. Todur, P. Malhotra, S. K. Mukherjee, and R. K. Bhatnagar. De novo transcriptome assembly and analysis of Sf21 cells using illumina paired end sequencing. *Biology Direct*, 10:44, 2015.

[59] V. Negre, T. Hotelier, A. N. Volkoff, S. Gimenez, F. Cousserans, K. Mita, X. Sabau, J. Rocher, M. Lopez-Ferber, E. d'Alencon, P. Audant, C. Sabourault, V. Bidegainberry, F. Hilliou, and P. Fournier. SPODOBASE: an EST database for the lepidopteran crop pest Spodoptera. *BMC Bioinformatics*, 7, 2006.

[60] F. Legeai, S. Gimenez, B. Duvic, J.-M. Escoubas, A.-S. Gosselin Grenet, F. Blanc, F. Cousserans, I. Séninet, A. Bretaudeau, D. Mutuel, P.-A. Girard, C. Monsempes, G. Magdelenat, F. Hilliou, R. Feyereisen, M. Ogliastro, A.-N. Volkoff, E. Jacquin-Joly, E. d'Alençon, N. Nègre, and P. Fournier. Establishment and analysis of a reference transcriptome for *Spodoptera frugiperda*. *BMC Genomics*, 15:704, 2014.

[61] M. W. Pfaffl. Quantification strategies in real-time pcr. In S.A. Bustin, editor, *A-Z of quantitative PCR*, pages 87–112. IUL Biotechnology Series, 2004.

[62] K. J. Livak and T. D. Schmittgen. Analysis of relative gene expression data using real-time quantitative PCR and the 2(-Delta Delta C(T)) Method. *Methods*, 25:402–408, 2001.

[63] Y. Lu, M. Yuan, X. Gao, T. Kang, S. Zhan, H. Wan, and J. Li. Identification and validation of reference genes for gene expression analysis using quantitative PCR in Spodoptera litura (Lepidoptera: Noctuidae). *PLoS One*, 8:e68059, 2013.

[64] N. Silver, S. Best, J. Jiang, and S. Thein. Selection of housekeeping genes for gene expression studies in human reticulocytes using real-time PCR. *BMC Molecular Biology*, 7:33, 2006.

[65] M. J. Miley, A. K. Zielinska, J. E. Keenan, S. M. Bratton, A. Radominska-Pandya, and M. R. Redinbo. Crystal Structure of the Cofactor-Binding Domain of the Human Phase II Drug-Metabolism Enzyme UDP-Glucuronosyltransferase 2B7. *Journal of Molecular Biology*, 369:498–511, 2007.

[66] S. Kaivosaari, P. Toivonen, L. M. Hesse, M. Koskinen, M. H. Court, and M. Finel. Nicotine glucuronidation and the human UDP-glucuronosyltransferase UGT2B10. *Molecular Pharmacology*, 72:761–768, 2007.

[67] O. Kerdpin, P. I. Mackenzie, K. Bowalgaha, M. Finel, and J. O. Miners. Influence of N-terminal domain histidine and proline residues on the substrate selectivities of human UDP-glucuronosyltransferase 1A1, 1A6, 1A9, 2B7, and 2B10. *Drug Metabolism and Disposition*, 37:1948–1955, 2009.

[68] F. Sanger, S. Nicklen, and A. R. Coulson. DNA sequencing with chain-terminating inhibitors. *Proceedings of the National Academy of Sciences of the United States of America*, 74:5463–5467, 1977.

[69] M. M. Bradford. A rapid and sensitive method for the quantitation of microgram quantities of protein utilizing the principle of protein-dye binding. *Analytical Biochemistry*, 72:248–254, 1976.

[70] C. Krempl, T. Sporer, M. Reichelt, S. J. Ahn, H. Heidel-Fischer, H. Vogel, D. G. Heckel, and N. Joussen. Potential detoxification of gossypol by UDP-glycosyltransferases in the two Heliothine moth species Helicoverpa armigera and Heliothis virescens. *Insect Biochemistry and Molecular Biology*, 71:49–57, 2016.

[71] A. Mueller. Untersuchungen zur Verteilung und Biosynthese von phenolischen Glycosiden in *Salicaceae*. Master's thesis, Friedrich-Schiller Universität, Jena, 2016.

[72] J.D. Thompson, D.G. Higgins, and T.J. Gibson. CLUSTAL W: improving the sensitivity of progressive multiple sequence alignment through sequence weighting, position-specific gap penalties and weight matrix choice. *Nucleic Acids Research*, 22:4673–4680, 1994.

[73] K. Tamura, G. Stecher, D. Peterson, Filipski A., and S. Kumar. MEGA6: Molecular Evolutionary Genetics Analysis version 6.0. *Molecular Biology and Evolution*, 30:2725–2729, 2013.

[74] UniProt: the universal protein knowledgebase. *Nucleic Acids Research*, 45:D158–D169, 2017.

[75] G. Taguchi, M. Nakamura, N. Hayashida, and M. Okazaki. Exogenously added naphthols induce three glucosyltransferases, and are accumulated as glucosides in tobacco cells. *Plant Science*, 164:231–240, 2003.

[76] J. Seppen, E. Steenken, D. Lindhout, P. J. Bosma, and Ronald P. J. Oude E. A mutation which disrupts the hydrophobic core of the signal peptide of bilirubin UDP-glucuronosyltransferase, an endoplasmic reticulum membrane protein, causes Crigler-Najjar type IIs. *FEBS Letters*, 390:294–298, 1996.

[77] A. Radominska-Pandya, S. M. Bratton, M. R. Redinbo, and M. J. Miley. The crystal structure of human UDP-glucuronosyltransferase 2B7 C-terminal end is the first mammalian UGT target to be revealed: the significance for human UGTs from both the 1A and 2B families. *Drug Metabolism Reviews*, 42:133–144, 2010.

[78] N. Saitou and M. Nei. The neighbor-joining mehtod: A new method for reconstructing phylogenetic trees. *Molecular Biology and Evolution*, 4:406–425, 1987.

[79] M. Nei and S. Kumar. *Molecular Evolution and Phylogenetics*. Oxford University Press, New York, 2000.

[80] Felsenstein J. Confidence limits on phylogenies: An approach using the bootstrap. *Evolution*, 39:783–791, 1985.

[81] F. Ponchel, C. Toomes, K. Bransfield, F. T. Leong, S. H. Douglas, S. L. Field, S. M. Bell, V. Combaret, A. Puisieux, A. J. Mighell, P. A. Robinson, C. F. Inglehearn, J. D. Isaacs, and A. F. Markham. Real-time PCR based on SYBR-Green I fluorescence: An alternative to the TaqMan assay for a relative quantification of gene rearrangements, gene amplifications and micro gene deletions. *BMC Biotechnology*, 3:18, 2003.

[82] B. Thornton and C. Basu. Real-time PCR (qPCR) primer design using free online software. *Biochemistry and Molecular Biology Education*, 39:145–154, 2011.

[83] O. Thellin, W. Zorzi, B. Lakaye, B. De Borman, B. Coumans, G. Hennen, T. Grisar, A. Igout, and E. Heinen. Housekeeping genes as internal standards: use and limits. *Journal of Biotechnology*, 75:291–295, 1999.

[84] M. W. Pfaffl, A. Tichopad, C. Prgomet, and T. P. Neuvians. Determination of stable housekeeping genes, differentially regulated target genes and sample integrity: BestKeeper–Excel-based tool using pair-wise correlations. *Biotechnology letters*, 26:509–515, 2004.

[85] J. Vandesompele, K. De Preter, F. Pattyn, B. Poppe, N. Van Roy, A. De Paepe, and F. Speleman. Accurate normalization of real-time quantitative RT-PCR data by geometric averaging of multiple internal control genes. *Genome Biology*, 3:research0034.1–research0034.11, 2002.

[86] C. L. Andersen, J. L. Jensen, and T. F. Orntoft. Normalization of real-time quantitative reverse transcription-PCR data: a model-based variance estimation approach to identify genes suited for normalization, applied to bladder and colon cancer data sets. *Cancer research*, 64:5245–5250, 2004.

[87] H. Shao, X. He, L. Achnine, J. W. Blount, R. A. Dixon, and X. Wang. Crystal structures of a multifunctional triterpene/flavonoid glycosyltransferase from Medicago truncatula. *Plant Cell*, 17:3141–3154, 2005.

[88] W. Offen, C. Martinez-Fleites, M. Yang, E. Kiat-Lim, B. G. Davis, C. A. Tarling, C. M. Ford, D. J. Bowles, and G. J. Davies. Structure of a flavonoid glucosyltransferase reveals the basis for plant natural product modification. *The EMBO Journal*, 25:1396–1405, 2006.

[89] A. Roy, W. B. Walker III, H. Vogel, S. Chattington, M. C. Larsson, P. Anderson, D. G. Heckel, and F. Schlyter. Diet dependent metabolic responses in three generalist insect herbivores *Spodoptera* spp. *Insect Biochemistry and Molecular Biology*, 71:91–105, 2016.

[90] M. D. Real, J. Ferre, and F. J. Chapa. UDP-glucosyltransferase activity toward exogenous substrates in *Drosophila melanogaster*. *Analytical Biochemistry*, 194:349–352, 1991.

[91] M. D. Real and J. Ferre. Biosynthesis of xanthurenic acid 8-*O*-beta-*D*-glucoside in Drosophila. Characterization of the xanthurenic acid:UDP-glucosyltransferase activity. *Journal of Biological Chemistry*, 265:7407–7412, 1990.

[92] T. Murai, N. Samata, H. Iwabuchi, and T. Ikeda. Human UDP-glucuronosyltransferase, UGT1A8, glucuronidates dihydrotestosterone to a monoglucuronide and further to a structurally novel glucuronide. *Drug Metabolism and Disposition*, 34:1102, 2006.

[93] S. B. Senafi, D. J. Clarke, and B. Burchell. Investigation of the substrate specificity of a cloned expressed human bilirubin UDP-glucuronosyltransferase: UDP-sugar specificity and involvement in steroid and xenobiotic glucuronidation. *Biochemical Journal*, 303:233–240, 1994.

[94] A. Wahlström, G. M. Pacifici, B. Lindström, L. Hammar, and A. Rane. Human liver morphine UDP-glucuronyl transferase enantioselectivity and inhibition by opioid congeners and oxazepam. *British Journal of Pharmacology*, 94:864–870, 1988.

[95] M. D. Green, C. D. King, B. Mojarrabi, P. I. Mackenzie, and T. R. Tephly. Glucuronidation of amines and other xenobiotics catalyzed by expressed human UDP-glucuronosyltransferase 1A3. *Drug Metabolism and Disposition*, 26:507–512, 1998.

[96] M. D. Green and T. R. Tephly. Glucuronidation of amine substrates by purified and expressed UDP-glucuronosyltransferase proteins. *Drug Metabolism and Disposition*, 26:860–867, 1998.

[97] J. L. Vaughn, R. H. Goodwin, G. J. Tompkins, and P. McCawley. The establishment of two cell lines from the insect *Spodoptera frugiperda* (lepidoptera; noctuidae). *In Vitro*, 13:213–217, 1977.

[98] F. F. Huang, C. L. Chai, Z. Zhang, Z. H. Liu, F. Y. Dai, C. Lu, and Z. H. Xiang. The UDP-glucosyltransferase multigene family in *Bombyx mori*. *BMC Genomics*, 9:563, 2008.

[99] J. P. Salminen, M. Lahtinen, K. Lempa, L. Kapari, E. Haukioja, and K. Pihlaja. Metabolic modifications of birch leaf phenolics by an herbivorous insect: detoxification of flavonoid aglycones via glycosylation. *Zeitschrift für Naturforschung C*, 59:437–444, 2004.

[100] M. Lahtinen, L. Kapari, and J. Kentta. Newly hatched neonate larvae can glycosylate: the fate of Betula pubescens bud flavonoids in first instar *Epirrita autumnata*. *Journal of Chemical Ecology*, 32:537–546, 2006.

[101] Y. Tamura, K. Nakajima, K. Nagayasu, and C. Takabayashi. Flavonoid 5-glucosides from the cocoon shell of the silkworm, *Bombyx mori*. *Phytochemistry*, 59:275–278, 2002.

[102] K. Herrmann. Flavonols and flavones in food plants: a review. *International Journal of Food Science & Technology*, 11:433–448, 1976.

[103] J. Mierziak, K. Kostyn, and A. Kulma. Flavonoids as important Molecules of Plant Interactions with the Environment. *Molecules*, 19:16240–16265, 2014.

[104] M. S. Simmonds. Flavonoid-insect interactions: recent advances in our knowledge. *Phytochemistry*, 64:21–30, 2003.

[105] F. Burghardt, H. Knuttel, M. Becker, and K. Fiedler. Flavonoid wing pigments increase attractiveness of female common blue (*Polyommatus icarus*) butterflies to mate-searching males. *Naturwissenschaften*, 87:304–307, 2000.

[106] E. A. Bernays and R. F. Chapman. Plant Secondary Compounds and Grasshoppers: Beyond Plant Defenses. *Journal of Chemical Ecology*, 26:1773–1794, 2000.

[107] V. Cambier, T. Hance, and E. de Hoffmann. Variation of DIMBOA and related compounds content in relation to the age and plant organ in maize. *Phytochemistry*, 53:223–229, 2000.

[108] J. Atkinson, J. Arnason, F. Campos, H. M. Niemeyer, and H. R. Bravo. Synthesis and Reactivity of Cyclic Hydroxamic Acids. In D. R. Baker, J. G. Fenyes, and J. J. Steffens, editors, *Synthesis and Chemistry of Agrochemicals III*, volume 504, pages 349–360. American Chemical Society, 1992.

[109] J. Magdalou, S. Fournel-Gigleux, and M. Ouzzine. Insights on membrane topology and structure/function of UDP-glucuronosyltransferases. *Drug Metabolism Reviews*, 42:159–166, 2010.

[110] S. Takeda, Y. Ishii, M. Iwanaga, A. Nurrochmad, Y. Ito, P. I. Mackenzie, K. Nagata, Y. Yamazoe, K. Oguri, and H. Yamada. Interaction of cytochrome P450 3A4 and UDP-glucoronosyltransferase 2B7: evidence for protein-protein association and possible involvement of CYP3A4 J-helix in the interaction. *Molecular Pharmacology*, 75:956–964, 2009.

[111] E. Isono and C. Schwechheimer. Co-immunoprecipitation and protein blots. *Methods in Molecular Biology.*, 655:377–387, 2010.

9 Supplements

9.1 List of chemicals

Acetonitrile (ACN)	VWR Chemicals (Radnor, USA)
Agarose	Carl Roth (Karlsruhe, Germany)
Ampicillin	Carl Roth ((Karlsruhe, Germany)
2-Benzoxazolinone (BOA)	Sigma-Aldrich (Steinheim, Germany)
β-mercaptoethanol	Sigma-Aldrich (Steinheim, Germany)
Bromphenol blue	Sigma-Aldrich (Steinheim, Germany)
Blasticidin S	Sigma-Aldrich (Steinheim, Germany)
Capsaicin	FLUKA, Sigma-Aldrich (Steinheim, Germany)
Catechol	Alfa Aesar (Karlsruhe, Germany)
p-coumaric acid	Sigma-Aldrich (Steinheim, Germany)
3,4-Dihydroxy-L-phenylalanine (*L*-DOPA)	Sigma-Aldrich (Steinheim, Germany)
K_2HPO_4 (dipotassium phosphate)	Sigma-Aldrich (Steinheim, Germany)
Na_2HPO_4 (disodium phosphate)	Carl Roth (Karlsruhe, Germany)
DTT (dithiotreitol)	Carl Roth (Karlsruhe, Germany)
DMSO	Acros Organics (New Jersey, USA)
Dopamine HCl	Sigma-Aldrich (Steinheim, Germany)
EDTA disodium salt	Carl Roth (Karlsruhe, Germany)
Esculetin	Carl Roth (Karlsruhe, Germany)
Esculin	Carl Roth (Karlsruhe, Germany)
Ethanol	Merck Millipore (Darmstadt, Germany)
Formic acid	Fischer Chemical (Geef, Belgium)
Gentamicin	Duchefa (Haarlem, Netherlands)
Glacial acetic acid	Carl Roth (Karlsruhe, Germany)

Gossypol	Sigma-Aldrich (Steinheim, Germany)
Glycerol	FLUKA, Sigma-Aldrich (Steinheim, Germany)
Glycine	Carl Roth (Karlsruhe, Germany)
H_2O_2 (hydrogen peroxide) 30% (w/w) in H_2O	FLUKA, Sigma-Aldrich (Steinheim, Germany)
6-Hydroxy-2-benzoxazolinone (6-OH-BOA)	Sigma-Aldrich (Steinheim, Germany)
Indole	Sigma-Aldrich (Steinheim, Germany)
Indole-3-acetic acid	Duchefa (Haarlem, Netherlands)
Isoquercitrin	Carl Roth (Karlsruhe, Germany)
Kanamycin	Duchefa (Haarlem, Netherlands)
LB-Agar (Luria/Miller)	Carl Roth (Karlsruhe, Germany)
low-fat powdered milk	FLUKA, Sigma-Aldrich (Steinheim, Germany)
Luminol	FLUKA, Sigma-Aldrich (Steinheim, Germany)
L-Tyrosine	Duchefa (Haarlem, Netherlands)
(±)-Menthol	FLUKA, Sigma-Aldrich (Steinheim, Germany)
Methanol	Merck Millipore (Darmstadt, Germany)
6-Methoxy-2-benzoxazolinone (MBOA)	Sigma-Aldrich (Steinheim, Germany)
KH_2PO_4 (monopotassium phosphate)	Sigma-Aldrich (Steinheim, Germany)
NaH_2PO_4 (monosodium phosphate)	Carl Roth (Karlsruhe, Germany)
1-Naphthol	FLUKA, Sigma-Aldrich (Steinheim, Germany)
p-Nitrophenol	FLUKA, Sigma-Aldrich (Steinheim, Germany)
4-Nitrophenyl-β-*D*-glucopyranosid	Carl Roth (Karlsruhe, Germany)
Phenyl-β-*D*-thioglucopyranosid	Sigma-Aldrich (Steinheim, Germany)

KCl (potassium chloride)	Carl Roth (Karlsruhe, Germany)
Quercetin	Sigma-Aldrich (Steinheim, Germany)
Quinine hydrochloride dihydrate	Sigma-Aldrich (Steinheim, Germany)
Salicylic aldehyde	FLUKA, Sigma-Aldrich (Steinheim, Germany)
Salicylic acid	Sigma-Aldrich (Steinheim, Germany)
Salicylic Acid 2-*O*-beta-*D*-Glucoside	Biozol (Eching, Deutschland)
NaCl (sodium chloride)	Carl Roth (Karlsruhe, Germany)
SDS (sodium dodecyl sulfate)	Carl Roth (Karlsruhe, Germany)
Sucrose	Duchefa (Haarlem, Netherlands)
Tris (tris(hydroxymethyl)-aminomethane)	Carl Roth (Karlsruhe, Germany)
tryptone	Sigma-Aldrich (Steinheim, Germany)
Tween® 20	Sigma-Aldrich (Steinheim, Germany)
UDP-α-*D*-glucose	Merck Millipore (Darmstadt, Germany)
Vanillin	Sigma-Aldrich (Steinheim, Germany)
yeast extract	Carl Roth (Karlsruhe, Germany)

9.2 List of primers

9.2.1 Primers used for quantitative real-time PCR (qPCR)

Table S1: Primers used for qRT-PCR analysis of SfUGTs responsible for benzoxazinoid detoxification and housekeeping genes from *Spodoptera frugiperda*. The list includes the sequences (5'-3' direction) and the size of the amplicon.

Gene	Name	Sequence	amplicon size [bp]
SfUGT5	qSfUGT5_1_F	5'-GTCGTTCAACGCTGAGAGATAC-3'	141
	qSfUGT5_1_R	5'-CGCAGTTTTACCATGTTCTCC-3'	
SfUGT11	qSfUG11_1_F	5'-CAACGAATGAAGAGGAATTCAAG-3'	104
	qSfUGT11_1_R	5'-AGGCTGGTCGTACATCACG-3'	
SfUGT14	qSfUG14_1_F	5'-CCGCTGCTATCGAAGAAAAC-3'	142
	qSfUGT14_1_R	5'-TCATGCCATACTTTGGATCG-3'	
SfUGT20	qSfUG20_1_F	5'-TCGCTAGAGGCTTTGCTTTG-3'	137
	qSfUGT20_1_R	5'-TCGGTCGTGGTAGATGTAGG-3'	
SfUGT29	qSfUG29_1_F	5'-TCGAAGGATTGCAGAGTGTG-3'	101
	qSfUGT29_1_R	5'-TGCTGTGTCCAAAGGATCTG-3'	
AK	Sf_AK_1_F	5'-TGGTATGGTGCAATGAGGAG-3'	132
	Sf_AK_1_R	5'-CATCGTGGGAGAAAGGAATG-3'	
EF1α	EFalpha_F	5'-GTCACCATTATTGACGCTCCCGGACACAGAG-3'	180
	EFalpha_R	5'-CTTGACACCGAGTGTGAAAGCGAGCAGAGC -3'	
GAPDH	Sf_GAPDH_1_F	5'-TGGATAACTTTGGCGAGAGG-3'	93
	Sf_GAPDH_1_R	5'-TGTCAACCTTGACGCTTACG-3'	
RpL10	Sf_RpL10_1_F	5'-ATTGGACAGCCCATCATGTC-3'	128
	Sf_RpL10_1_R	5'-AAGCCCCATTTCTTGGAGAC-3'	
UCCR	Sf_UCCR_1_F	5'-GCCATCGATGACACAAAGTG-3'	128
	Sf_UCCR_1_R	5'-ATGGACGTCAATCCTTCACC-3'	

9.2.2 Primers used for the amplification of new SfUGT candidates

Table S2: Primers used for the amplification of new UGT candidates. The list includes the sequences (5'-3' direction) with underlined start codon and the binding positions in the coding DNA sequences of the respective genes.

Gene	Name	Sequence	Position in the coding DNA sequence
SfUGT10	Sf_fUGT10_F	5'-CCGTTCGAAATGAAGGCT-3'	-9 - 9
	Sf_fUGT10_R	5'-ATTCTTCTTCTTATGCGCTAGTCT -3'	1610 - 1632
SfUGT26	Sf_fUGT26_F	5'-TTTGTAAATATGAAGCATAAAGTAATCG -3'	-9 - 19
	Sf_fUGT26_R	5'-GTGACTCTTCTCTTTTTTATTAGTCG-3'	1541 - 1566
SfUGT32	Sf_fUGT32_F	5'-AGAACAAAAATGGCGGATT-3'	-9 - 10
	Sf_fUGT32_R	5'-ATTCTTCTTCTCTTTTATATTCTTCTGAG -3'	1540 - 1566
SfUGT35	Sf_fUGT35_F	5'-TGTGCCGTAATGAAGTGG-3'	-9 - 9
	Sf_fUGT35_R	5'-CATTATTTTCTTTTTGCATATTTTCA-3'	1508 - 1533
SfUGT39	Sf_fUGT39_F	5'-AGCACAGAGATGAGGCCG-3'	-9 - 9
	Sf_fUGT39_R	5'-ATTGGGTTTCACTTTGTACTTCC-3'	1632 - 1610
SfUGT40	Sf_fUGT40_F	5'-TTAATAATAATGGAAAAGTTAATATGTTTT-3'	-9 - 21
	Sf_fUGT40_R	5'-ATTCTTCTTCTCTTTTATATTCTTCTGA-3'	1538 -1566
SfUGT41	Sf_fUGT41_F	5'-ATAGCCACAATGTCTCAGTTAACA-3'	-9 - 12
	Sf_fUGT41_R	5'-CTCACATTTTATTCTGATTCTCAAAT -3'	1556 - 1581
SfUGT42	Sf_fUGT42_F	5'-AGTGAGAACATGTTGCTGTGC-3'	-9 - 9
	Sf_fUGT42_R	5'-GTCTGCCTTAAGCTTCTTTAAAGT-3'	1564 - 1587
SfUGT43	Sf_fUGT43_F	5'-CGCGTCAAGATGTCACGT-3'	-9 - 6
	Sf_fUGT43_R	5'-GCTTTGTTTCAGTTTAATGTATTGAT-3'	1553 - 1578
SfUGT46	Sf_fUGT46_F	5'-GAAACCAACATGTCTCTAGTAAAGC-3'	-9 - 13
	Sf_fUGT46_R	5'-TGCGCGCTTAATTTTAATAATAG-3'	1625 - 1647

9.2.3 Primers used for the site-directed mutagenesis in the coding sequence of the catalytic region of UGTs

Table S3: Primers used for the site-directed mutagenesis in the coding DNA sequence of the catalytic region of two UDP-glycosyltransferases (SfUGTs) from *Spodoptera frugiperda*. The list includes the sequences (5'-3' direction) with underlined mutation site.

Gene	Name	Sequence
SfUGT5	1_SfUGT5_AT-TG_fwd	5'-ACCCTTCAATCAGCCTGCAAGTGGTTTTCCGA-3'
	1_SfUGT5_AT-TG_fwd	5'-TCGGAAAACCACTTGCAGGCTGATTGAAGGGT-3'
SfUGT29	5_SfUGT29_CAC-TTG_fwd	5'-CACACTGGAAAAAGTTTGCAAATGGTATTTGAT-3'
	5_SfUGT29_CAC-TTG_rev	5'-ATCAAATACCATTTGCAAACTTTTTCCAGTGTG-3'

9.2.4 Primers used for Sanger Sequencing

Table S4: Primers used for Sanger sequencing to confirm the sequence and right orientation of putative SfUGT genes of qPCR amplicons in the respective expression or sequencing vector. The list includes the sequences (5'-3' direction) and the size of the amplicon.

Vector	Name	Sequence	Position in the coding DNA sequence
pIB/V5-His-TOPO®	OpIE2_Fwd	5'-CGCAACGATCTGGTAAACAC-3'	511 - 530
	OpIE2_Rev	5'-GACAATACAAACTAAGATTTAGTCAG-3'	753 - 776
pCR®4Blunt-TOPO®	T7_primer	5'-CCCTATAGTGAGTCGTATTA-3'	328 - 347
	M13_Rev	5'-CAGGAAACAGCTATGAC-3'	205 - 221

9.3 Coding sequences of new SfUGT candidates

9.3.1 SfUGT10

Coding DNA sequence, 1542 bp

ATGAAGGCTACATTAGCAGCGCTGATGCTGTGTCTCTCCAGTGGGTTTGCTTACAAGATCCTGTGCATCCTT
CCTGTACCTTCGAAGAGTCATGACCACCTGTCTCTTGGTATCGTGAAGCCACTTCTGAAGGCTGGTCATCAG
GTGACATGGGCCACCCCGTATGAGAAGAAGAATATGCATGAAAACTTGACTGTGATAGAACTGAAGGAGAT
TCGGGAATTTGTTGAATCGGTGGACATCATGAGTAAAACGGACCTGGGCTTCCAGTACATGCGGAGCTTCG
CCCGGAACATCTCCATCGGTACTGCTCAGCATCCTGAGCTGCAGCGGGTGCTGGTGGAACAGCAGTTCGAT
GCTGTAGTGTCCATCTGGTTCATGAACGATTTCGAGGCTGGCTACGCAGCCATCCAGCAAGTGCCCTGGAT
CCTGGTGAGCTCTGTAGGCTATCACCCTTACCTGGAGAAGCAGGTGGACCAGGTCAGGTCCATCGCCACCG
TGCCTCTAGCATTCAATGACAACGGAGACCGACCCATGAATACCGTGAGGAGGTTCATCAATGGACTGATC
TATATGGTCATGAATTTCGATGAGTGGTTCGACAAACCCACCCTAACCTCTACATACGAATCCCTCTTCAGT
CCCCTAGCTGCAAGGAGAGGAGTACCTCTCCCCCCCTTTGAAAACGCCTACCACAACGTGTCCATACTCCTG
GCGAACTCCCATGAGTCTATTGGGTACCCCATGAGCCTACCCCCAAATGTCATCAACATAGCTGGGTATCAT
ATTGAAGAACCTGCGCCGTTGCCTAAGGACTTGCAAGACTTGCTGGACGGATCACCTCAAGGCGTGATCTA
CTTCAGCATGGGATCCATCCTACGCTCCGCAGCCCTAAAGCCTCACACTCGGGATGCTCTGCTGAAGCTGTT
CGCCTCCCTCCCTTACACAGTGCTGTGGAAGTTTGAGGAGCCTCTGAAGGACCTCCCTCCTAATGTCCACGT
CAGGTCTTGGATGCCTCAACTTAGTATACTTGTCCACAAGAACGTCCGTCTATTCATCACCCACGGTGGCCT
CCTCAGCACCTTGGAAGCGGTCTACGCTGGAGTACCACTCCTGGCGATACCGGTGTTCGGAGACCAGCCCT
CGAATGCTGAACGCGCTGAACTAGCTGGGTATGCTGTGAAGGTGGAGTTTAAAGATGACATGGTACCTGAT
GTGGAGGCAGCGCTGAAGAAGATGCTTAGTACTGATGTCTACTACAACAAAGTGAAGCAGATTTCTAAAAC
GTTCCGTCTACGCCCGGTTCCACCATCAGACCTGGTCAACTTCTACATAGAGTTGGCTATAGAGACCAAAGG
TGCATATCACATTCGCTCACCAGCGCTGGAATACAAATGGTATGAGCGATGGATGCTTGACTTTGTGCTCAT
TGTACTAGCCATGCTTGTCCTGTTCATCACGCTTGTCAAACTTCTCGTAACTAGCTGTCTCAGAAGAATACT
AGGCAAGAAGCAGAAGAGACTAGCGCATAAGAAGAAGAAT

Translated protein sequence, 514 aa, x kDa

MKATLAALMLCLSSGFAYKILCILPVPSKSHDHLSLGIVKPLLKAGHQVTWATPYEKKNMHENLTVIELKEIREFVE
SVDIMSKTDLGFQYMRSFARNISIGTAQHPELQRVLVEQQFDAVVSIWFMNDFEAGYAAIQQVPWILVSSVGYHPY
LEKQVDQVRSIATVPLAFNDNGDRPMNTVRRFINGLIYMVMNFDEWFDKPTLTSTYESLFSPLAARRGVPLPPFE
NAYHNVSILLANSHESIGYPMSLPPNVINIAGYHIEEPAPLPKDLQDLLDGSPQGVIYFSMGSILRSAALKPHTRDALL
KLFASLPYTVLWKFEEPLKDLPPNVHVRSWMPQLSILVHKNVRLFITHGGLLSTLEAVYAGVPLLAIPVFGDQPSN
AERAELAGYAVKVEFKDDMVPDVEAALKKMLSTDVYYNKVKQISKTFRLRPVPPSDLVNFYIELAIETKGAYHIRS
PALEYKWYERWMLDFVLIVLAMLVLFITLVKLLVTSCLRRILGKKQKRLAHKKKN

9.3.2 SfUGT26

Coding DNA sequence, 1566 bp

ATGAAGCATAAAGTAATCACCAGTATTTGTATACTAAGTCTATTAATATCGAGTGAGGCTCTAAGGATTCTA
GTATGTTATCCTATGACGTCCAAGAGCCACAGTATCTTAGGCTATGGTATCGTCAATCGACTGCTGGAAGCT
GGACATGAGGTGGTTCATATAACATCATTTCCAAATGGCAAAGTGGTTCAAAACCTCACTGAAATCGATGT
ATCATCTATAGCAGATGTATTCAAGAAGGATGCTGATGGAGTTGAAGCATTCAAATTGAAAAACTTAATCG
GAAAGGGCAACTTTGGGGACTCCGCTCTGTTTTTGTATTACGTTTATACAATACATAGAAACTTTTTGGAAG
AGCCCAGTGTTGTGAAATTGTTCAGTGACCCCAAAGAGAAGTTTGACGCTGTTGTTTTGGAGTGGTTCTTC
AATGAGATGAATGCTGGAATTCCAGCGCTGTTCAACTGTCCTCTAATCTGGGTATGTTCGACGGAGCCTCA
CTGGCAATCCATGAGAGTGATGGATGGGATCACCAACCCAGCATACACTCTAGACATATTTACACACAACAA
GCTGCCCTTGAACTTCTGGCAACGTGCTGAAGGACTGTGGAAGGTTGTGAAGAAAGCTGCCCAGGTGCTAA
TTCTCAACCAGTTTGAAAAAAGGGCGTACTATTCGATATACCCAGAGATCGCAGCCAAGCGAGGTGTAACA
ATGCCTTCATATGAAGAGGCGGTATACAATGGATCCTTCATGCTGATTAACGCTCATCCTTCCATTGGAGGA
GCCATAAAGCTCCCTCAAAATGCAGCAAACATCGCTGGTTACCACATAGATAAACTCAAACCTTTACCGAAG
GATCTGCAAAAAATAATGGACGAAGCGAAACACGGCGTCATTTACTTCAGCTTGGGATCTATCGTCCAAAG
CGATGGCATGTCTGAACAGATGCAAAAATCTATTCTGAATATGTTCAGTAAATATAAGCAGACTGTCATCTG
GAAGTTCGAGAGTGACATGAAGGACAATGTACCTGCTAACGTTCATCTTGTAAAATGGGCTCCACAGCAGA
GTATATTAGCCCATCCTAGCCTGAAACTGTTCATCACACATGGCGGTCAGCTCTCCACATCAGAAGCCATAC
ATTACGGAATACCTCTAGTTGGTATCCCTGTGATGGCTGACCAAGTCCTCAACATGATTTCCGTAGAAAACA
AGGGTTTTGGAGTCAAAGTTACCTTATCTGAAGACATGATACCAGAACTTGATGCAGCTGTCAGAAAAGTA
CTGACTGATGACGCATACAGAAAAAAATCCAAAGAAATTTCAGCTCTATTCCATGATCGTGTGATGACGCCA
GGCGCTGCTGTCCCATATTGGATAGAATACGTTGTGCGGACGCATGGTGCACGTCATCTCCGATCCCCTGC
AGTCGATGTCCCACTGTATCAAAAGCTTTACTTAGATCTAGCAGCATTCATAGCTGTAGTTGTAATTGTACT
CAAAAAGGCTGTGAAATATTTAATGAAGAAGAGAAATGCGACTAATAAAAAAGAGAAGAGTCAC

Translated protein sequence, 522 aa, x kDa

MKHKVITSICILSLLISSEALRILVCYPMTSKSHSILGYGIVNRLLEAGHEVVHITSFPNGKVVQNLTEIDVSSIADVFK
KDADGVEAFKLKNLIGKGNFGDSALFLYYVYTIHRNFLEEPSVVKLFSDPKEKFDAVVLEWFFNEMNAGIPALFNC
PLIWVCSTEPHWQSMRVMDGITNPAYTLDIFTHNKLPLNFWQRAEGLWKVVKKAAQVLILNQFEKRAYYSIYPEI
AAKRGVTMPSYEEAVYNGSFMLINAHPSIGGAIKLPQNAANIAGYHIDKLKPLPKDLQKIMDEAKHGVIYFSLGSIV
QSDGMSEQMQKSILNMFSKYKQTVIWKFESDMKDNVPANVHLVKWAPQQSILAHPSLKLFITHGGQLSTSEAIHYG
IPLVGIPVMADQVLNMISVENKGFGVKVTLSEDMIPELDAAVRKVLTDDAYRKKSKEISALFHDRVMTPGAAVPY
WIEYVVRTHGARHLRSPAVDVPLYQKLYLDLAAFIAVVVIVLKKAVKYLMKKRNATNKKEKSH

9.3.3 SfUGT35

Coding DNA sequence, 1533 bp

ATGAAGTGGTTAATATTATTAGGTCTGATATATTTTATATGTGATGTGGAAGGTCTAAAAGTGTTGGTATG
TTTCCCTTTACCCGTGAAGAGTTTAAGTATTTTGGGACAAGGAGCAGTCAGGCATCTGATGGAAGCTGGTC
ATGATGTAACATATATAACAGTGTATCCACTGAAATTGCAAGCGAAAAATTTTCGTCAAATTGATATCAGCA
GCAACGTTGCCCTAGTTGCAAAGGATGAAACCTTGACAATGGGGTACGTTCTTAATCATAAACTGGAAAGA
AACCATCCATATCAGATTCAAGAGTTTGCACAAGAAGCCGTAAGAATGACATTTAACCATGAGAACGTGAA
AAAGCTTTTGGAAGACCCAAATGTACATTTCGACGTTATCATTACGGACTTGATGGAATCAGAAGTGTATA
CTGGATTGGCGGTTTTATACAACTGTCCCATGGTATGGCTGTACTCCATGGGGGCACACTGGCAAGTACTG
CGACTGATAGACGTGGCTTCGAACCCTGCTTACGACCCGGACTACTTATCACCAAACATGCCTCCATTCACA
TTCGCACAAAGAGTGGAAGAACTGTGGTCGAGGATTTATTGGCAATACCTTAAAACATTCTACACCCAACCT
GAGGAGCGTAGGATATACGAGGCGGTCTTTGGCCCTCTGATGGCTAAACGTGGAAGAGTGCTTCCAGATTA
TGAAGATGTCATGTACAATGCTTCACTGGTATTTGCAAATGAACATGACGCGACACGCAACCGCTTGAGTA
CTCCACAGAACTTCAAGTATATCGGTGGATTCCATATTGAGGAACCGGTGAAGCCACTGCCAAAGGATCTT
CAAGAGCTCATAGACAATTCAAAACATGGCGTCATATATTTCAGTATGGGTTCATTTTTAAAAAGCAATTCT
TTGCCAAGGAAACTGGTCATGGAATTACTCCAGATGTTCGGAGAATTGAAACAAACAGTCATTTGGAAATT
CGAAGATAATAGTTTGCAAGATGTCCCGAAGAACGTTCATATTGTAAATTGGGCTCCACAACCGAGTATTTT
AGCTCATCCGAACGTCAGAATGTTCATCTCACACGGAGGTCAGCTCTCTTCTTTAGAAGCCATCCACTTTGG
AAAGCCTGTCATTGGAGTACCAGTATTCTTCGACCAGTTCACCAATATCTTTAAAGCAGAACGAAATGGATA
TGCTCTAAGAGTGCCATTGTCCCATAATTTGCCAAGAGACTTGAAACCTGCCATTAATACGATGTTAACTGA
TGATCGTTATGCCAAGAAAGCCAAAGAGCTGTCGGCTCTCTACCACGATCGTTTGACGAAGCCAGGCCAGG
CTCTCGTGTACTGGGTGGAACACGTAGTGCGCACACGGGGTGCTCATCACCTGCGCTCTCCAGCACTCCAC
GTACCTTTATACCAACGACTTTATCTCGATCTCTTAGCAATAATCCTTACTGTAGTATCTACGTTAATGTTA
CTGCTATTGAAAATATGCAAAAAGAAAATAATG

Translated protein sequence, 511 aa, 58.96 kDa

MKWLILLGLIYFICDVEGLKVLVCFPLPVKSLSILGQGAVRHLMEAGHDVTYITVYPLKLQAKNFRQIDISSNVALV
AKDETLTMGYVLNHKLERNHPYQIQEFAQEAVRMTFNHENVKKLLEDPNVHFDVIITDLMESEVYTGLAVLYNCP
MVWLYSMGAHWQVLRLIDVASNPAYDPDYLSPNMPPFTFAQRVEELWSRIYWQYLKTFYTQPEERRIYEAVFGP
LMAKRGRVLPDYEDVMYNASLVFANEHDATRNRLSTPQNFKYIGGFHIEEPVKPLPKDLQELIDNSKHGVIYFSMG
SFLKSNSLPRKLVMELLQMFGELKQTVIWKFEDNSLQD

9.3.4 SfUGT39

Coding DNA sequence, 1617 bp

ATGAGGCCGCGGCTCCTATGGCTGGTCCTCGCGTGGGCGGCGTCGGCGGAGGCAGCTCGCCTGCTCGCTGT
CTTGCCCACCAACACCAAGAGCCACTACGCGATGTACGGCCGGCTTCTCGATGCACTGGCCAGGAAGGACC
ACCACCTTACTATCGTTTCGCACTTCCCAATGAAAAATCCTCGACCGAATGTTCATCAAATAAGCCTCGCGG
GGACGATACCAGAAATCACTAACAATCTTACGAAGCAAAATGAATCATTAAAGCCCGATTTTATAAGAAACT
TGGAACAGATAATGAAAGAATGCGTGGACGCATGTGAGACTGCTGCCAAAGTACCAGCGGTCAAGGCATTA
TTCAATTCAACAGAGACTTTCGATCTGGTCATAGTTGAAGTGTTTGGAAGCGATTGCTTCCTACCTCTAGGC
AAGAAATATGGAGCTCCTGTGGTCGGCTTCCTCTCAAGTGTTCCACTCCCCTGGTTGAACGAGCAGCTTGG
AAACCCTGAAGCGACTGCCTACGTACCATCTTATATGGTCGGATATGGTCAACGGATGTCGCTATGGGAAA
GATTTGCTAACACCATGGCGGTGATCATAGCAAAAATGTTGTATAGATACAAATCGCAAATTCCGTCACAG
ACTATATCGGACAGACTTTTTGGACCGGGACCGAAATTGGAAACATTGGCACAAAACTATAGTTTGGTTTT
GTCGAACAGTCATTTCAGCATCAACGAAGTGAGGCCATTAGTTCCTGCTTTAGTAGAAGTTGGAGGGCTCC
ACTTAGACGATTCCCCAGTTCTTTCACGTCACATGCAAAATCTTTTGGACGCTTCAACGGAAGGCGTGATCT
ACTGGAGCTTCGGATCAATGTCGCGGATAGAAACAATACCAAGTGATACACTCTCACGAATATTTGACGTG
CTGTCGGAGCTACCTCAGACGGTGTTCATCAAGATGGACAGGCGTATGCTGGCCCAGAACCTCACAGTGCC
TGACAACGCATACACCATGGATTGGATACCACAGCATGCTACTTTATGTCACCCGAACGTGAAGCTGTTTAT
ATCGCACGGTGGACTGCTGGGCACACAAGAGGCTGTGGCCTGTGGGGTCCCCATGTTGATGGTGCCGCTGT
ACGCAGACCAGGCACTCAATGCACGAGCGATGGCTGACAGGGGTGTCGCACAAATTGTTACTCTCAAAAAT
ACCGATAAAGACACATGGAGACGAAAACTACGGGTGTTATTAACAGATCAACGATATAAAAATAGAGCAAT
GGAGTTGAAGAATATATTCTTGGATCGGCCGGTGAAGCCTTTGGATATGGGCGTTTACTGGATAGAATATG
TGCTGAGACATAGAGGAGCGTCGCACTTGCGGTCGCCCGCACTCGACCTCACCTACCCGCAGTACATGCTAC
TCGACGTAGTAGCACTAAGTACTGCCGTGGCGGTACTCACCATATACATACTACATAAGCTATTTAGGTACC
TATGTACGCGATGCATTCGCTGGTGGCCGAAAGAAAAATTAGTCTTCGAAAAGAGACTGTTGAGAAAGAAC
ATTAGTTTCTTCTTATGTATTTTATGGAAGTACAAAGTGAAACCCAAT

Translated protein sequence, 539 aa, 61.28 kDa

MRPRLLWLVLAWAASAEAARLLAVLPTNTKSHYAMYGRLLDALARKDHHLTIVSHFPMKNPRPNVHQISLAGTIP
EITNNLTKQNESLKPDFIRNLEQIMKECVDACETAAKVPAVKALFNSTETFDLVIVEVFGSDCFLPLGKKYGAPVV
GFLSSVPLPWLNEQLGNPEATAYVPSYMVGYGQRMSLWERFANTMAVIIAKMLYRYKSQIPSQTISDRLFGPGPKL
ETLAQNYSLVLSNSHFSINEVRPLVPALVEVGGLHLDDSPVLSRHMQNLLDASTEGVIYWSFGSMSRIETIPSDTLSR
IFDVLSELPQTVFIKMDRRMLAQNLTVPDNAYTMDWIPQHATLCHPNVKLFISHGGLLGTQEAVACGVPMLMVPL
YADQALNARAMADRGVAQIVTLKNTDKDTWRRKLRVLLTDQRYKNRAMELKNIFLDRPVKPLDMGVYWIEYVL
RHRGASHLRSPALDLTYPQYMLLDVVALSTAVAVLTIYILHKLFRYLCTRCIRWWPKEKLVFEKRLLRKNISFFLCI
LWKYKVKPN

9.3.5 SfUGT40

Coding DNA sequence, 1566 bp

ATGGAAAAGTTAATATGTTTTTTGTTTTGTGCGGTTGTAAGTTTGTGTTCATGTGATGCTTACAAGATCTTA
GCTGTGTTCCCGGTGCCGAGTCCCAGCCATGGGATCCTCGGAGACAATATGATTAAACATCTTCTTAATGCT
GGACATGAAGTAACCTACATAACGCCGTATGCAAGCAGACAGAAAAGTAATCCGAAATTACATATAGTGGA
TGTCACTGACCATCATAGCTTTTTTAATCCGGACATCCTAGACCTCACAGAGATTCTGGAAGGGACAGTGAA
CTTCAAGGATCACAACTTCGTGTTTTCTATGATGATGCACATTGCAGCAATGACGTTAGAACACAAGAATGT
CCAGAAGCTCATGAAAGATCCCCAACAGAAGTTTGATGTGATCATTGGCGAATACATGTTTACAGATCTGT
ATTCTACATTCCCAGCGGTATTCCAATGCCCCTACATCTGGTTTTCAACAGTTGAACCACATTGGATGGTAA
TGAACCTGGTCCATAGTCCGATGAACCCAGCTTATAATGGAGACTATATGTATGCCAATATACCACCATTCA
ACTTCATGCAAAGAGTCCAGGAGCTGTGGCTTCAATTGACTGGACTTTATCATCATAACAATGACTATTACC
AACGTGAAGAAGCAGTGTACCTAAAACATGTGGTCCCTATCTTGAAGGAGCAAGGCAAACCAGTACCTGAT
TATAATGTGCTGAAGTATAATGCATCACTACTGCTGGGCAACTCGCAAGTGGCAATTGGTAATGCAGTGCC
AATGCCACCAAGCTACAAGCACATTGGAGGTTACCATATTGATGATGAGGTTAAGCCCTTACCAGAGGATT
TGAAGAAGATTTTGGATAATGCCAAGAATGGCGTTATTTACTTCAGCATGGGCTCCAATTTGAAGAGCAAG
GACTTACCAGATGATCTAAAGAAAGGTCTGTTGGAAGTATTCGGGGGACTGAAGCAAACTGTCTTGTGGAA
GTTTGAAGAGAATCTACCGAACCAGCCTAAGAACGTTCATATAGTGCAGTGGGCACCACAGCAAAGTTTAT
TAGCACATCCCAATTTGAAGTTGTTCGTCACCCACGGTGGCCTCCTATCGCTCACCGAGGCGGTCCATTTCG
GAGTTCCAGTCATTGCCATTCCAGTCTTCGCTGACCAGTTCCTCAATGCAAACCAAATTCAACATAAAAGAA
TTGGAGAAAAAGTTGATCTTTCCCACAATTTGCCCAAGGATCTGAAGGTCGCTTTGGATAAAGTTCTCGGT
GATCTTCCCAGGTACACTGCCAAAGTTAAGGAGATGTCTGTAGCATACCACGACAGTCCGATGAAGCCAAA
AGAAGCATTGAACTTCTGGGTGGAGCACGTGGTGCGCACGCGCGGCGCCCCACACCTGCGCTCGGTGGCGC
TACAAGTGCCGCTGTACCAACAAGCGTACCTAGATCTGCTAGCTGTGCTACTGGCAGCTGCTGTTGGTATAT
TGCTGGTGGTTAGGAGGATTTTAAGCTTCTTTAAACCTCAGAAGAATATAAAAGAGAAGAAGAAGAAT

Translated protein sequence, 522 aa, 59.40 kDa

MEKLICFLFCAVVSLCSCDAYKILAVFPVPSPSHGILGDNMIKHLLNAGHEVTYITPYASRQKSNPKLHIVDVTDHHS
FFNPDILDLTEILEGTVNFKDHNFVFSMMMHIAAMTLEHKNVQKLMKDPQQKFDVIIGEYMFTDLYSTFPAVFQC
PYIWFSTVEPHWMVMNLVHSPMNPAYNGDYMYANIPPFNFMQRVQELWLQLTGLYHHNNDYYQREEAVYLKH
VVPILKEQGKPVPDYNVLKYNASLLLGNSQVAIGNAVPMPPSYKHIGGYHIDDEVKPLPEDLKKILDNAKNGVIYFS
MGSNLKSKDLPDDLKKGLLEVFGGLKQTVLWKFEENLPNQPKNVHIVQWAPQQSLLAHPNLKLFVTHGGLLSLTE
AVHFGVPVIAIPVFADQFLNANQIQHKRIGEKVDLSHNLPKDLKVALDKVLGDLPRYTAKVKEMSVAYHDSPMKP
KEALNFWVEHVVRTRGAPHLRSVALQVPLYQQAYLDLLAVLLAAAVGILLVVRRILSFFKPQKNIKEKKN

9.3.6 SfUGT42

Coding DNA sequence, 1536 bp

ATGTTGCTGTGCTATTTAATCAGTGTTTTAATCAGTGTCAATGAAGCAGCTAGAATCCTAGCAGTGTTTCCA
ACACCATCGATCAGTCACCAAATAGTATTCAGACCTTTAACTCAAGAACTAGCCAGAAGAGGCCATGACGTC
ACAATCATCACTCCTGATCCAGCCTTCCCAAAAGGAGAGACACCAGCTAACATCACAGAAATCGACGTACAT
GACATTTCATACAAACTATGGCACGACAGACTACTAACATCGATGGGTAAAGGAGAACAGGATGATTTGAA
AAGTCAAATAGAAATCTATTACGCAACAATACTGGAAATAGTACTACAACAGCTACAGAATAAAGAAGTAC
AAAAAGTGATTAGTGATAAACATAAGAAGTTTGATCTCTTATTTCTTGAAGCGTGTGTGAGACCCGCTCTTT
TATACTCTCATATCTACAACGCCCCTGTAATTCAAATCAGTTCGTTTGGGGCCATGCCTGGGAATTTAGAAG
CTGTTGGAGCACCGGACCATCCAATTCTCTATCCAAACATATTTCGACAAAAAACTAATAATATAACTACGA
AAGAGAAATTTGTGGAAATCTTCAAGTACTATGCCTTTAATATGATCCACAAAGGTTTTGAAGTGACTGAG
ACGGCAGCTATTAGGAAAGTCATTGGGCCTAATATGCCAGAAGTGGGGGAGTTGTTTAAAAACGTTCATAT
GTTGTTTCTAAATGTTCATCCAGTGTTTGAAGGTATTCGTCCTGTTCCTCCTAATGTTATTTACATGGGTGG
TTTGCATCAAAATCCTGTGAAGGAATTACCTAAAGATCTCAAGTCCTATTTGGACAATTCTAAGAATGGCGT
CATCTATGTAAGTTTCGGTACAAACGTGATAACTGATCAGTTGCCTAATCAAGTTCAAGATTTGATCAAAGT
GCTATCTCGCCTGCCTTATGATGTGCTACTTAAATGGGACGATGACGAACTACCTGGACGACCTAAAAATAT
TAGAGTTTCTAAATGGCTGCCGCAATCAGATTTGCTACGTCACCCAAACGTAAAACTATTCATAATGCAAGG
AGGTCTACAATCTACAGATGAAGCTATAACAGCAGGAGTACCTCTGATTGGTCTACCCATGCTAGCAGATCA
ATGGTTCAATGTGGAACGATATGAGTATCATGGAATAGGAATCAGAATTGATTGGGATACTTTTACTGAAG
AAAAATTCGAAAATGCTGTTACTAAAATAATTGGTAGTGAGAGCTATCGCCAAAACGTCATCAAGCTCCAAA
CTTTAATACACGATCAGCCAATGCGTCCACTAGAGCGCGCCGTGTGGTGGACGGAGCACGTGCTGCGTCAC
GGCGGCGCGAGACATCTGCGTGGACCTGCAGCCAACATGTCGTGGGCAGAGTACCACGAATTAGATTTAGT
CCTCTTCTTAATAACTAGCCTACTAATTCTAGTATTTATATTCATAGCACTTGTTTATTATGTTTGTAGATA
TTGCGTAACTTTAAAGAAGCTTAAGGCAGAC

Translated protein sequence, 512 aa, 58.61 kDa

MLLCYLISVLISVNEAARILAVFPTPSISHQIVFRPLTQELARRGHDVTIITPDPAFPKGETPANITEIDVHDISYKLWH
DRLLTSMGKGEQDDLKSQIEIYYATILEIVLQQLQNKEVQKVISDKHKKFDLLFLEACVRPALLYSHIYNAPVIQISSF
GAMPGNLEAVGAPDHPILYPNIFRQKTNNITTKEKFVEIFKYYAFNMIHKGFEVTETAAIRKVIGPNMPEVGELFK
NVHMLFLNVHPVFEGIRPVPPNVIYMGGLHQNPVKELPKDLKSYLDNSKNGVIYVSFGTNVITDQLPNQVQDLIKV
LSRLPYDVLLKWDDDELPGRPKNIRVSKWLPQSDLLRHPNVKLFIMQGGLQSTDEAITAGVPLIGLPMLADQWFN
VERYEYHGIGIRIDWDTFTEEKFENAVTKIIGSESYRQNVIKLQTLIHDQPMRPLERAVWWTEHVLRHGGARHLRG
PAANMSWAEYHELDLVLFLITSLLILVFIFIALVYYVCRYCVTLKKLKAD

9.3.7 SfUGT46

Coding DNA sequence, 1566 bp

ATGTCTCTAGTAAAGCTTTTGACTGTGGTTGCTTCTCTGGCTTTATCGATACCGACTAGTGATGGTGCTAAA
ATTCTGGGATTCTTCCCATTTCCGTCTATCAGTCACCAAGTCGTGTTCAGACCTCTGATGCAGGAACTCGCT
CGAAGAGGCCACGAAGTGACAGTCATCACACCAGATCCAGCCTTCCCCAAAGGAGGAACACCAGCCAATTT
GACCGAGATCGATGTCCACGATGCGTCATACCGCATATGGCACGAACAATTCGTTGGCACACCGAAAGGGC
ATAAAGGGAATTTTGTAAAAGATTTCAATATAATTTTCAACCTAAATGTAAAAATAGTTGATGTTGAATTAA
AAGATGTGGAAGTGCAAAGATTGCTTAATGATAAGAACCAGACGTTTGATCTGATATTCGCCGAAGCGATG
ATGAGACCTGCTGTAGTACTGTCCCATATATACAACGCTCCAGTGATTCTAATGAGTTCTTATGGAACGTTC
AGTGACAATTACGCAGTCATGGGTGCACCTATTCATCCATTTTTGTACCCGTTCTCTGTCAGTAGGAGATTG
CATAGTACATCTTTGTGGGACAAAATTGGACATTTGTACGATTACATAAGGATTGAGATTATACAGAGAAA
CAGCTACGTTGAAGAGAATCGAATGCTCAGATCACATTTTGGAGCGAACCTCCCATCGATTCAAGAGATGA
ACAACAATGTCGCTATGATGTTTTTGAATATGTATCCTGTTTTCGAAGGGAACCACCCCGTTCCTCCTTCTG
TTATACACATGGGTGGTATTCATCAGATTCCTGACAAGCCGTTGCCTAAGGACTTAAAATCATACCTAGATT
CTTCTAAAAACGGCGTAATCTACGTCAGTTTTGGTACAAACGTGGATCCAACATTGTTGCCTCCAGAGAAAA
TTGCAATGTTCATACGAGCATTCTCCAGATTGCCCTACGACGTGCTATGGAAGTGGAACAAGGACGAACTG
CCGGGACGTACGGACAATATCAAGATATCTAAATGGCTTCCACAGTCCGACCTGCTGAAACACCCAAAAATC
AAAGCATTCATAACACAAGGAGGTCTACAATCAACAGATGAGGCTATAACTGCGAGAGTACCTCTGATTGG
TATACCAATGTTTGGTGACCAATGGTACAATGTAGTCAAGTATGAAAAGCTGAAGATTGGACTGAAGTTGG
AATTAGACACCATTACTGAAGAAATTCTAGAAAATGCTATTCACAAAGTTATTGATGATGACAGTTATCGAC
GTAACATAGAAAAACTGAGAAGTGTTATGCAAGATGAACCAATGGCACCTCTAGAGCGCGCCGTGTGGTGG
ACGGAGCACGTGCTGCGTCACGGCGGCGCGAGACATCTGCGTGGACCTGCAGCCAACATGTCGTGGGCAGA
GTACCTCGAACTAGAATTAGTACTAACACTTCTCCTAGCCCTAATCATCACCACAGCTACCATCATTCTGCT
AGCTAAATATATATACGATCAAGTTTTAAGAAAATACATCGCTATTATTAAAATTAAGCGCGCA

Translated protein sequence, 522 aa, 59.51 kDa

MSLVKLLTVVASLALSIPTSDGAKILGFFPFPSISHQVVFRPLMQELARRGHEVTVITPDPAFPKGGTPANLTEIDVH
DASYRIWHEQFVGTPKGHKGNFVKDFNIIFNLNVKIVDVELKDVEVQRLLNDKNQTFDLIFAEAMMRPAVVLSHIY
NAPVILMSSYGTFSDNYAVMGAPIHPFLYPFSVSRRLHSTSLWDKIGHLYDYIRIEIIQRNSYVEENRMLRSHFGANL
PSIQEMNNNVAMMFLNMYPVFEGNHPVPPSVIHMGGIHQIPDKPLPKDLKSYLDSSKNGVIYVSFGTNVDPTLLPP
EKIAMFIRAFSRLPYDVLWKWNKDELPGRTDNIKISKWLPQSDLLKHPKIKAFITQGGLQSTDEAITARVPLIGIPM
FGDQWYNVVKYEKLKIGLKLELDTITEEILENAIHKVIDDDSYRRNIEKLRSVMQDEPMAPLERAVWWTEHVLRH
GGARHLRGPAANMSWAEYLELELVLTLLLALIITTATIILLAKYIYDQVLRKYIAIIKIKRA

9.4 Substrates used for enzymatic glucosylation activity assays

Table S5: List of substrates used for *in vitro* enzymatic assays and all parameters observed during LC-MS analysis of glucosylation product formation.
The list includes the name of all substrates tested in this work. The mass [m/z] of the expected glucosylation products and the product masses observed during a full-range (m/z = 60 - 1200) LC-Iontrap-MS analysis in both, positive and negative ionization mode are listed. Product retention times (R_t) [min] correspond to the respective HPLC methods used for separation. All used HPLC methods are summarized in 9.5. The extracted ion chromatograms (EICs) for analytes measured with Iontrap-MS are shown. For EICs separated by a semicolon (;), the sum of both EIC traces was used for quantification. The chosen ionization mode used for quantification is shown in brackets. For analytes determined by multiple reaction monitoring (MRM) with the API3200 MS/MS system, the Quadrupole 1 and 3 masses (Q1/Q3) used for quantification are listed. All MRM analyses were performed in negative ionization mode.
IAA: Indole acetic acid; BOA: 2-benzoxazolinone; 6-OH-BOA: 6-hydroxy-2-benzoxazolinone; MBOA: 6-methoxy-2-benzoxazolinone; DIMBOA: 2,4-dihydroxy-7-methoxy-1,4-benzoxazin-3-one; HMBOA: 2-hydroxy-7-methoxy-1,4-benzoxazin-3-one.

#	Name	expected product mass [m/z]	Observed product mass [m/z] (Iontrap)	R_t (product) [min]	HPLC method	EIC (ionization mode)	Q1/Q3 (MRM
1	Indole	279	280 $[M+H]^+$, 324 $[M+FA]^-$, 314 $[M+Cl]^-$	9.9	D	314; 324 (-)	
2	IAA	337	382 $[M+FA]^-$, 372 $[M+Cl]^-$	10.1	D	372; 382 (-)	
3	BOA	297	298 $[M+H]^+$, 336 $[M+K]^+$, 296 $[M-H]^-$, 342 $[M+FA]^-$	7.8	D	298; 336 (+)	
4	6-OH-BOA	313	312 $[M-H]^-$, 348 $[M+Cl]^-$, 358 $[M+FA]^+$ 312 $[M-H]^-$	5.4 4.5	D	312 (-)	
5	MBOA	327	328$[M+H]^+$, 326 $[M-H]^-$, 362 $[M+Cl]^-$, 372 $[M+FA]^-$	4.12	B		372/164
6	DIMBOA	327	328$[M+H]^+$, 326 $[M-H]^-$, 362 $[M+Cl]^-$, 372 $[M+FA]^-$	4.12	A		418/372
7	HMBOA	357	356$[M-H]^-$, 392 $[M+Cl]^-$, 402 $[M+FA]^-$	4.19	A		402/356
8	4-Nitrophenol	301	300 $[M-H]^-$, 336 $[M+Cl]^-$, 346 $[M+FA]^-$	3.86	A		336/138
9	1-Naphthol	306	306 $[M-H]^-$, 341 $[M+Cl]^-$, 351 $[M+FA]^-$	0.92	B		305/143

#	Name	expected product mass [m/z]	Observed product mass [m/z] (Iontrap)	R_t (product) [min]	HPLC method	EIC (ionization mode)	Q1/Q3 (MRM)
10	Salicylic aldehyde	284	283 $[M-H]^-$, 319 $[M+Cl]^-$, 329 $[M+FA]^-$	2.84	C		329/121
11	Salicylic acid	300	299 $[M-H]^-$, 335 $[M+Cl]^-$, 345 $[M+FA]^-$	2.79	C		299/137
12	Vanillin	314	313 $[M-H]^-$, 349 $[M+Cl]^-$, 359 $[M+FA]^-$	7.5	D	313; 359 (-)	
13	Catechol	272	271 $[M-H]^-$, 317 $[M+Cl]^-$, 317 $[M+FA]^-$	7.8	D	271; 307 (-)	
14	*L*-Tyrosine	343	n. d.	n. d.	E		
15	*L*-DOPA	359		n. d.	E		
16	Dopamine	315	n. d.	n. d.	E		
17	Quercetin	464	463 $[M-H]^-$	10.2 11.3 11.8	D	463 (-)	
18	(±)-Menthol	318	353 $[M+Cl]^-$, 363 $[M+FA]^-$, 341 $[M+Na]^+$, 357 $[M+K]^+$	13.8 14.2	D	341; 357 (+)	
19	Esculetin	340	339 $[M-H]^-$, 375 $[M+Cl]^-$, 341 $[M+H]^+$, 363 $[M+Na]^+$	3.35	A		339/177
20	Capsaicin	467	466 $[M-H]^-$, 512 $[M+FA]^-$	15.1	D	467; 512 (-)	
22	Thiophenol	272	271 $[M-H]^-$, 317 $[M+FA]^-$	4.12	A		217/109

#	Name	expected product mass [m/z]	Observed product mass [m/z] (Iontrap)	R_t (product) [min]	HPLC method	EIC (ionization mode)	Q1/Q3 (MRM)
21	Gossypol	680	679 $[M\text{-}H]^-$	3.98 4.17 4.52	B		679/517
23	Quinine	n. d.	486	n. d.	D		

9.5 Used HPLC methods

9.5.1 HPLC methods used with the Agilent 1200 HPLC system

Table S6: HPLC methods performed on the Agilent 1200 (Agilent Technologies, Boeblingen, Germany) HPLC system. A sample volume of 5 μl was applied and separated using a Zorbax Eclipse XDB-C18 column (4.6 x 50 mm, 1.8 μm) in combination with 0.05% formic acid (FA) in water and acetonitrile (ACN) as mobile phases A and B. The flow rate was 1.1 ml/min. Analytes were subsequently analyzed by multiple reaction monitoring (MRM) using the API3200 triple quadrupole system (see 9.6.

Method	Solvent A	Solvent B	Gradient
A	0.05% FA	ACN	0 - 0.5 min, 95% A; 0.5 - 6 min, 95-67.5% A; 6.02 - 7 min, 100% B; 7.1 - 9.5 min, 95% A
B	0.05% FA	ACN	0 - 0.5 min, 70% A; 0.5 - 5 min, 30-100% B; 5 - 6 min, 100% B; 6 - 6.1 min, 0-70% A; 6.1 - 8.5 min, 70% A
C	0.05% FA	ACN	0 - 0.5 min, 95% A; 0.5 - 4.5 min, 95-35% A; 4.52 - 5 min, 100% B; 5 - 5.1 min, 0-95% A; 5.1 - 8 min, 95% A

9.5.2 HPLC methods used with the Agilent 1100 HPLC system

Table S7: HPLC methods performed on the Agilent 1200 (Agilent Technologies, Boeblingen, DE) HPLC system. A sample volume of 10 μl was applied and separated using a EC 250/4.6 Nucleodur Sphinx RP 5 column (250 x 4.6 mm, 5 μm) in combination with 0.2% formic acid (FA) in water and acetonitrile (ACN) as mobile phases A and B. The flow rate was 1.0 ml/min. Analytes were subsequently analyzed by full-range (m/z = 60 - 1200) Iontrap-MS using the Esquire 6000 MS^n system.

Method	Solvent A	Solvent B	Gradient
D	0.2% FA	ACN	0 - 15 min, 10 – 59% B; 15 -15.01 min, 59 - 100% B; 15.01 - 17 min, 100% B; 17 - 17.01 min, 100-90% B; 17.1 - 21 min, 90 % B
E	0.2% FA	ACN	0 - 2.5 min, 0.5% B; 2.5 - 8 min, 0.5 - 6.9% B; 8.1 - 11 min, 6.9 - 100% B; 11 - 11.01 min, 100 - 0.5% A; 11.01 - 15 min, 0.5% A

9.6 Parameters for multiple reaction monitoring (MRM)

Table S8: Parameters for Multiple Reaction Monitoring (MRM) used for the analysis of product formation by enzymatic assays. CE: collision energy; CEP: collision cell entrance potential; CXP: collision cell exit potential; DP: declustering potential; EP: entrance potential; DIMBOA-Glc: 2,4-dihydroxy-7-methoxy-1,4-benzoxazin-3-one glucoside; HMBOA-Glc: 2-hydroxy-7-methoxy-1,4-benzoxazin-3-one glucoside; MBOA-Glc: 6-methoxy-2-benzoxazolinone glucoside; Q1: Quadrupol 1; Q3: Quadrupol 3; SA-Glc: salicylic acid glucoside; Inf.: MRM parameters were obtained by infusion experiment with compound optimization; Lit.: literature.

Analyte	**Q1 [m/z]**	**Q3 [m/z]**	**time [ms]**	**DP [V]**	**EP [V]**	**CEP [V]**	**CE [V]**	**CXP [V]**	**Lit.**
MBOA-Glc	372	164	10	-15	-4.5	-18	-20	-4	[35, 54]
DIMBOA-Glc	418	372	10	-22	-4	-25	-18	-5	[35, 54]
HMBOA-Glc	402	356	10	-22	-4	-25	-18	-5	[35, 54]
4-Nitro-phenol-Glc	346	138	10	-20	-6	-24	-18	-4	Inf.
1-Napthtol-Glc	305	134	10	-35	-8	-20	-20	-15	[70]
Helicin	329	121	10	-20	-8	-18	-20	-2	[71]
SA-Glc	299	137	10	-25	-8.5	-16	-18	-4	[71]
Esculin	339	177	10	-45	-8.5	-20	-30	-4	Inf.
Gossypol-Glc	679	517	10	-30	-8	-42.21	-40	-4	[70]
Thio-phenol-Glc	317	109	10	-15	-3.5	-18	-22	-2	Inf.

9.7 Substrate specificities of SfUGTs expressed in insect cells

9.7.1 Total and net amounts of glucosides formed by UGT-transfected microsomal fractions

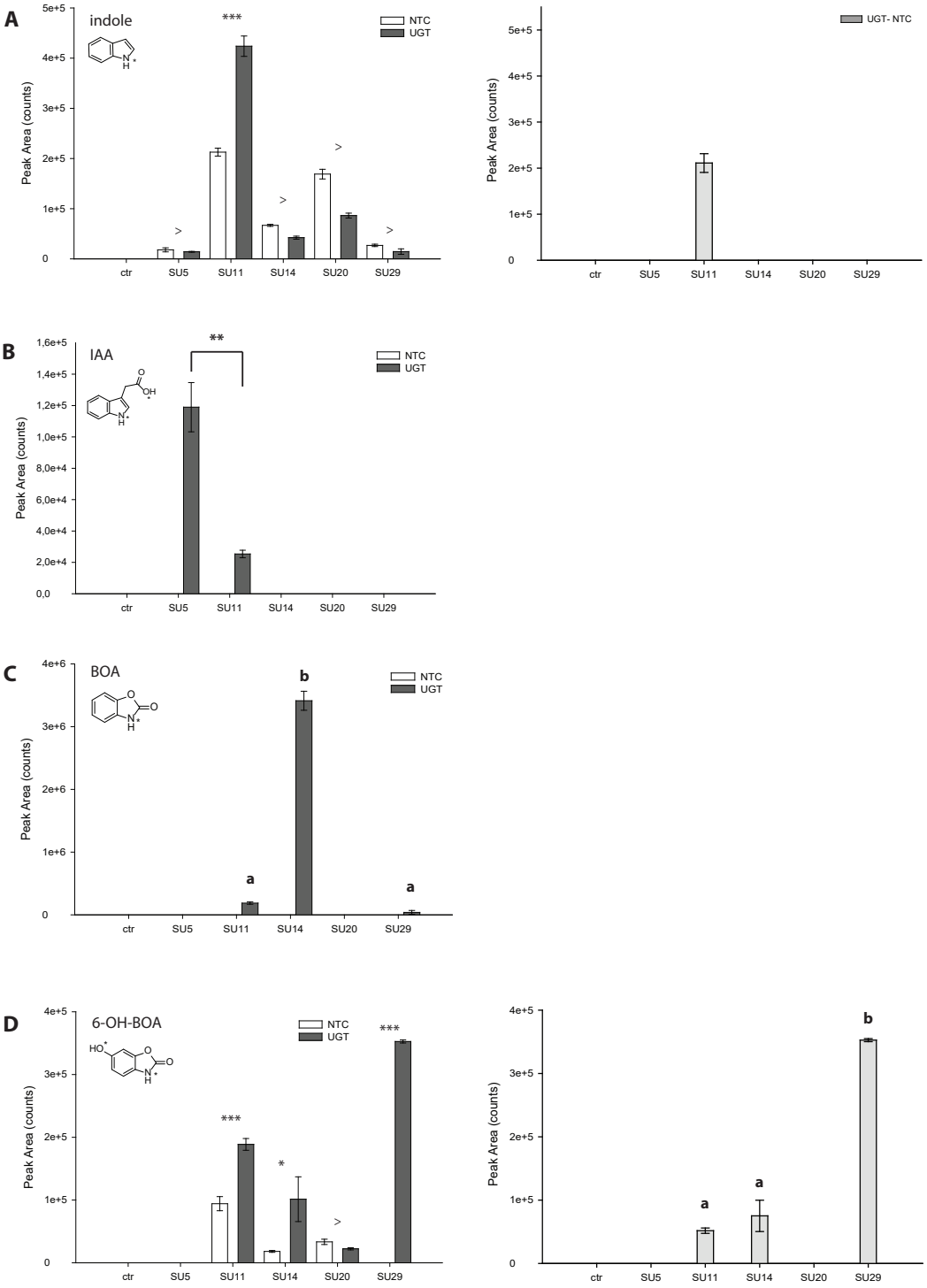

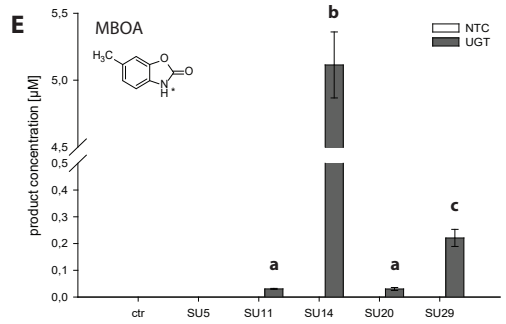
E
MBOA
NTC
UGT
product concentration [µM]
5,5
5,0
4,5
0,5
0,4
0,3
0,2
0,1
0,0
a
b
a
c
ctr
SU5
SU11
SU14
SU20
SU29

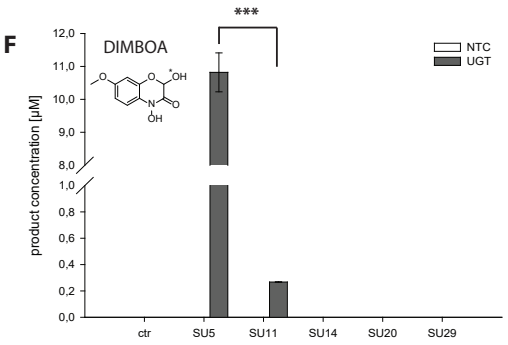
F
DIMBOA
NTC
UGT
***
product concentration [µM]
12,0
11,0
10,0
9,0
8,0
1,0
0,8
0,6
0,4
0,2
0,0
ctr
SU5
SU11
SU14
SU20
SU29

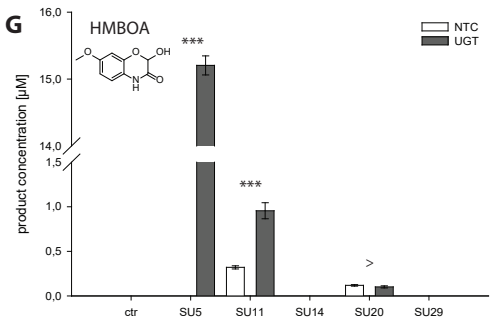
G
HMBOA
NTC
UGT
***
***
>
product concentration [µM]
16,0
15,0
14,0
1,5
1,0
0,5
0,0
ctr
SU5
SU11
SU14
SU20
SU29

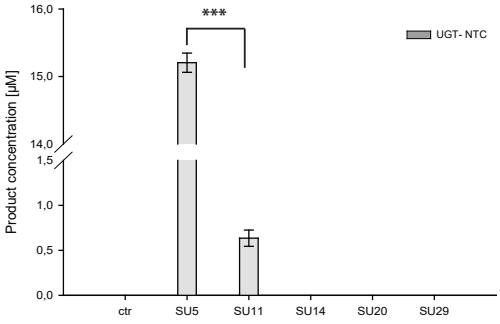
***
UGT- NTC
Product concentration [µM]
16,0
15,0
14,0
1,5
1,0
0,5
0,0
ctr
SU5
SU11
SU14
SU20
SU29

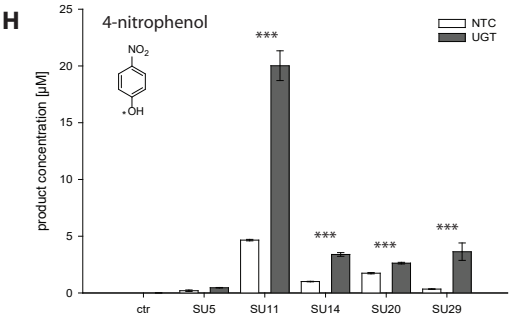
H
4-nitrophenol
NTC
UGT
***
***
***
***
product concentration [µM]
25
20
15
10
5
0
ctr
SU5
SU11
SU14
SU20
SU29

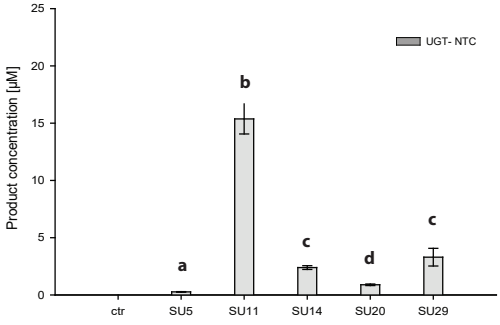
UGT- NTC
Product concentration [µM]
25
20
15
10
5
0
a
b
c
d
c
ctr
SU5
SU11
SU14
SU20
SU29

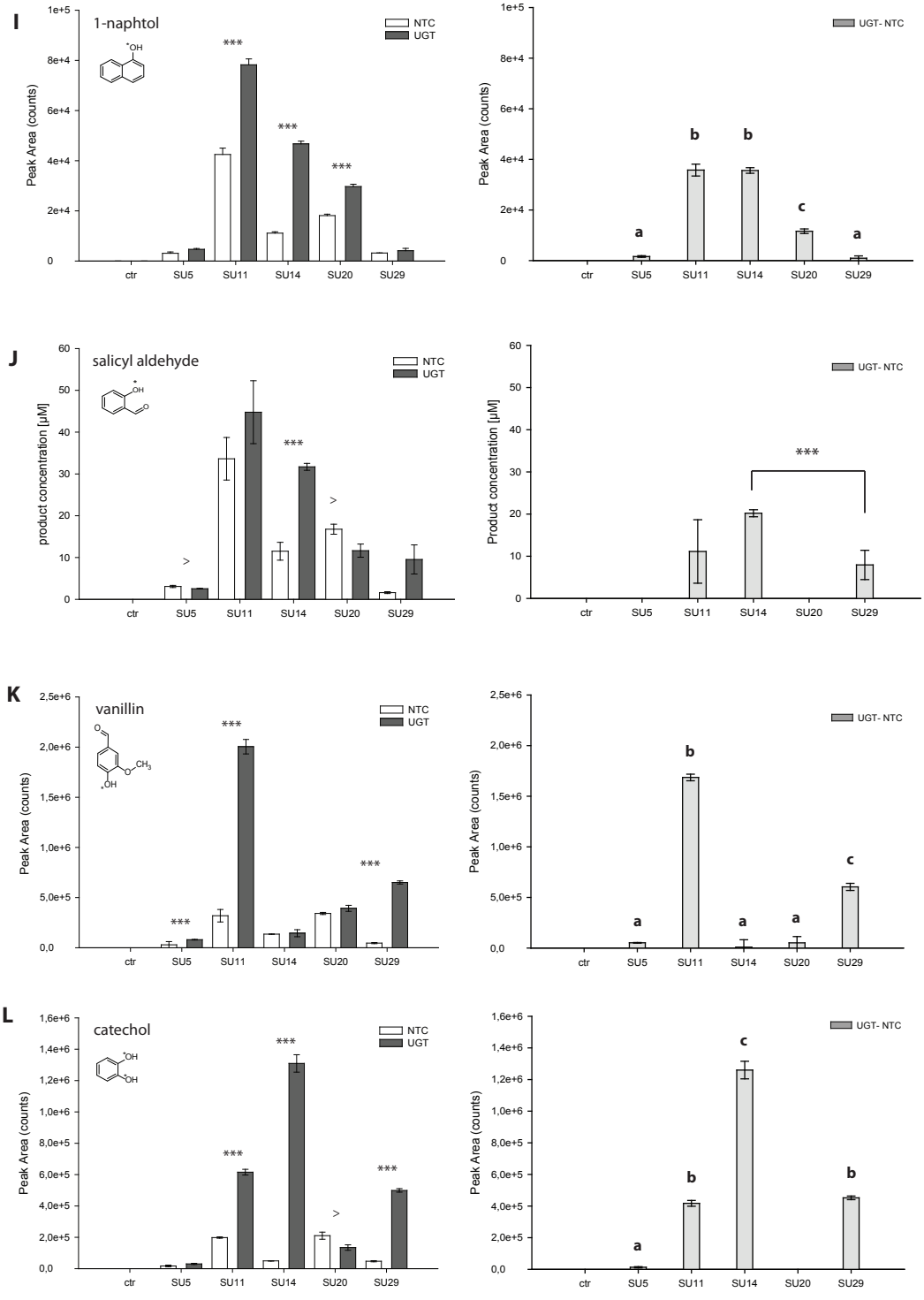
I
1-naphtol
NTC
UGT
Peak Area (counts)
1e+5
8e+4
6e+4
4e+4
2e+4
0
***
***
***
ctr
SU5
SU11
SU14
SU20
SU29
UGT- NTC
a
b
b
c
a
J
salicyl aldehyde
product concentration [µM]
>
>
Product concentration [µM]
60
50
40
30
20
10
K
vanillin
2,5e+6
2,0e+6
1,5e+6
1,0e+6
5,0e+5
0,0
L
catechol
1,6e+6
1,4e+6
1,2e+6
1,0e+6
8,0e+5
6,0e+5
4,0e+5
2,0e+5

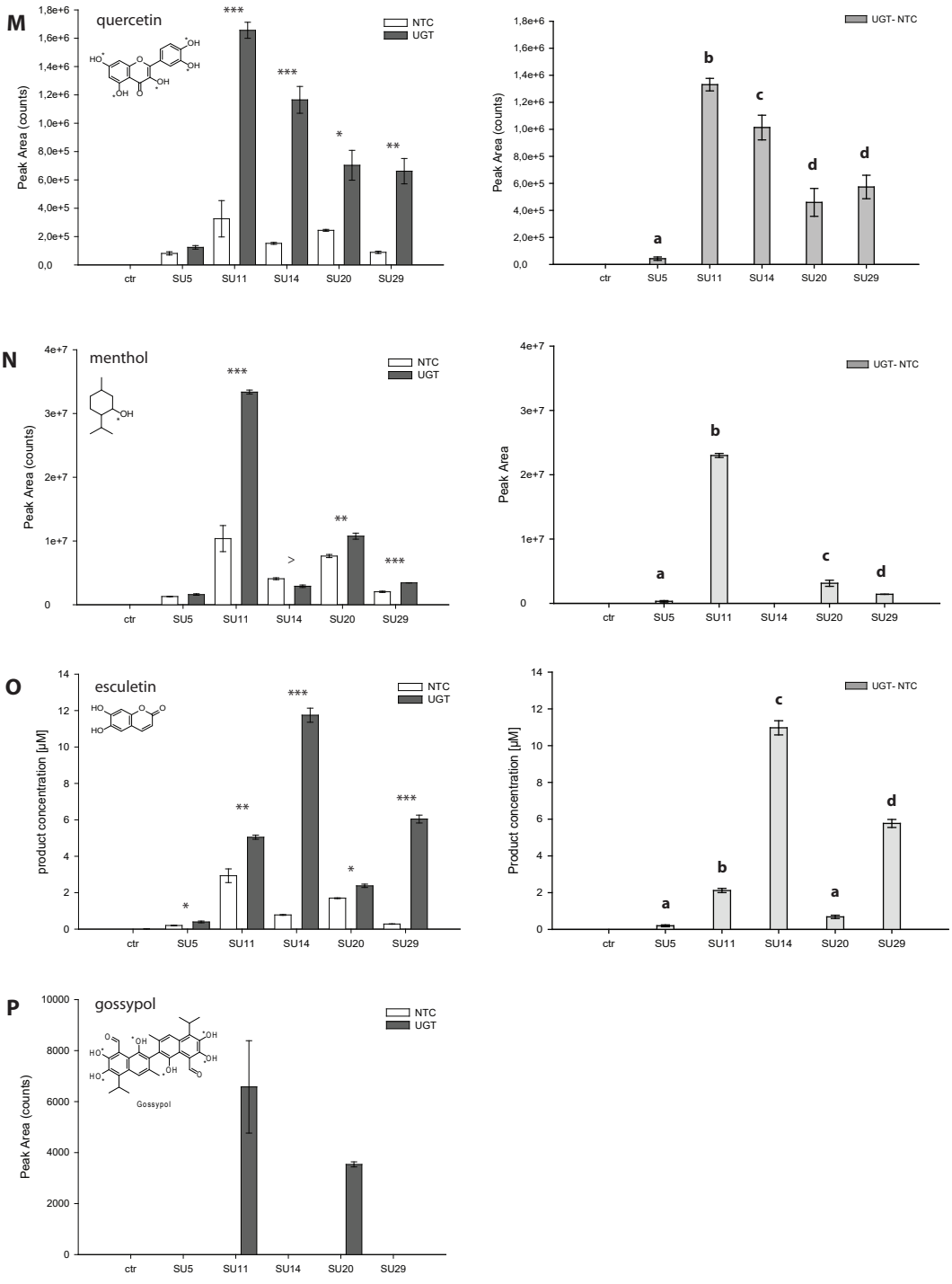
M
quercetin
NTC
UGT
Peak Area (counts)
1,8e+6
1,6e+6
1,4e+6
1,2e+6
1,0e+6
8,0e+5
6,0e+5
4,0e+5
2,0e+5
0,0
***
***
*
**
ctr
SU5
SU11
SU14
SU20
SU29
UGT- NTC
a
b
c
d
d
N
menthol
4e+7
3e+7
2e+7
1e+7
0
>
Peak Area
O
esculetin
product concentration [µM]
14
12
10
8
6
4
2
0
Product concentration [µM]
P
gossypol
Gossypol
10000
8000
6000
4000
2000

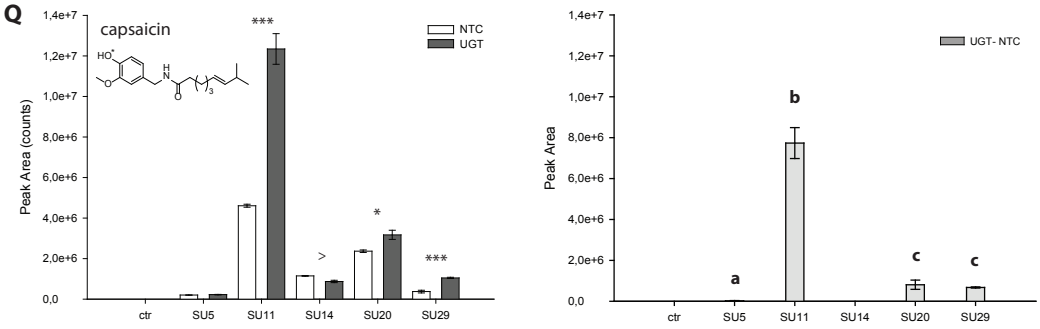

Figure S1: Substrate specificities of SfUGTs 5, 11, 14, 20 and 29 among 20 structurally various substrates. Results of the substrate screening are illustrated in two bar charts per tested substrate. The first chart (left) compares the product formation of each UGT-transfected microsomal fraction (UGT, dark-gray bars) to the UGT activity observed for the corresponding total protein amount of a non-transfected control (NTC, white bars). Results from a t-test, comparing the UGT activity to its respective NTC, are indicated by asterisks ($P < 0.05$ (*), $P < 0.01$ (**) and $P < 0.001$ (***). The second chart (right) shows the net amounts of glucosides formed by the recombinant UGT resulting after subtracting of glucoside amount formed by the NTC (UGT-NTC, light-gray bars). When NTC activity exceeded the UGT activity (indicated by a > in the left bar chart), net glucoside formation was set to 0. Results from one-way analysis of variance (ANOVA), comparing the net glucoside amounts formed by each enzyme, are indicated by small letters (a-d). Detailed information on the statistical analysis are listed in 9.9.1.

9.7.2 Enzymatic assays resulting in different isomers of glucosides

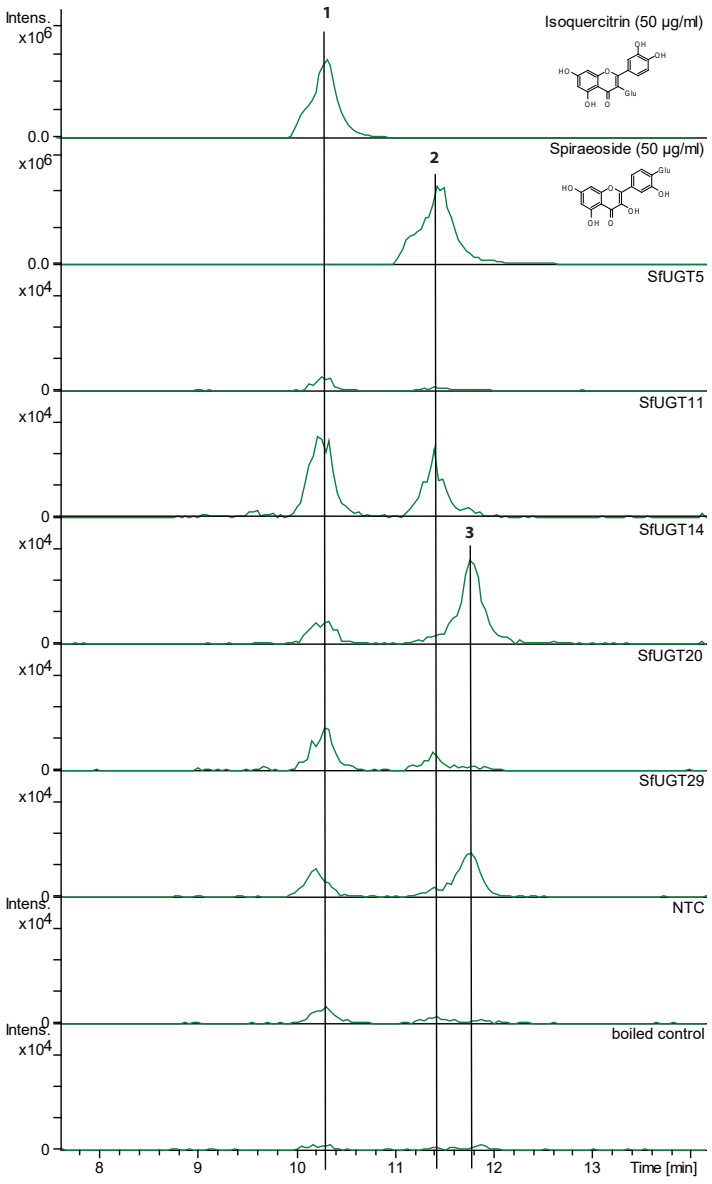

Figure S2: Comparison of the formation of isomers formed during the glucosylation of 6-OH-BOA.

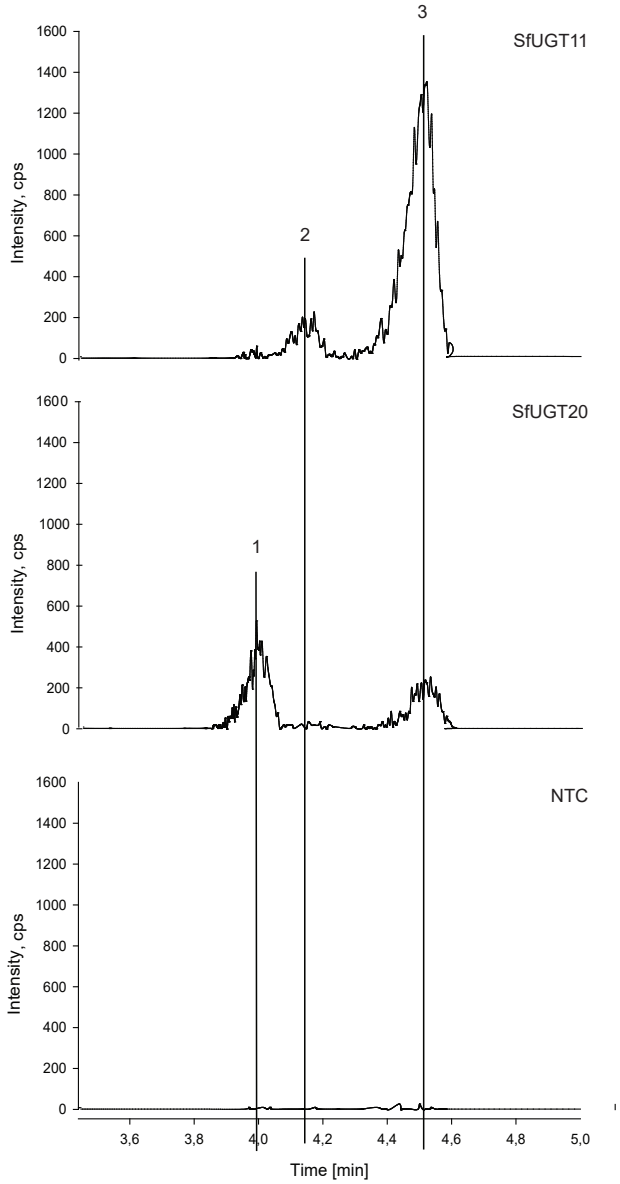

Figure S3: Comparison of the formation of isomers formed during the glucosylation of gossypol.

9.8 Total amounts of glucosides formed by SfUGTs 5 and 29 and their respective H35L mutants

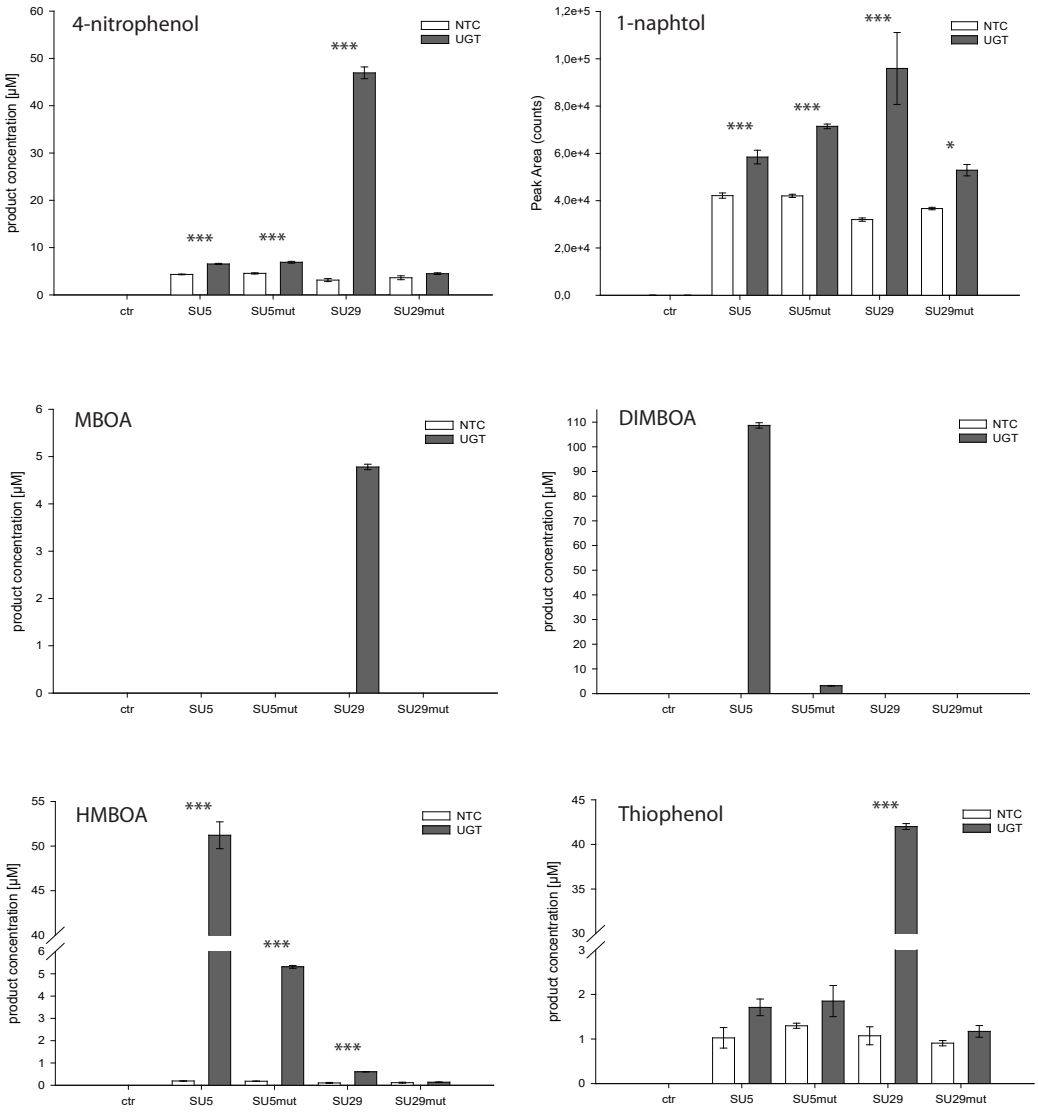

Figure S4: Mutational analysis of the importance of the catalytic H35 in UGTs from *S. frugiperda*.
The net amounts of glucosides formed by SfUGT-containing microsomes extracted from transfected insect cells are illustrated as mean ± standard error of three replicate determinations. Net glucoside amounts were calculated via subtraction of the glucoside amounts formed by non-transfected controls from the total amount of glucosides formed by UGT-transfected cells. Total protein amounts were adjusted according to the calculated relative expression levels via western blot. Differences between the net glucoside formation of mutant UGTs (SfUGT_*mut*) and their corresponding wild type (SfUGT) were analyzed via Student's t-test. Results are indicated by asterisks (* - $P < 0.05$, **- $P < 0.01$, *** - $P < 0.001$). Gain or loss of activity in the mutant protein compared to the wild type is given in %.

9.9 Statistical analysis

9.9.1 Substrate screening

Table S9: Statistical Analysis of Substrate Screening. a - data was log-transformed before analysis.

substrate	**test**	**comparison**	**results**	
Indole	t-test	SU11 vs. NTC	$P < 0.001$	
Indole-3-acetic acid	t-test	SU5 vs. NTC	$P < 0.001$	
		SU11 vs. NTC	$P < 0.001$	
		△SU5 vs. △SU11	$P = 0.004$	
BOA	One-way ANOVA	△SU11, △SU14, △SU29	$P < 0.001$; $F = 422.434$	
	Student Newman Keuls	**comparison**	**P-value**	**P < 0.05?**
		△SU11 vs. △SU14	< 0.001	Yes
		△SU14 vs. △SU29	< 0.001	Yes
		△SU11 vs. △SU29	0.748	No
6-OH-BOA	t-test	SU11 vs. NTC	$P < 0.001$	
		SU14 vs. NTC	$P = 0.019$	
		SU29 vs. NTC	$P < 0.001$	
	One-way ANOVA	△SU11, △SU14, △SU29	$P < 0.021$; $F = 7.801$	
	Student Newman Keuls	**comparison**	**P-value**	**P < 0.05?**
		△SU29 vs. △SU14	0.022	Yes
		△SU29 vs. △SU11	0.026	Yes
		△SU11 vs. △SU14	0.456	No
MBOA	One-way ANOVA [a]	△SU11 - △SU29	$P < 0.001$; $F = 350.683$	
	Student Newman Keuls [a]	**comparison**	**P-value**	**P < 0.05?**
		SU14 vs. SU20	< 0.001	Yes
		SU14 vs. SU11	< 0.001	Yes
		SU14 vs. SU29	< 0.001	Yes
		SU29 vs. SU20	< 0.001	Yes
		SU29 vs. SU11	< 0.001	Yes
		SU11 vs. SU20	< 0.792	No
DIMBOA	t-test	SU5 vs. SU11	$P < 0.001$	
HMBOA	t-test	SU5 vs. NTC	$P < 0.001$	
		SU11 vs. NTC	$P < 0.001$ [a]	
		△SU5 vs. △SU11	$P < 0.001$	
4-nitrophenol	t-test	SU5 vs. NTC	$P < 0.02$	
		SU11 vs. NTC	$P < 0.001$	
		SU14 vs. NTC	$P < 0.001$	
		SU20 vs. NTC	$P < 0.001$	
		SU29 vs. NTC	$P < 0.001$ [a]	
	One-way ANOVA [a]	△SU5 - △SU29	$P < 0.001$; $F = 123.364$	
	Student Newman Keuls [a]	**comparison**	**P-value**	**P < 0.05?**
		△SU11 vs. △SU5	< 0.001	Yes
		△SU11 vs. △SU20	< 0.001	Yes
		△SU11 vs. △SU14	< 0.001	Yes
		△SU11 vs. △SU29	< 0.001	Yes
		△SU29 vs. △SU5	< 0.001	Yes

4-nitrophenol	Student Newman Keuls [a]	△SU29 vs. △SU20	< 0.001	Yes
		△SU29 vs. △SU14	0.198	No
		△SU14 vs. △SU5	< 0.001	Yes
		△SU14 vs. △SU20	< 0.001	Yes
		△SU20 vs. △SU14	< 0.001	Yes
1-naphthol	t-test	SU5 vs. NTC	P = 0.063	
		SU11 vs. NTC	P < 0.001	
		SU14 vs. NTC	P < 0.001	
		SU20 vs. NTC	P < 0.001	
		SU29 vs. NTC	P = 0.377	
	One-way ANOVA	△SU5 - △SU29	P < 0.001; F = 180.286	
	Student Newman Keuls	**comparison**	**P-value**	**P < 0.05?**
		△SU11 vs. △SU29	< 0.001	Yes
		△SU11 vs. △SU5	< 0.001	Yes
		△SU11 vs. △SU20	< 0.001	Yes
		△SU11 vs. △SU14	0.930	No
		△SU14 vs. △SU29	< 0.001	Yes
		△SU14 vs. △SU5	< 0.001	Yes
		△SU14 vs. △SU20	< 0.001	Yes
		△SU20 vs. △SU29	< 0.001	Yes
		△SU20 vs. △SU5	< 0.001	Yes
		△SU5 vs. △SU29	0.720	No
Salicyl aldehyde	t-test	SU11 vs. NTC	P = 0.287	
		SU14 vs. NTC	P < 0.001	
		SU29 vs. NTC	P = 0.056	
		△SU11 vs. △SU29	P < 0.001	
Vanillin	t-test	SU5 vs. NTC	P < 0.001	
		SU11 vs. NTC	P < 0.001	
		SU14 vs. NTC	P = 0.907	
		SU20 vs. NTC	P = 0.474	
		SU19 vs. NTC	P < 0.001	
	One-way ANOVA	△SU5 - △SU29	P < 0.001; F = 224.074	
	Student Newman Keuls	**comparison**	**P-value**	**P < 0.05?**
		△SU11 vs. △SU14	< 0.001	Yes
		△SU11 vs. △SU20	< 0.001	Yes
		△SU11 vs. △SU5	< 0.001	Yes
		△SU11 vs. △SU29	< 0.001	Yes
		△SU29 vs. △SU14	< 0.001	Yes
		△SU29 vs. △SU20	< 0.001	Yes
		△SU29 vs. △SU5	< 0.001	Yes
		△SU5 vs. △SU14	0.809	No
		△SU5 vs. △SU20	0.992	No
		△SU20 vs. △SU14	0.551	No
Catechol	t-test	SU5 vs. NTC	P = 0.114	
		SU11 vs. NTC	P < 0.001	
		SU14 vs. NTC	P = 0.907	

		SU29 vs. NTC	P < 0.001	
	One-way ANOVA	△SU5 - △SU29	P < 0.001; F = 305.524	
	Student Newman Keuls	**comparison**	**P-value**	**P < 0.05?**
		△SU14 vs. △SU5	< 0.001	Yes
		△SU14 vs. △SU11	< 0.001	Yes
		△SU14 vs. △SU29	< 0.001	Yes
		△SU29 vs. △SU5	< 0.001	Yes
		△SU29 vs. △SU11	0.433	No
		△SU11 vs. △SU5	< 0.001	Yes
Quercetin	t-test	SU5 vs. NTC	P = 0.068	
		SU11 vs. NTC	P < 0.001	
		SU14 vs. NTC	P < 0.001	
		SU20 vs. NTC	P = 0.011	
		SU29 vs. NTC	P = 0.003	
	One-way ANOVA	△SU5 - △SU29	P < 0.001; F = 43.331	
	Student Newman Keuls	**comparison**	**P-value**	**P < 0.05?**
		△SU11 vs. △SU5	< 0.001	Yes
		△SU11 vs. △SU20	< 0.001	Yes
		△SU11 vs. △SU29	< 0.001	Yes
		△SU11 vs. △SU14	0.015	Yes
		△SU14 vs. △SU5	< 0.001	Yes
		△SU14 vs. △SU20	0.001	Yes
		△SU14 vs. △SU29	0.002	Yes
		△SU29 vs. △SU5	0.002	Yes
		△SU29 vs. △SU20	0.314	No
		△SU20 vs. △SU5	0.003	Yes
Menthol	t-test	SU5 vs. NTC	P = 0.063	
		SU11 vs. NTC	P < 0.001	
		SU20 vs. NTC	P = 0.004	
		SU29 vs. NTC	P < 0.001	
	One-way ANOVA	△SU5, △SU11, △SU20, △SU29	P < 0.001; F = 1363.681	
	Student Newman Keuls	**comparison**	**P-value**	**P < 0.05?**
		△SU11 vs. △SU5	< 0.001	Yes
		△SU11 vs. △SU29	< 0.001	Yes
		△SU11 vs. △SU20	< 0.001	Yes
		△SU20 vs. △SU5	0.015	Yes
		△SU20 vs. △SU29	0.003	Yes
		△SU29 vs. △SU5	0.029	Yes
Esculetin	t-test	SU5 vs. NTC	P = 0.018	
		SU11 vs. NTC	P = 0.006	
		SU14 vs. NTC	P < 0.001	
		SU20 vs. NTC	P = 0.002	
		SU29 vs. NTC	P < 0.001	
	One-way ANOVA	△SU5 - △SU29	P < 0.001; F = 459.567	
	Student Newman Keuls	**comparison**	**P-value**	**P < 0.05?**
		△SU14 vs. △SU5	< 0.001	Yes
		△SU14 vs. △SU20	< 0.001	Yes
		△SU14 vs. △SU11	< 0.001	Yes
		△SU14 vs. △SU29	< 0.001	Yes

		△SU29 vs. △SU5	< 0.001	Yes
		△SU29 vs. △SU20	< 0.001	Yes
		△SU29 vs. △SU11	< 0.001	Yes
		△SU11 vs. △SU5	< 0.001	Yes
		△SU11 vs. △SU20	< 0.001	Yes
		△SU20 vs. △SU5	0.133	No
Capsaicin	t-test	SU5 vs. NTC	P = 0.194	
		SU11 vs. NTC	P < 0.001	
		SU20 vs. NTC	P = 0.026	
		SU29 vs. NTC	P < 0.001	
	One-way ANOVA [a]	△SU5, △SU11, △SU20, △SU29	P < 0.001; F = 77.628	
	Student Newman Keuls	**comparison**	**P-value**	**P < 0.05?**
		△SU11 vs. △SU5	< 0.001	Yes
		△SU11 vs. △SU29	< 0.001	Yes
		△SU11 vs. △SU20	< 0.001	Yes
		△SU20 vs. △SU5	< 0.001	Yes
		△SU20 vs. △SU29	0.833	No
		△SU29 vs. △SU5	< 0.001	Yes
Gossypol	t-test	SU11 vs. SU20	P = 0.169	

9.9.2 Mutational analysis

Table S10: Statistical Analysis of Mutational Analysis. a - data log-transformed, b - data transformed to reciprocal

substrate	**test**	**comparison**	**results**
4-nitrophenol	t-test	SU5 vs. NTC	P < 0.001
		SU5mut vs. NTC	P < 0.001
		SU29 vs. NTC	P < 0.001
		SU29mut vs. NTC	P = 0.707
		△SU5mut vs. △SU5mut	P = 0.575
		△SU29 vs. △SU29mut	P < 0.001
1-naphthol	t-test	SU5 vs. NTC	P = 0.006
		SU5mut vs. NTC	P < 0.001
		SU29 vs. NTC	P < 0.014
		SU29mut vs. NTC	P < 0.001 [b]
		△SU5mut vs. △SU5mut	P = 0.013
		△SU29 vs. △SU29mut	P < 0.036
DIMBOA	t-test	SU5 vs. SU5mut	P < 0.001
HMBOA	t-test	SU5 vs. NTC	P < 0.001 [a]
		SU5mut vs. NTC	P < 0.001 [a]
		SU29 vs. NTC	P < 0.001
		SU29mut vs. NTC	P = 0.439
		△SU5mut vs. △SU5mut	P = 0.013
		△SU29 vs. △SU29mut	P = 0.049
Thiophenol	t-test	SU5 vs. NTC	P = 0.082
	Mann-Whitney Rank Sum	SU5mut vs. NTC	P = 0.200
	t-test	SU29 vs. NTC	P < 0.001
		SU29mut vs. NTC	P = 0.704

		△SU5mut vs. △SU5mut	P = 0.760
		△SU29 vs. △SU29mut	P < 0.001

9.9.3 New SfUGTs

Table S11: Statistical Analysis of Activity Assays of new UGT candidates.

substrate	**test**	**comparison**	**results**
4-nitrophenol	t-test	SU10 vs. NTC	P = 0.195
		SU26 vs. NTC	P = 0.094
		SU35 vs. NTC	P = 0.034
		SU39 vs. NTC	P < 0.001
		SU40 vs. NTC	P = 0.001
		SU42 vs. NTC	P < 0.001
		SU46 vs. NTC	P < 0.001
1-naphthol	t-test	SU10 vs. NTC	P < 0.001
		SU26 vs. NTC	P = 0.149
		SU35 vs. NTC	P = 0.003
		SU39 vs. NTC	P < 0.001
		SU40 vs. NTC	P = 0.011
		SU42 vs. NTC	P < 0.001
		SU46 vs. NTC	P < 0.001
HMBOA	t-test	SU10 vs. NTC	P = 0.374
		SU26 vs. NTC	P < 0.001
		SU35 vs. NTC	P = 0.304
		SU39 vs. NTC	P = 0.041
		SU40 vs. NTC	P = 0.005
		SU42 vs. NTC	P = 0.002
		SU46 vs. NTC	P = 0.318

9.9.4 qPCR

Table S12: Statistical Analysis of Mutational Analysis. g - gut, t - testes, fb - fat bodies, c - cuticle, mt - Malpighian tubules.

tested variable	**test**	**comparison**	**results**	
DIMBOA-UGT activity	One Way Repeated Measures Analysis of Variance	all tissues	P < 0.001, F = 27.725	
	Holm-Sidak multiple comparison	**comparison**	**P-value**	**P < 0.05?**
		g vs. c	< 0,001	Yes
		g vs. t	< 0,001	Yes
		g vs. fb	< 0,001	Yes
		g vs. mt	< 0,001	Yes
		mt vs. c	0,521	No
		mt vs. t	0,526	No
		mt vs. fb	0,651	No
		fb vs. c	0,958	No
		fb vs. t	0,931	No

		t vs. c	0,907	No
MBOA-UGT activity	One Way Repeated Measures Analysis of Variance	all tissues	P = 0.05, F = 3.853	
	Holm-Sidak multiple comparison	**comparison**	**P-value**	**P < 0.05?**
		fb vs. c	0,082	No
		fb vs. g	0,098	No
		fb vs. mt	0,517	No
		fb vs. t	0,513	No
		t vs. c	0,624	No
		mt vs. c	0,602	No
		t vs. g	0,594	No
		mt vs. g	0,535	No
		g vs. c	0,976	No
		t vs. mt	0,941	No
SU5	Normality Test (Shapiro-Wilk)	Passed (P = 0.089)		
	Equal Variance Test	Failed (P < 0.050)		
	Friedman Repeated Measures Analysis of Variance on Ranks	all tissues	P = 0.043, chi-square = 9.867	
		group	**median**	**25%**	**75%**
		c	0.779	0.700	1.835
		fb	1.238	0.282	2.910
		g	14.129	5.304	25.487
		mt	4.864	3.624	5.153
		t	0.703	0.461	0.897
SU11	One Way Repeated Measures Analysis of Variance	all tissues	P = 0.018, F = 5.729	
	Holm-Sidak multiple comparison	**comparison**	**P-value**	**P < 0.05?**
		t vs. mt	0,046	Yes
		t vs. c	0,044	Yes
		t vs. g	0,043	Yes
		t vs. fb	0,396	No
		fb vs. mt	0,514	No
		fb vs. c	0,474	No
		fb vs. g	0,433	No
		g vs. mt	1,000	No
		g vs. c	0,998	No
		c vs. mt	0,969	No
SU14	One Way Repeated Measures Analysis of Variance	all tissues	P = 0.013, F = 6.432	
	Holm-Sidak multiple comparison	**comparison**	**P-value**	**P < 0.05?**
		fb vs. c	0,028	Yes
		fb vs. g	0,032	Yes
		fb vs. mt	0,109	No

		t vs. c	0,191	No
		t vs. g	0,212	No
		fb vs. t	0,552	No
		t vs. mt	0,520	No
		mt vs. c	0.650	No
		mt vs. g	0,604	No
		g vs. c	0,868	No
SU20	One Way Repeated Measures Analysis of Variance	all tissues	P = 0.073, F = 3.249	
SU29	One Way Repeated Measures Analysis of Variance	all tissues	P < 0.001, F = 19.417	
	Holm-Sidak multiple comparison	**comparison**	**P-value**	**P < 0.05?**
		t vs. mt	< 0,001	Yes
		t vs. g	0,002	Yes
		fb vs. mt	0,009	Yes
		c vs. mt	0,023	Yes
		t vs. c	0,022	Yes
		t vs. fb	0,059	No
		fb vs. g	0,056	No
		c vs. g	0.143	No
		g vs. mt	0,196	No
		fb vs. c	0,442	No

10 Acknowledgements

At this point I would like to thank **Prof. Jonathan Gershenzon** for giving me the opportunity of conducting my Master's thesis in the Department of Biochemistry in the Max Planck Institute for Chemical Ecology and their support during my project and supporting me in my project. Also I would like to thank **Prof. Christian Hertweck** for his support, and reading my thesis.

I particularly want to thank my supervisors **Dr. Felipe Wouters** and **Dr. Daniel Giddings Vassão** for their guidance, numerous discussions and words of encouragement. **Felipe**, I especially want to thank you for introducing me into your project and helping me in the lab at the beginning of my thesis, for being such a great and positive person and for all the life advises you gave me! Big thanks also to you **Daniel**, for letting me work in your lab, for many discussions, for proofreading my thesis, for the best peanut cookies ever, and for supporting me whenever I needed help! Muito obrigado!

A huge thanks goes to **Katrin Luck**, the best and most patient teacher of Molecular Biology both, Felipe and me could have had. Thank you for your help and advice and for the encouraging words during all the times when was desperately trying to stay motivated. Thank you! And also, not to forget, **Nathalie Lackus** for being my secret supervisor, helping me with the mutational analysis, always kindly offering me her enzymes and always keeping me motivated with chocolate and good words. Thank you so much!

I also want to thank **Dr. Michael Reichelt** for teaching me practical everything that I know about analytical chemistry. Thank you for answering numerous questions and for your ideas regarding my project.
I would like to thank all the people of the Department of Biochemistry for the great working atmosphere and especially my group members **Anton**, **Micheal**, **Abinaya**, **Verena**, **Selina** and **Max** for the help and nice environment in the lab, for coffee breaks and a lot of great moments. It was great to work with you!

A big thanks goes to the Department of Entomology, especially to **Theresa**, **Wiebke** and **Michel** who supported me during my time here. Theresa, thank you for teaching me everything about westernblots and expression analysis and for all questions that you answered regarding my thesis. **Wiebke** and **Michel**, thanks for your help and for all the nice talks.

Finally, I want to thank my family and friends for supporting me and being patient with me during this time, for listening to me and encouraging me.

11 Selbständigkeitserklärung

Hiermit versichere ich, dass ich die vorliegende Arbeit selbstständig verfasst und keine anderen als die angegebenen Quellen und Hilfsmittel benutzt habe.

Ort, Datum Elena Seibel